# Non-linear Dynamics

# LPHYS2114

Lecture notes

2025 – 2026

Michel Crucifix

Faculté des Sciences

UCLouvain

## Contents

Git version HEAD:4310720 of Fri Mar 6 21:55:22 2026 +0100

# 1 Motivation and structure

## 1.1 Foreword

I am a physicist specialised in climate dynamics, and I have been working dynamical systems as models of the climate since 2006. My approach tends to be pragmatic, as I am ultimately interested in the behaviour of the real world system that I am attempting to model with dynamical systems. So will be this lecture. The divide between *continuous* dynamical systems and *discrete* dynamical systems has been conserved, as well as many exercises and the overall evaluation structure. I have the pleasure to thank warmly Prof. Wamsley-Hagendorf — who gave this course many years before me — and Prof. Luc Haine for their help and collaboration in preparing this course.

The course programme should roughly follow the succession of chapters, but not quite as some chapters are longer than other. The basis is 10 2-hour lessons (this including 3 spare weeks in the 13-week official program), plus weekly exercise sessions organised by Loic Sablon.

In preparing this lecture, I have relied on several reference books. Although the current notes are meant to be the formal material upon which evaluation is based, the circumstances are such that writing is work in progress and students are most welcome to check them and provide corrections or suggestions. This text and related material is provided as a free git repository. Many of the books below are available online, and some can be bought at an advantageous rate with the Springer MyCopy program.

- S.H. Strogatz, Nonlinear dynamics and chaos. Westview Press (2015).
- S. Wiggins, Introduction to Applied Nonlinear Dynamical Systems and Chaos, Springer (2003)

- R. Hilborn, Chaos and Nonlinear Dynamics: An Introduction for Scientists and Engineers (2nd edn) , Oxford University Press (2000)
- H. Dijkstra, Nonlinear Physical Oceanography, A Dynamical Systems Approach to the Large Scale Ocean Circulation and El Niño, Springer Science+Business Media (2000)
- Alligood K., T. Sauer and J. Yorke (1997), Chaos: An Introduction to Dynamical Systems, Springer (NewYork)
- Perko L. (2001), Differential Equations and Dynamical Systems, Springer, ISBN 978-1-4612-6526-9

The lecture is marked by a written exam

Last but not least, I am thankful to students who spotted small and big mistakes and communicated them to me. By doing so they improved the document and made life easier for their followers.

## 1.2 Motivating example: ice sheet

To motivate the course and its objective, consider the following example from glaciology.

An ice sheet is a large accumulation of ice. The largest ice sheets take thousands of years to millennia to form. If the climate is stable enough (say, it is *constant*), the ice sheet may reach a *stable equilibrium*.

This equilibrium results from a balance between *accumulation* of snow above the *snowline* (which is determined by the external climate conditions), and the *ablation* of ice that is being pushed below the snow line.

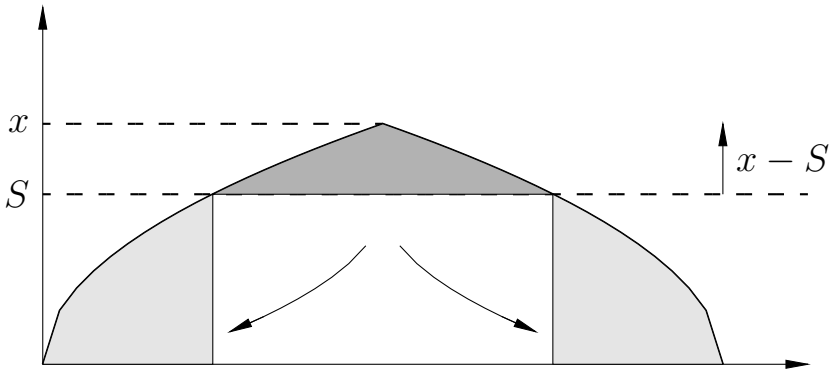


**Fig. 1.1**

Intuitively, we may perceive that if climate warms a little, the altitude of the ice sheet will decrease (implying less net accumulation), but the flow of ice towards the ice sheet will be reduced as well, so that a new balance will be reached.

However, we may already anticipate that if the climate warms *too much*, and the top surface of the ice sheet will drown under the snowline, at which point we expect a catastrophic meltdown of the icesheet.

We witness here a non-linear phenomenon. There is what some might call a *tipping point*, a point of warming above which the qualitative behaviour of the object changes. In this course, we would like to use mathematical modelling and a mathematical language to describe this behaviour, and many others. We will be introduced to the theory and learn the techniques that allow us to describe the expected behaviour of such systems.

The standard theory is the theory of *dynamical systems*. In essence, a dynamical system is the combination of a state space, say $\Omega$, and a *rule* that determines the evolution of every point of the state space.

This is perhaps a bit abstract, so consider again our ice sheet example.

Call the altitude of the summit of the ice sheet $x$. This is a positive real number, so $x \in \mathbb{R}^+$. The altitude of the snowline is $S$. We consider

that it is constant, so in the following we will view it as a *parameter*.

Here, we have *summarised* the state of our real-world system (the ice sheet) with a single variable $x$. That variable evolves in $\mathbb{R}^+$. In our case the $\Omega$ space is $\mathbb{R}^+$. Now we need a rule for the evolution of an ice sheet that would have an altitude $x$.

One (standard) approach is to write a *differential equation*. Simply, we equate $\frac{\mathrm{d}x}{\mathrm{d}t}$ with a function of the state $x$, and the parameter $S$. At this point, we need a bit of physical intuition. $x$ will evolve as a balance between accumulation and ablation. The difference between accumulation and ablation is called *net accumulation*. One (simplistic) way of putting it, is that net accumulation is proportional to the distance between $x$ and $S$. It would be an equation of the kind

$$\frac{\mathrm{d}x}{\mathrm{d}t} = x - S \tag{1}$$

**CLASS ROOM DISCUSSION 1**

Consider an initial condition $x_0 = x(t_0)$. Finding $x_t$ for $t > t_0$ is an initial value problem, which is a particular case of a Cauchy problem. Find the solutions. Show that their behaviour differ depending on the initial condition. Explain also what is wrong with this model. How can we fix it ?

After discussion, we see that we need a *negative feedback* to prevent ice to grow until infinity when it starts above the snowline. We won't discuss too much the phenomenological details here, but say that the negative feedback is related to the flow of ice towards the ice sheet ablation zone, which is enhanced when the ice sheet grows very big. So our final equation would resemble:

$$\frac{\mathrm{d}x}{\mathrm{d}t} = x - ax^2 - S \text{ if } x > 0, \text{ and } \frac{\mathrm{d}x}{\mathrm{d}t} = \max(0, -S) \text{ if } x = 0, \tag{2}$$

where $a$ is a parameter. Again, we look after qualitative behaviours, and for (mathematical) simplicity we will set $a = 1/4$. In practice we cannot be so relaxed about fixing parameters, but this is for the sake of the demonstration.

What is going on now ?

**CLASS ROOM DISCUSSION 2**

A fixed point $x_f$ of the differential equation is an element of the domain $\Omega$ such that the system is invariant at that point. That is, if $x(t_0) = x_f$ for a given $t = t_0$, then $x(t) = x_f$ for any time $t$ of the time domain. How do you find the fixed points associated with the dynamical system in (2) ?

After discussion, we find that the number of fixed points depends on the value of the parameter $S$: one fixed point for $S < 0$ $2(1+\sqrt{(}1-S))$, one fixed point for $S > 1$ (x=0), and three fixed points between these values (which ones ?)

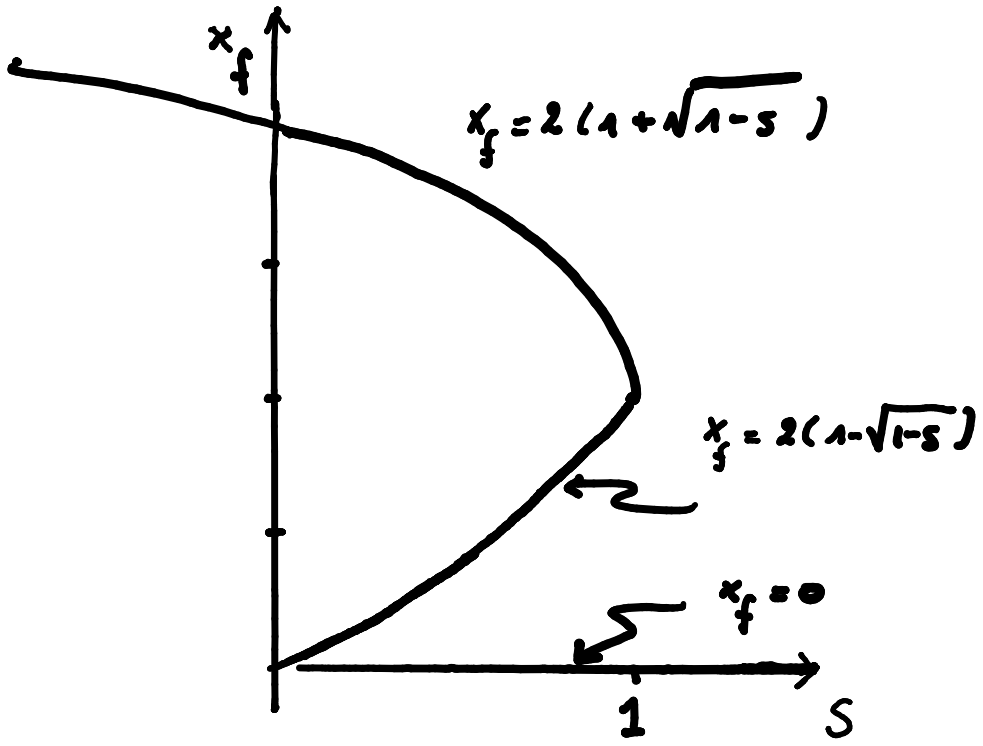


Now we would like to determine the behaviour of the system for initial conditions between these points. One approach would be to resolve the ordinary differential equation (2). For $S = 0$ it is doable (hint: use the separation of variables: put all $\mathrm{d}x$ terms on one side; the $\mathrm{d}t$ terms on the other side; integrate and solve for $x$) but it is cumbersome and the strategy will actually not work in most cases. In other words, most non-linear ordinary differential equations have no analytical solutions.

Hence, a more fruitful strategy is to study the behaviour of $S(t)$ *near* (in French: *dans le voisinage the*) fixed points, and use theory to connect the flow lines between fixed points.

The model we have been starting with is of the form $\frac{\mathrm{d}x}{\mathrm{d}t} = f(x;\psi)$ with, here, $\psi := S$. By definition of a fixed point, $f(x_f;\psi) = 0$ (the dependency on $\psi$ is dropped for clarity). Define $\delta x := x - x_f$.

$$\frac{\mathrm{d}(x - x_f)}{\mathrm{d}t} \doteq \frac{\mathrm{d}\delta_x}{\mathrm{d}t} = \underbrace{\left.\frac{\partial f(x;\psi)}{\partial x}\right|_{x_f}}_{\lambda} \delta x + \mathcal{O}(\delta x^2) \tag{3}$$

This is a linear differential equation for $\delta x$ with constant coefficient. That is, near enough to the fixed point, $\delta x$ decays (if $\lambda < 0$) or grows (if $\lambda > 0$) exponentially with e-folding time $1/\lambda$. This distinguishes a point that is *locally stable* from a point that is *locally unstable*.

**CLASS ROOM DISCUSSION 3**

Reconsider the solutions of the bifurcation diagram. Which ones are stable, and which one unstable? What we see appearing are branches of *stable* and *unstable* solutions.

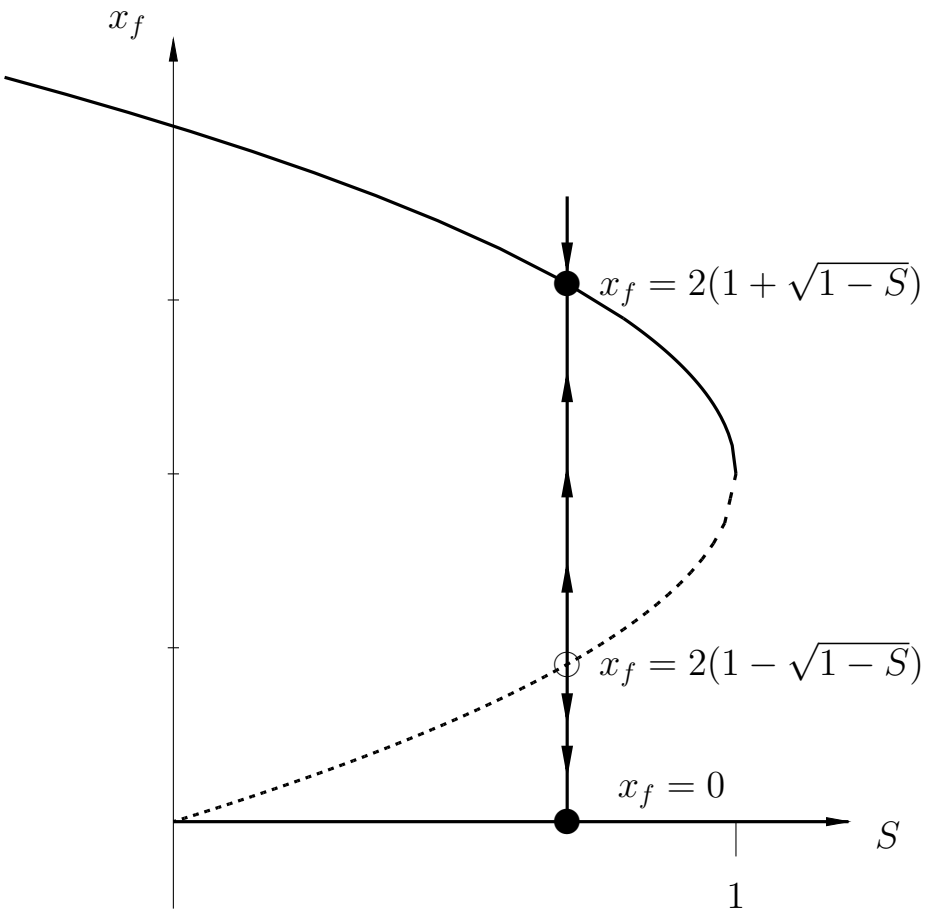


**Fig. 1.2**

Hence, even though we have avoided to resolve the ordinary differential equation (we avoided to solve the initial value problem), but provided that we have identified all fixed points, and characterised their local stability, we have gained a good qualitative picture of the system's behavior. For any value of $S$, we can picture the *flow* associated with the dynamical system, that is, for any point $x$ of the domain $\Omega$, we know the direction taken by $x$ as time progresses.

This is an example of qualitative analysis of a non-linear dynamical system, which, as we see it here, is reasonably simple but not simplistic. We have identified *invariant sets*, that is, sets of points that are

left unchanged by the *flow*. In this example, invariant sets are fixed points. We have also identified *bifurcation points*, that is, points of the parameter space $S$ where the number or the stability of the invariant sets (again, here, fixed points).

In this first lecture, meant to motivate the course, we have been informal and did not justify our findings with theorems; nor did we attempt to be too systematic and rigorous with definitions. But we understand our objectives: identify the nature of invariant sets, estimate their stability, and depict the behaviour of the system between these invariant sets.

Specifically, the lecture will be divided into two broad sections:

- ▷ continuous dynamical systems (expressed as ordinary differential equations)
- ▷ discrete dynamical systems (expressed as iterations)

Dynamical systems will be deterministic (but informally, from time to time I will mention the interest and possibilities brought about by stochastic dynamical systems), and we will not go beyond three dimensions.

## 1.3 Evaluation

Exercises will be evaluated and provide a *fifth* of the final evaluation that can no longer be modified. There will be a *written* exam (June and September sessions) that is focused on exercises. Exams of the previous years are available on Moodle. They will be focused on applications, knowledge of the theory being instrumental in solving the problems.

# 2 Continuous Flows: existence and uniqueness

## 2.1 Definition of trajectories, orbit, and linear stability

(based on [Wig03], section 7)

Consider the following dynamical system:

$$\dot{\boldsymbol{x}} \overset{\text{def}}{=} \frac{\mathrm{d}}{\mathrm{d}t}x = \boldsymbol{f}(\boldsymbol{x}, t), \text{ with } \boldsymbol{x} \in \Omega \tag{4}$$

**DEFINITION 1 Autonomous dynamical system**

The system is said to be *autonomous* if there is no explicit dependence of $\boldsymbol{f}$ on $t$, and non-autonomous otherwise.

For simplicity, we will admit that $\Omega = \mathbb{R}^n$, where $n$ is the phase-space dimension.

**DEFINITION 2 Trajectory**

A *trajectory* $\boldsymbol{x}(t, t_0, x_0)$ (or *phase curve*), for $t \in I$ is a solution of the differential equation (4), passing through $\boldsymbol{x}_0$ at time $t_0$ over an interval of existence $I$.

**DEFINITION 3 Orbit**

An orbit through $\boldsymbol{x}_0$ is the set of points in phase space passing of a trajectory passing through $\boldsymbol{x}_0$.

## 2.2 Equilibrium solutions, stability and asymptotic stability

In this section we briefly formalise and extend notions that have already been introduced in the motivating chapter (section 1.2).

We consider an *autonomous* vector field

$$\frac{\mathrm{d}\boldsymbol{x}}{\mathrm{d}t} = \boldsymbol{f}(\boldsymbol{x}), \quad \boldsymbol{x} \in \mathbb{R}^n$$

A fixed point (also said: *equilibrium solution*) is a point $\boldsymbol{x}_f \in \mathbb{R}^n$ such that $f(\boldsymbol{x}_f) = 0$.

We distinguish the Lyapunov stability from the asymptotic stability. Roughly speaking, $\boldsymbol{x}_f$ is *stable* (shorthand for *Lyapunov stable*) if solutions starting close enough to $\boldsymbol{x}_f$ remain near it. It is *asymptotically stable* if these solutions eventually converge to $\boldsymbol{x}_f$.

**DEFINITION 4 Lyapunov Stability**

The fixed point $\boldsymbol{x}_f$ is (Lyapunov) stable if, given $\varepsilon > 0$, there exists a $\delta > 0$ such that, for any other trajectory $y(t)$ satisfying $|\boldsymbol{x}_f - \boldsymbol{y}(t_0)| < \delta$, then $|\boldsymbol{x}_f - \boldsymbol{y}(t)| < \varepsilon$ for $t > t_0$, $t_0 \in \mathbb{R}$.

**DEFINITION 5 Asymptotic Stability**

A fixed point $x_f$ is asymptotically stable if it is Lyapunov stable *and* for any other solution $y(t)$ there exists a constant $b > 0$ such that, if $|\boldsymbol{x}_f - \boldsymbol{y}(t_0)| < b$, then $\lim_{t\to\infty} |\boldsymbol{x}_f - \boldsymbol{y}(t)| = 0$.

**CLASS ROOM DISCUSSION 4**

Illustrate these notions graphically

## 2.3 Properties of vector fields: existence, uniqueness, differentiability and flows

In this section we develop a technical notion to deal wit the notions of "long term" and "observable" behaviours of *orbits* of *dynamical systems*. This will later allow us to develop the notions of *attracting sets* and *attractors*. Again, we restrict the discussion to dynamical systems in the form of vector fields, that is:

$$\frac{\mathrm{d}}{\mathrm{d}t}x = f(\boldsymbol{x}, t), \text{ with } \boldsymbol{x} \in \Omega \tag{5}$$

and, again, for simplicity, we will admit that $\Omega = \mathbb{R}^n$. Here, we further suppose that $\boldsymbol{f}(\boldsymbol{x}, t)$ is $\mathbf{C}^r$-differentiable, with $r \geq 1$ on the open set $U \subset \mathbb{R}^n \times \mathbb{R}$.

**THEOREM 1 Existence**

Let $(\boldsymbol{x}_0, t_0) \in U$. Then, there *exists* a solution of (5) through the point $\boldsymbol{x}_0$ at $t = t_0$, denoted $\boldsymbol{x}(t, t_0, \boldsymbol{x}_0)$ for $|t - t_0|$ sufficiently small. The solution is unique. Moreover, $\boldsymbol{x}(t, t_0, \boldsymbol{x}_0)$ is a $\mathbb{C}^r$ function of $t$, $t_0$, and $\boldsymbol{x}_0$.

The proof is available in specialised books [e.g. HD13, chap. 6 for linear systems and chap. 17 for more general systems].

It has also been proved that the unique solution can be (uniquely) *extended* to the boundaries of any compact subset (closed and bounded)

of $U$. However, this says nothing about what is going on once the solution has reached the boundaries.

**CLASS ROOM DISCUSSION 5**

Consider the following example: $\frac{\mathrm{d}x}{\mathrm{d}t} = x^2, \quad x \in \mathbb{R}$. Find the analytical solution, and show that the solution blows up and that the interval of existence of solutions through $x_0$ at $t = 0$ depends on $x_0$. Tip: use the methods of variable separation.

There in another handy theorem, that says that if $\boldsymbol{f}(\boldsymbol{x}, t, \psi)$ is differentiable with respect to the parameter $\psi$, then the solution is also differentiable with respect to that parameter.

## 2.4 Special properties of autonomous fields

We now consider two important propositions that apply to autonomous dynamical systems, and that we will be able to prove. For simplicity, we consider a dynamical system admitting solutions over all times.

**THEOREM 2 Time shifted trajectories are trajectories in autonomous fields.**

If $\boldsymbol{x}(t)$ is a solution of $\frac{\mathrm{d}}{\mathrm{d}t}x = \boldsymbol{f}(\boldsymbol{x})$, then $\boldsymbol{x}(t+\tau)$ is also a solution of that equation for any $\tau$.

Proof: By definition, $\frac{\mathrm{d}\boldsymbol{x}(t)}{\mathrm{d}t} = \boldsymbol{f}\left(\boldsymbol{x}\left(t\right)\right)$. Hence, we have

$$\left.\frac{\mathrm{d}\boldsymbol{x}(t+\tau)}{\mathrm{d}t}\right|_{t=t_0} = \left.\frac{\mathrm{d}\boldsymbol{x}(t)}{\mathrm{d}t}\right|_{t=t_0+\tau} = \boldsymbol{f}\left(\boldsymbol{x}\left(t_0+\tau\right)\right) = f\left(\boldsymbol{x}\left(t+\tau\right)\right)|_{t=t_0}.$$

To pack this up:

$\left.\frac{\mathrm{d}\boldsymbol{x}(t+\tau)}{\mathrm{d}t}\right|_{t=t_0} = \boldsymbol{f}\left(\boldsymbol{x}\left(t+\tau\right)\right)|_{t=t_0}$ is true for any $t_0 \in \mathbb{R}$. In other words, $\boldsymbol{x}(t+\tau)$ is a solution of the dynamical system. □

The formal maths make it a bit confusing, but the intuition is reasonably clear: two time-shifted trajectories that pass through the same point *correspond to the same orbit* !

This has an important implication: in an autonomous dynamical system, there is *one single* orbit that passes through any point $\boldsymbol{x}_0$. There is a more formal proof in [Wig03], but the intuition seems to be reasonably clear from the uniqueness theorem.

In other words,

**THEOREM 3 Non-crossing orbits**

Orbits *never cross* each other in an autonomous dynamical system.

## CLASS ROOM DISCUSSION 6

Consider the following diagram. This is a phase portrait: a diagram which qualitatively represents some trajectories such as to provide a general idea of the behavour of trajectories in the phase spaced. In this case, several trajectories seem to converge to a same point. How would you prove that the intersection is necessarily a fixed point? What does it say about the time a trajectory will need to reach the fixed point?

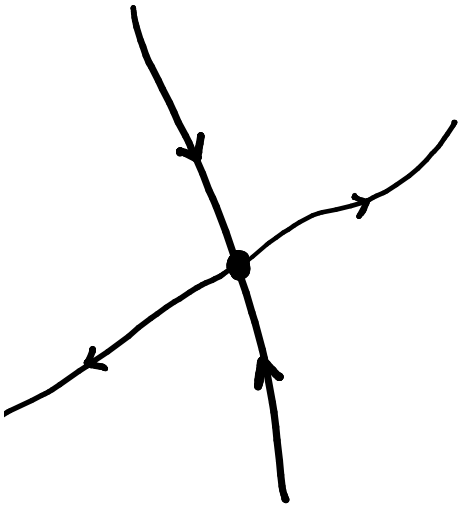

## 2.5 Flows

At this point, we have understood (at least intuitively) that the future fate a point in the phase space, in an autonomous system, does not depend on the time at which the snapshot has been taken. This is

after all consistent with the definition of an autonomous system (the evolution dictated by $\boldsymbol{f}$ does not depend explicitly on time). In other words, for any point $(\boldsymbol{x}_0, t_0)$, the point of the trajectory $\boldsymbol{x}(t, t_0, \boldsymbol{x_0})$ reached at time $t$ depends only on the initial condition $t_0$, and the time elapsed $\tau = t - t_0$. We can thus define a function $\phi(t - t_0, \boldsymbol{x_0}) = \boldsymbol{x}(t, t_0, \boldsymbol{x_0})$.

We proceed in two steps. First, we denote the family of functions $\phi^\tau$, defined such that $\phi^\tau(\boldsymbol{x_0}) = x(t_0 + \tau, t_0, \boldsymbol{x_0})$ which, we have seen, is independent of $t_0$. We observe the following properties:

- ▷ $\phi^0$ is the identify function;
- ▷ $(\phi^\tau)^{-1} = \phi^{-\tau} : \phi_\tau$ is thus an invertible function.
- ▷ $\phi^t \in \mathbb{C}^r$.

**DEFINITION 6 Flow of an autonomous differential equation**

The family of functions $\phi\tau$ associated with the differential equation $\dot{\boldsymbol{x}} = \boldsymbol{f}(\boldsymbol{x})$, $\boldsymbol{f} \in \mathbb{C}^r$, which satisfy the above properties, is called a flow.

In our notation we have been a little ambiguous about the domain of $\phi$. Above we have applied $\phi^\tau$ to elements of the phase-space domain. However, we could also map the function on subsets $U$ of this domain, as illustrated on the figure below:

$\phi^{\tau_1+\tau_2}(U) = \phi^{\tau_2} \circ \phi^{\tau_1}(U)$.

Again, this flow function is invertible.

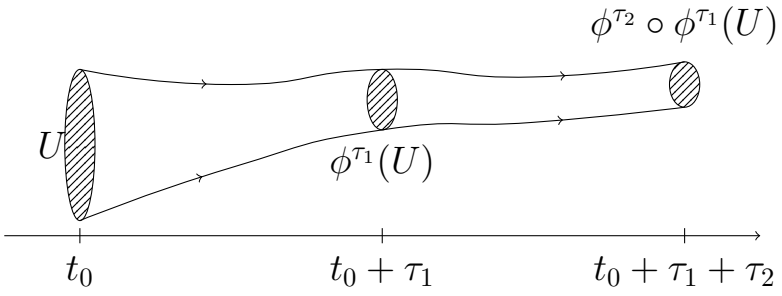


Given that we have required the vector field defined by $\boldsymbol{f}$ to be continuous and differentiable, the mapping defined by the flow $\phi$ also inherits some nice properties as we have seen it: it is invertible and differentiable. Therefore, it turns out that the flow generated by the vector field defined on $\mathbb{R}^n$ belongs to a wider class of mathematical objects called *diffeomorphism*, which are continuous, invertible mappings of so-called "differential manifolds". The vector space defined on $\mathbb{R}^n$ is a particular case of differential manifold. This establishes a link between ordinary differential equations and differential geometry. The term "diffeomorphism" will therefore appear from time to time in some of the definitions below, specifically in section where we define attractors and attracting sets.

The flow provides an intuitive impression that is reminiscent of a fluid flow. It may be converging; diverging but streamlines never cross each other.

At this point, we may already perceive that dynamical systems will fall in different categories. A bit informally, we will mainly encounter and distinguish

1. Those associated with flow which (on average) diverge. Such flows can be considered to be globally unstable because trajectories tend to grow towards the limits of the domain; such dynamical systems have only local validity: they cannot be used to study asymptotic behaviours as time unfolds.
2. Those associated with flows that (on average) converge. Trajecto-

ries tend to cluster towards attracting regions (a notion that still needs to be formalised). These flows are called *dissipative* : information about initial is, in practice, lost because a potentially large volume of initial conditions gets collapsed into a small volume of possible final states (the attractor);

3. Those associated with flow that neither diverge nor converge. The phase-space volume of $U$ is conserved through time.

**CLASS ROOM DISCUSSION 7**

The latter category represents the class of *Hamiltonian flows*. Can you guess why? Tip: think of Liouville's theorem.

At this point we may already have some intuitions which will be generalised in the coming chapters. The stability or instability of fixed points in an autonomous system is related to the overall structure of the vector field defined by the function $\boldsymbol{f}$ (which is here a vector). If it is rather diverging around the fixed point we expect instability; if it is converging, stability. In a 2-dimensional vector field, divergence and convergence can be assessed with the divergence operator $\nabla \cdot \boldsymbol{f}$. This is the trace of the Jacobian of the vector field, and it measures the overall compression of the flow. However, we may also anticipate that we might have divergence in one direction, and perhaps compression in another. These directions, as we will find out, are the eigenvectors of the Jacobian, and the related stability are given by the related eigenvalues.

The figure below represents a *dissipative* flow that has at least one positive Lyapunov exponent. The phase space volume is shrinking over time (meaning that the *sum* of eigenvalues is negative, even though one is positive). However, because one eigenvalue is positive, the flow gets stretched in one direction, so that to initially close initial conditions get increasingly distant with each other as time grows.

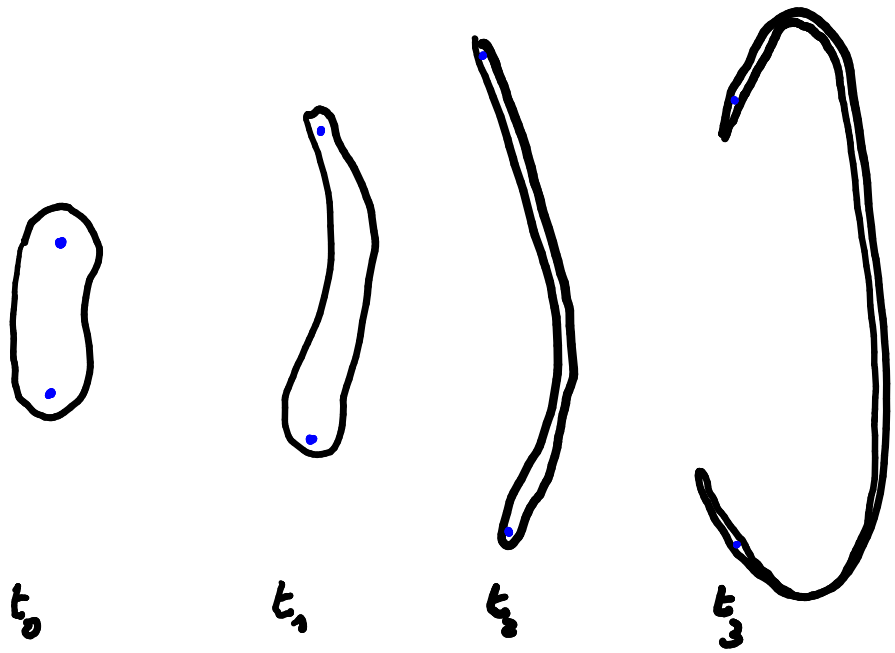


This is the basic explanation to the possibility of sensitive dependence to initial conditions, that is one of the cornerstones of chaos.

One generally distinguishes dissipative chaos (in dissipative flows) from Hamiltonian chaos (in Hamiltonian flows). Poincaré first discovered sensitive dependence to initial conditions in the 3-body problem, which is characterised by a Hamiltonian flow. The meteorologist Edwar Lorenz is famous for having popularised the notion of dissipative chaos.

All these notions will have to be made more precise and proved, but hopefully the relevant ideas are already pretty much in place.

# 3 Vector fields on the line: bifurcations and normal forms

We now consider the autonomous dynamical system on the line, with parameter $\psi$ which, for simplicity, we view as one-dimensional.

## 3.1 Monotonous character of the trajectories

$$\frac{\mathrm{d}x}{\mathrm{d}t} = f(x;\psi), \text{ with } x \in \mathbb{R}, \ \psi \in \mathbb{R}, \tag{6}$$

with $f$ continuous and differentiable over $x$ and $\psi$.

We start with a remarkable properties of the trajectories:

**THEOREM 4 No local extrema.**

Trajectories of (6) do not have local maxima and minima.

Proof: If there was a local extrema at time $t$, $x(t)$ at that point would need to have a zero-derivative, it must therefore be a fixed point; thus the trajectory must be constant and it cannot have local extrema. □

It comes up that trajectories on the line must either be constant (fixed point), strictly increasing (towards infinity, or towards a fixed point), or strictly decreasing (ditto).

## 3.2 Stability of the fixed point

**DEFINITION 7 Hyperbolic fixed points on the line**

Fixed points on the line are said to be hyperbolic if the derivative $\frac{\mathrm{d}f}{\mathrm{d}x}$ is either strictly negative or positive

**THEOREM 5 Stability of hyperbolic fixed points on the line**

Fixed points with $\frac{\mathrm{d}f}{\mathrm{d}x}|_{x=x_f} < 0$, or $\frac{\mathrm{d}f}{\mathrm{d}x}|_{x=x_f} > 0$, are asymptotically stable or unstable, respectively

Consider $x_f$ a fixed point, so that by definition $f(x_f) = 0$. Suppose first that $\frac{\mathrm{d}f}{\mathrm{d}x}|_{x=x_f}$ is strictly negative. Then it comes that there one can find a (small) open neighbourhood around $x_f$ such that $f(x)$ is strictly positive for $x < x_f$ in this neighbourhood, and $f(x)$ is strictly negative for $x < x_f$. It comes up that orbits in this neighbourhood will asymptotically converge (since they are monotonous) to $x_f$. One can also verify that the conditions for Lyapunov stability are fulfilled. There is thus asymptotic stability.

By the same token, one verifies asymptotic *instability* when $\frac{\mathrm{d}f}{\mathrm{d}x}|_{x=x_f} > 0$. □

Hyperbolic fixed points with negative derivative are a *sink*; those with positive derivative are a *source*.

Stability is no-longer trivial for non-hyperbolic fixed points, since one cannot affirm that $\frac{\mathrm{d}f}{\mathrm{d}x}$ changes sign. We show an example below.

**CLASS ROOM DISCUSSION 8**

Consider again the motivating example with the ice sheets. Are the fixed points hyperbolic? Everywhere ? (tip: it is enough to restrict the discussion to the case $x \neq 0$. )

## 3.3 The saddle-node bifurcation

We now consider changes in $\psi$ that may affect the existence or the *nature* of the fixed point. To this end, consider the following example: $f(x;\psi) = x + e^{-x} - \psi$.

The fixed point may be visualised graphically, using the fixed point equation $e^{-x} = \psi - x$.

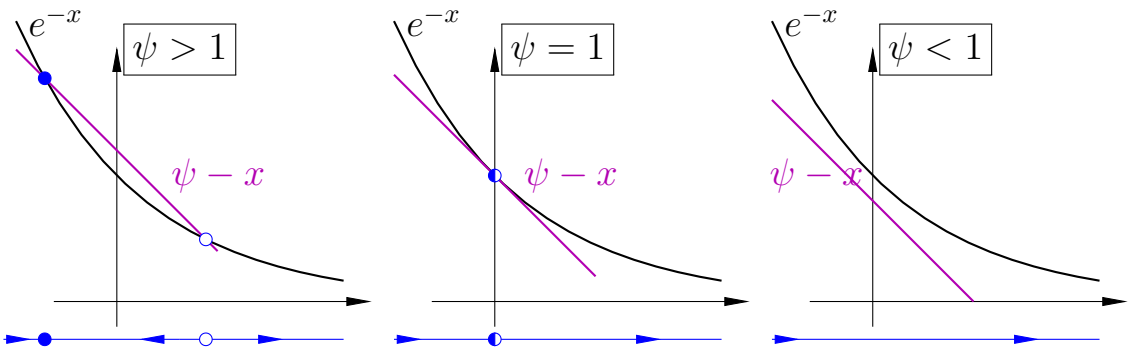


**Fig. 3.1**

The arrows in blue represent the flow with arrows, which converge or diverge from the fixed points depending on their stability. This is the *phase portrait* which, in this case, is one dimensional. We will see, later, 2-d or even higher dimensional phase portraits.

As is clear from the phase portraits, the number of fixed points changes

from 2 hyperbolic fixed points for $\psi > 1$, to one non-hyperbolic fixed point at $\psi = 0$, to zero for $\psi - 1$. Hence, the parameter $\psi = 1$ marks a qualitative change in the flow. This is a singularity, which is called a *bifurcation point*.

In this section we will learn to *detect* bifurcation points in vector fields on the line and classify them.

To this end, let us continue with the example with have just started. The bifurcation occurs at $\psi = 1$ and we would like to study the behaviour of $f$ near this bifurcation point.

To this end, we develop the function according to Taylor (recall that we have taken care of its differentiability):

$$\begin{aligned} f(x;\psi) =& f(x_0;\psi_0) + \left.\frac{\partial f}{\partial \psi}\right|_{x_0,\psi_0} (\psi - \psi_0) + \left.\frac{\partial f}{\partial x}\right|_{x_0,\psi_0} (x - x_0) + \\ & \frac{1}{2} \left.\frac{\partial^2 f}{\partial x^2}\right|_{x_0,\psi_0} (x - x_0)^2 + \\ & \frac{1}{2} \left.\frac{\partial^2 f}{\partial \psi^2}\right|_{x_0,\psi_0} (\psi - \psi_0)^2 + \\ & \left.\frac{\partial^2 f}{\partial \psi \partial x}\right|_{x_0,\psi_0} (x - x_0)(\psi - \psi_0) \\ & + \dots \\ =& \underbrace{1 - \psi - \frac{1}{2}x^2}_{\text{normal form}} + \dots \end{aligned}$$

Hence, if we develop the vector field around the bifurcation point, it takes a specific form that depends on the first and second-order derivatives on $x$ and $\psi$. This specific form is called a *normal form*, and the normal form characterises the bifurcation. In general you

need some linear transformation of the variable and the parameter to find the text book normal form. In this case, we need $\psi' = 1 - \psi$, $x' = x/\sqrt{2}$ and also invert time $t' = -t$ to obtain the normal form

$$\frac{\mathrm{d}x'}{\mathrm{d}t'} = \psi' + x'^2.$$

This is the normal form of the *saddle-node* bifurcation (also called a *fold bifurcation*): it is the collision of a stable and an unstable fixed point, with both vanishing beyond the bifurcation point. We have met this exact bifurcation in the motivating example.

The position of stable and unstable fixed points, as a function of the parameter $\psi$ is summarised by the *stability* diagram. The set of fixed point solutions are organised as branches, which may be stable (solid lines), or unstable (dashed lines).

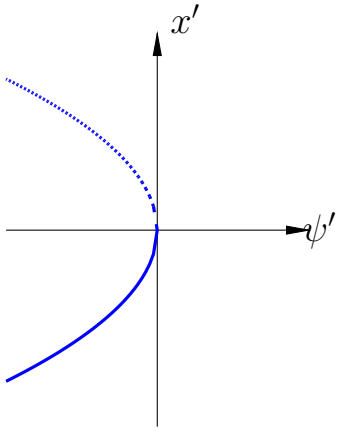


**Fig. 3.2**

The classical convention for the normal form makes it that the solutions disappear for $\psi'$ positive and, and the stable branch is obtained for negative $x$; however any affine transformation of this graph will actually represent a saddle-node bifurcation. This leads to the following theorem.

**THEOREM 6 Sufficient conditions for a saddle-node bifurcation on the line.**

A saddle-node bifurcation occurs on $x_0, \psi_0$ when:

1. $f(x_0; \psi_0) = 0$;
2. $\frac{\partial f}{\partial x}(x_0; \psi_0) = 0$;
3. $\frac{\partial^2 f}{\partial x^2}(x_0; \psi_0) \neq 0$;
4. $\frac{\partial f}{\partial \psi}(x_0; \psi_0) \neq 0$;

The intuition beyond this theorem is reasonably clear. The first condition imposes the existence of the fixed point; the second one is the non-hyperbolic character of the fixed point (neither linear stable nor linearly unstable). The third and fourth conditions set the locally parabolic character of the solutions near the bifurcation point.

More formally, from the implicit function theorem, (1) and (4) imply that there must exist a function $\psi(x)$ on an interval $I \subset \mathbb{R}$ such that $f(x, \psi(x)) = 0$ and $\psi(x_0) = \psi_0$.

This is the curve of fixed points, as a function of $\psi$. On a branch of solution parameterised as $(x, \psi(x))$, by definition, $f = 0$, so that $\mathrm{d}f$ is also zero along the branch:

$$\mathrm{d}f = \frac{\partial f(x, \psi(x))}{\partial x}\,\mathrm{d}x + \frac{\partial f(x, \psi(x))}{\partial \psi}\,\mathrm{d}\psi,$$

leading

$$\frac{\mathrm{d}\psi}{\mathrm{d}x} = -\frac{\frac{\partial f(x,\psi(x))}{\partial x}}{\frac{\partial f(x,\psi(x))}{\partial \psi}};$$

The assumptions (1) and (4) imply that $\frac{\mathrm{d}\psi}{\mathrm{d}x} = 0$. And

$$\frac{\mathrm{d}^2\psi}{\mathrm{d}x^2} = +\frac{\frac{\partial^2 f(x,\psi(x))}{\partial x^2}\frac{\partial f(x;\psi(x))}{\partial \psi} + \frac{\partial f(x,\psi(x))}{\partial x}\frac{\partial^2 f(x;\psi(x))}{\partial \psi \partial x}}{\left(\frac{\partial f(x;\psi(x))}{\partial \psi}\right)^2},$$

which then must be different from zero from (3) and (4). Both indicate that the solution curve $\psi(x)$ has a minimum or a local maximum in $x = x_0$ and therefore must bear the characteristic of a saddle-node bifurcation.

## 3.4 The fork bifurcation

The normal form for the pitchfork bifurcation (or simply: fork bifurcation) is

$$f(x;\psi) = \psi x + \sigma x^3,$$

where $\sigma$ is either $-1$ or $1$. $\sigma = -1$. We consider both.

### 3.4.1 $\sigma = -1$ The supercritical fork bifurcation

The supercritical fork bifurcation is the one which is most commonly introduced. It admits the trivial solution $x_f = 0$ throughout the entire real line. The stability of the solution is directly given by the sign of $\psi$: stable for negative $\psi$, and stable for positive.

For $\psi > 0$, it also admits the solutions $x_f = \pm\sqrt{\psi}$, which is stable.

The bifurcation diagram clearly reveals how, going from negative to positive values of the parameter $\psi$, the bifurcation at $\psi = 0$ consists in a loss of stability of the trivial solution, and the emergence of two stable solutions of distance gently growing from the zero-line as $\psi$ increases. Here is the stability diagram:

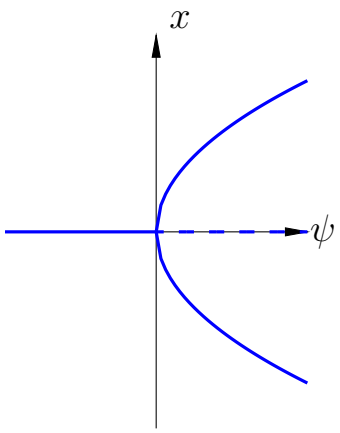


**Fig. 3.3**

### 3.4.2 $\sigma = 1$ The subcritical pitchfork bifuration

Compared to the supercritical case, nothing changes for the stability along the $x = 0$ line: stable for negative $\psi$, unstable for positive ones.

$f(x;\psi) = \psi x + \sigma x^3$,

Now, the side solutions only exist for *negative* $\psi$, at $x_f = \pm\sqrt{|\psi|}$. The derivative

$$\left.\frac{\partial f(x;\psi)}{\partial x}\right|_{x=\pm\sqrt{|\psi|}} = 2|\psi|$$

is positive (use $\sqrt{\psi^2} = |\psi|$). That solution is unstable.

Hence, going from negative to positive $\psi$, we have, on the negative side, three solutions but only the central is stable, and on the positive side, only the trivial solution that is unstable, that is, the flow escaping that solution.

This is how the normal form works, but we understand that in practice,

it will only be a local description of the flow because we do not expect, in a physical system, the state variable to run away to infinity. Hence, in practical applications, higher order terms are expected to catch up the solution.

A classical scenario is found by adding a fifth-order term as:

$$f(x;\psi) = \psi x + x^3 - x^5$$

Consider the particular case $\sigma = 1$. We find that, in addition to the trivial solution $x = 0$, we have now two to four additional solutions, depending on what comes under the square root:

$$x_f(\psi) = \pm\frac{1}{\sqrt{2}}\sqrt{1 \pm \sqrt{4\psi + 1}},$$

where all combinations of $+$ and $-$ are potentially admitted, with the restriction of keeping real solutions only.

Specifically, considering real solutions only, we have four solutions for $\frac{1}{4} \leq \psi \leq 0$. It may be verified (exercise) that, they come as two symmetric groups of two around the zero axis, and they are successively stable and unstable. One thus finds two fold bifurcations at $\psi = \frac{1}{4}$. Then, for $\psi > 0$, the only two *stable* solutions.

Hence, as one moves from negative to positive $\psi$, we see here a scenario quite different from the supercritical bifurcation. The stable trivial solution vanishes, and the only place to land is already located at a distance $\frac{1}{2}\sqrt{1+\sqrt{2}}$ of the origin.

This would be the typical scenario, in physics, of a stick being compressed, and suddenly bending towards a new stable state, either on the left or on the right. This will be a case of spontaneous symme-

try breaking, since once a stable state has been found, it is hard to come back to the original solution, and even harder to reach to other solution.

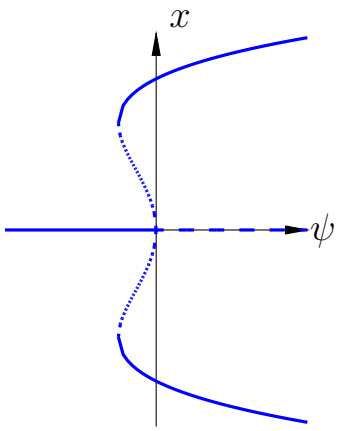


**Fig. 3.4**

## 3.5 Transcritical solution

The normal form for the transcritical bifurcation is:

$$f(x;\psi) = \psi x - x^2$$

Again, besides the trivial solution, the stability of which is given by the sign of $\psi$, we have one additional solution $x_f = \psi$, which is unstable for negative $\psi$, and stable for positive $\psi$. The stability diagram thus makes it clear how 'stabilities' are exchanged at the bifurcation point $(x;\psi) = (0,0)$.

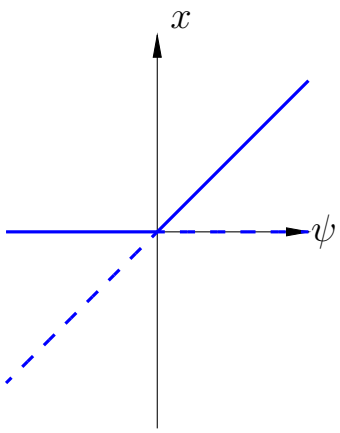


**Fig. 3.5**

## 3.6 Summary of the bifurcations on the line

- ▷ saddle node: two fixed points collapsing and annihilating each other
- ▷ transcritical: two fixed points exchanging stability
- ▷ supercritical fork : one fixed point losing stability, sending trajectories towards two adjacent fixed points.
- ▷ subcritical fork : one fixed point losing stability, but nearby solutions (which were unstable) also vanish. Trajectories will generally reach more remote fixed points.

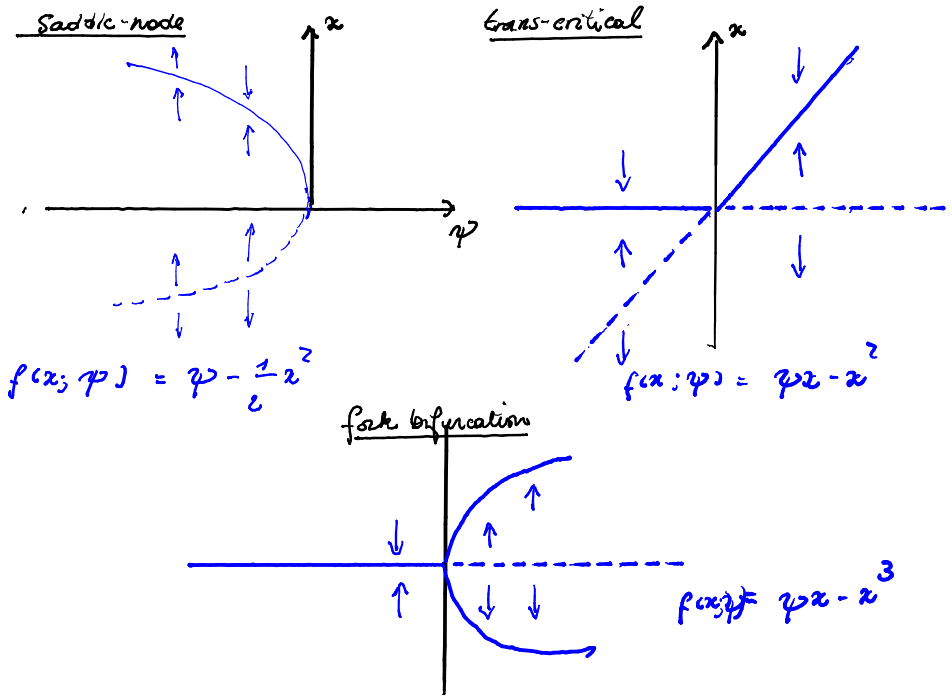


## CLASS ROOM DISCUSSION 9

Think of physical examples corresponding to these bifurcations.

# 4 Vector fields on the plane: stable and unstable manifolds



## 4.1 Linear fields on the plane

### 4.1.1 General solution

We consider the vector field defined in $\mathbb{R}^2 \to \mathbb{R}^2$, with $\boldsymbol{x} \in \mathbb{R}^2$.

Before we start anything, we will have to define the notion of invariant set.

**DEFINITION 8 Invariant set**

A set $S$ is said to be invariant *under the vector field* $\dot{\boldsymbol{x}} = \boldsymbol{f}(\boldsymbol{x}, t)$ if for any $\boldsymbol{x}_0 \in S$, its trajectory $\boldsymbol{x}(t, t_0, x_0) \in S$ (see def. of trajectory in sect. 2.1)

Technically, much of what follows here actually applies to *invariant manifolds*, which are invariant sets that that are locally differentiable (you can describe them locally as a vector space). We will not insist on this difference here. Note that, by definition, an *orbit* is an invariant set, but an invariant set is not necessarily an orbit.

Now, this chapter is specifically dedicated to linear, autonomous dynamical systems. In other words, they can be written in matrix notation:

$$\dot{\boldsymbol{x}} = A\boldsymbol{x}.$$

The flow associated with such linear fields are linear diffeomorphisms (the space is deformed continuously and linearly).

The Jordan canonical form theorem tells [1] us that, if $A$ is a real two by two matrix, there is a non-singular real matrix $T$ such that $A = TJT^{-1}$, and $T$ is made of two columns with vectors $\boldsymbol{u}$ and $\boldsymbol{v}$. Depending on the eigenvalue and eigenvectors of $A$, $J$ will be of one of three forms:

- *Case A*: Two independent eigenvectors ($\boldsymbol{u}$ and $\boldsymbol{v}$), real eigenvalues : $J = \begin{pmatrix} \lambda_1 & 0 \\ 0 & \lambda_2 \end{pmatrix}$;
- *Case B*: Complex eigenvalues $\lambda_r \pm i\omega$: $J = \begin{pmatrix} \lambda_r & \omega \\ -\omega & \lambda_r \end{pmatrix}$;
- *Case C*: A single independent eigenvector ($\boldsymbol{u}$), with one single real eigenvalue $J = \begin{pmatrix} \lambda & 1 \\ 0 & \lambda \end{pmatrix}$.

Geometrically, $T$ is the composition of a rotation, dilation and reflection around the origin. Vectors $\boldsymbol{u}$ and $\boldsymbol{v}$ are not necessarily orthogonal. We only have this guarantee when the matrix $A$ is symmetric.

### 4.1.2 Hyperbolicity

**DEFINITION 9 Hyperbolic fixed point.**

A fixed point is hyperbolic if all the eigenvalues of $\mathrm{D}f(x_f)$ have either a strictly positive or a strictly negative real part.

We will be able to *prove* that a fixed point with all *negative* eigenvalues (said to be linearly stable) is asymptotically stable. But we leave it for later. At this point, we already know enough to understand the idea of sink and source:

[1] More on this D.1. The relevant intuition is that the original space is deformed and rotated so that the vectors $\boldsymbol{u}$ and $\boldsymbol{v}$ are aligned on the $x-$ and $y-$axes. We can see this as follows. The original equation $\dot{\boldsymbol{x}} = A\boldsymbol{x}$ can be rewritten as $T^{-1}\dot{\boldsymbol{x}} = JT^{-1}\boldsymbol{x}$. So this is an linear equation with operator $J$ for the vector $T^{-1}\dot{\boldsymbol{x}}$. When $\boldsymbol{x}$ is $\boldsymbol{u}$, then $T^{-1}\boldsymbol{x} = (1\ 0)^\mathsf{T}$ (verify this by multiplying both sides by $T$ and replace $\boldsymbol{x}$ by $\boldsymbol{u}$; the index $\mathsf{T}$ on the right-hand-side is there to denote a column matrix).

1. A hyperbolic fixed point is called a *sink* if all eigenvalues of the Lyapunov spectrum have negative real parts.
2. A hyperbolic fixed point is called a *source* if all eigenvalues of the Lyapunov spectrum have positive real parts.
3. A hyperbolic fixed point is called a *saddle* if some but not all eigenvalues of the Lyapunov spectrum have positive real parts
4. A non-hyperbolic fixed point with purely imaginary eigenvalues, and non-zero is a *center*.

### 4.1.3 Case A: Real eigenvalues and linearly independent eigenvectors : invariant manifolds and linear transient growth

The general solution to the ordinary differential equation is

$$\boldsymbol{x}(t) = C_1 e^{\lambda_1 t}\boldsymbol{u} + C_2 e^{\lambda_2 t}\boldsymbol{v},$$

where $\boldsymbol{u}$ and $\boldsymbol{v}$ are the eigenvectors, and $\lambda_1$ and $\lambda_2$ the respective eigenvalues.

The fixed point $(0, 0)$ is asymptotically attracting if it is a hyperbolic fixed point with $\lambda_{1,2} < 0$. Furthermore, for an initial condition along the eigenvector $\boldsymbol{u}$, that is, $\boldsymbol{x}_0 = \alpha\boldsymbol{u}$, the particular solution is $\boldsymbol{x} = \alpha e^{\lambda_1 t}\boldsymbol{u}$. In other words, in the particular case of an initial condition along an eigenvector, the orbit is a line.

In other words, the lines defined respectively by $\alpha\boldsymbol{u}$ and $\beta\boldsymbol{v}$, $\alpha, \beta \in \mathbb{R}$ have a special property: if you are on the line. They are invariant sets and given that we are in a 2-D domain, these lines effectively partition the state space. If a trajectory is born on one side of the set, it remains there.

At this point we can already have some intuitive grasp on what is going on. Some of these lines are associated with an exponentially growing solution (the associated $\lambda$ is positive): This is an *unstable* manifold. Some, to the contrary, bring you asymptotically to the fixed point

$(0,0)$. They are *stable*. Whether they are stable or unstable depends on the eigenvalue.

$\lambda_1 < \lambda_2 < 0$

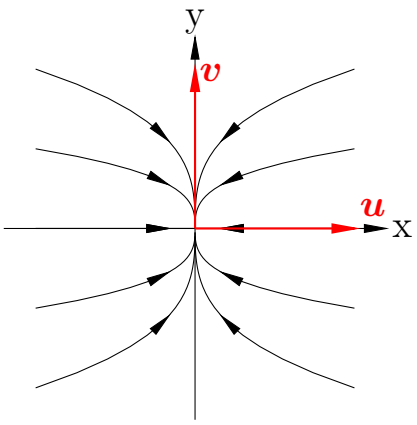


**Fig. 4.1**

However, these are particular cases: even when both eigenvalues are real, the orbit is *not* a line. Consider the case of a hyperbolic sink $(\lambda_1, \lambda_2 < 0)$. One can view that $-\lambda_1$ and $-\lambda_2$ act as the inverse of attracting time scales. For example, $|\lambda_1| \gg |\lambda_2|$ imply that the trajectory will be quickly attracted towards the $u-$component of the trajectory will vanish quickly, so that it will be quickly attracted towards the manifold associated with the second eigenvalue. The $\beta\boldsymbol{v}$ will act as a *slow manifold*.

A further counter-intuitive behaviour may occur in the case $\boldsymbol{u}$ and $\boldsymbol{v}$ are non-orthogonal. As the $u$-component quickly vanishes (in this example), the *norm* of the vector

$$\boldsymbol{x}(t) = C_1 e^{\lambda_1 t}\boldsymbol{u} + C_2 e^{\lambda_2 t}\boldsymbol{v},$$

may display a *transient growth*. This phenomenon, called *non-normal growth* is common in fluid dynamics and has been suggested to be important in the early phases of the dynamics of the ocean-atmosphere phenomenon El-Nino [2].

[2] Von der Heydt and Dijkstra, https://dspace.library.uu.nl/bitstream/handle/1874/314407/naw5_2013_14_3_195.pdf?sequence=1

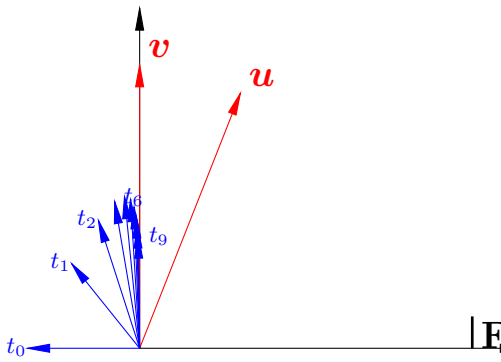


**Fig. 4.2**

### 4.1.4 Case B: Complex eigenvalues : spiral and center

The eigenvectors associated with the matrix form $B$ are $(1, i)$ and $(1, -i)$ $i = \sqrt{-1}$. Thus, the general solution reads (with $x$, $y$ the components of the solution):

$$\begin{pmatrix} x \\ y \end{pmatrix} = Ae^{(\lambda_r + i\omega)t} \begin{pmatrix} 1 \\ i \end{pmatrix} + Be^{(\lambda_r - i\omega)t} \begin{pmatrix} 1 \\ -i \end{pmatrix}$$

Requiring $x$ and $y$ to be real imposes $2A = 2B = C = C_0 e^{i\phi_0}$, where $C \in \mathbb{C}$ and $C_0$, $\phi_0 \in \mathbb{R}$.

We then observe that $x + iy$ behaves as a complex phasor $\mathbf{q}$, with amplitude growing or shrinking exponentially depending on the sign of $\lambda_r$, and rotating clockwise with $\omega$:

$$\mathbf{q} = x + iy = Ce^{\lambda_r} e^{-i\omega t}$$

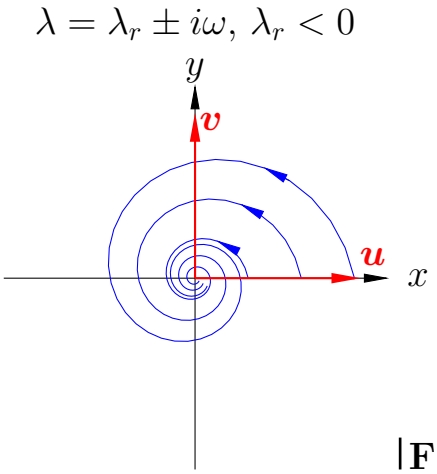


**Fig. 4.3**

Two more examples:

The frictionless, linear harmonic oscillator is defined by (after a suitable choice of length unit):

$$\begin{pmatrix} \dot{q} \\ \dot{p} \end{pmatrix} = \begin{pmatrix} 0 & 1 \\ -\omega^2 & 0 \end{pmatrix} \begin{pmatrix} q \\ p \end{pmatrix}.$$

This is a typical example of linear vector field with purely imaginary eigenvalues $\lambda_{1,2} = \pm i\omega$, $i = \sqrt{-1}$.

With a development similar to above, the couple $q$ and $p/\omega$ can be interpreted as the real and imaginary parts of a same phasor $\mathbf{q}$ animated by a clockwise motion of constant radius

$$\mathbf{q} = q + i\left(\frac{p}{\omega}\right) = C_0 e^{-i\omega(t-\phi_0)},$$

where $C_0$ and $\phi_0$ are real and set by the initial condition:

## CLASS ROOM DISCUSSION 10

Can you see that you now have an *infinity* of orbits which can are arbitrarily far apart from each other ? Which are they ? How can you say that this property must be specific of non-dissipative systems ? (Class discussion sect. 2.5)

Now consider the slightly more realistic case of a harmonic oscillator with friction coefficient $\nu$, but for easier computation we assume a time-scale redimensionalisation such that $\omega = 1$:

$$\begin{pmatrix} \dot{q} \\ \dot{p} \end{pmatrix} = \begin{pmatrix} 0 & 1 \\ -1 & -\nu \end{pmatrix} \begin{pmatrix} q \\ p \end{pmatrix}$$

The eigenvalues are found with the characteristic equation $\lambda^2+\lambda\nu-1 = 0$. The eigenvalues are $\lambda = \frac{1}{2}(-\nu \pm \sqrt{\nu^2-4})$, which are complex conjugate with negative real part for $\nu < 2$. We anticipate a damped oscillation. We still use the convention $\lambda = \lambda_r \pm i\omega$, with $\lambda_r$ and $\omega$ real.

The general solution is now:

$$\mathbf{q} = \left(q + \frac{\lambda_r}{\lambda_r^2+\omega_e^2}\right) + i\left(p\frac{\omega_e}{\lambda_r^2+\omega_e^2}\right) = C_0 e^{\lambda_r t} e^{-i(\omega_e t - \phi_0)}.$$

This *dissipative oscillator* is thus associated with a non-hyperbolic fixed point that is a *center*, asymptotically attracting, with *spiraling* trajectories. The phase-space interpretation is a bit less straigtforward than in the harmonic oscillator because the real and imaginary parts of the phasor are not just $q$ and $p$ but an affine transformation of them. This is the affine transformation which was needed to give the matrix a canonical form.

### 4.1.5 Case C: Jordan form matrix

In this case, the general solution of the trajectories is $\boldsymbol{x}(t) = (C_1 e^{\lambda t} + C_2 t e^{\lambda t})\boldsymbol{u} + C_2 e^{\lambda t}\boldsymbol{v}$. Again, $\boldsymbol{u}$ and $\boldsymbol{v}$ are the columns of the matrix $T$ needed to bring $A$ into canonical form (here, for illustration, they are orthogonal, but they do not need be.

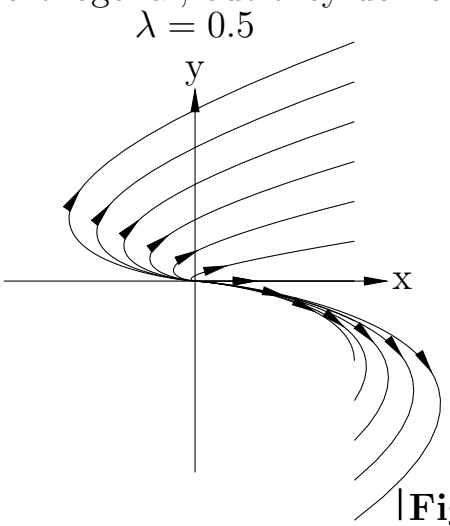


**Fig. 4.4**

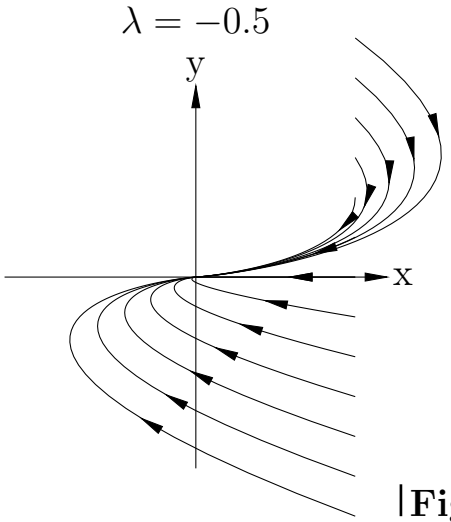


**Fig. 4.5**

**CLASS ROOM DISCUSSION 11**

Can you see that for linear fields to generate bounded trajectories within $\mathbb{R}^2$, fixed points must be either hyperbolic sinks, or centers? Sources will generate trajectories flowing to infinity.

## 4.2 Non-linear vector fields in the plane

### 4.2.1 Topological equivalence with the linearised system around hyperbolic fixed points

As we see now, non-linear dynamics are needed to combine hyperbolic sources with bounded behaviour, which, in the plane, will typically generate attracting orbits. We will review at a later stage the dynamics of attracting orbits, but for the moment we would like to take advantage of what we have learned about hyperbolic sources and sinks in the linear regime. The theory allows us to show that *near* a hyperbolic fixed point, the non-linear flows behaves *like* a linear system with the same eigenspectrum.

To get there, we start with an example that, unusual fact, can be solved analytically.

$\dot{x} = x + y^2,$
$\dot{y} = -y.$

The fixed point is $(x_0, y_0) = (0, 0)$. Writing, more generically, the system as:

$\dot{x} = f(x, y),$
$\dot{y} = g(x, y)$

we find that we can *linearise* the system as follows (writing $x' = x - x_0 = x$):

$$\dot{x} = f(x_0, y_0) + \left.\frac{\partial f}{\partial x}\right|_{(x_0,y_0)} x' + \left.\frac{\partial f}{\partial y}\right|_{(x_0,y_0)} y' + N_x(x, y), \tag{7}$$

$$\dot{y} = g(x_0, y_0) + \left.\frac{\partial g}{\partial x}\right|_{(x_0,y_0)} x' + \left.\frac{\partial g}{\partial y}\right|_{(x_0,y_0)} y' + N_y(x, y), \tag{8}$$

where $N_{x,y}$ include all the non-linear terms. The *tangent linear system is*, per definition:

$$\dot{x} = f(x_0, y_0) + \left.\frac{\partial f}{\partial x}\right|_{(x_0,y_0)} x' + \left.\frac{\partial f}{\partial y}\right|_{(x_0,y_0)} y',$$

$$\dot{y} = g(x_0, y_0) + \left.\frac{\partial g}{\partial x}\right|_{(x_0,y_0)} x' + \left.\frac{\partial g}{\partial y}\right|_{(x_0,y_0)} y',$$

or, written in a more compact form, and considering that, by definition of the fixed point, $f(x_0, y_0)$ and $g(x_0, y_0) = 0$:

$$\begin{pmatrix} \dot{x} \\ \dot{y} \end{pmatrix} = \mathrm{D}_{(f,g)}(x_0, y_0) \begin{pmatrix} x \\ y \end{pmatrix},$$

with $\mathrm{D}_{(f,g)}(x_0, y_0)$ the Jacobian of $(f, g)$ evaluated at the fixed point. In the specific example chosen here,

$$\mathrm{D}_{(f,g)}(x_0, y_0) = \begin{pmatrix} 1 & 0 \\ 0 & -1 \end{pmatrix}.$$

It is already diagonal, with eigenvectors along the $x$ and $y$ axes, and eigenvalues $\lambda_1 = 1$ and $\lambda_2 = -1$. The phase portrait is thus fairly straightforward:

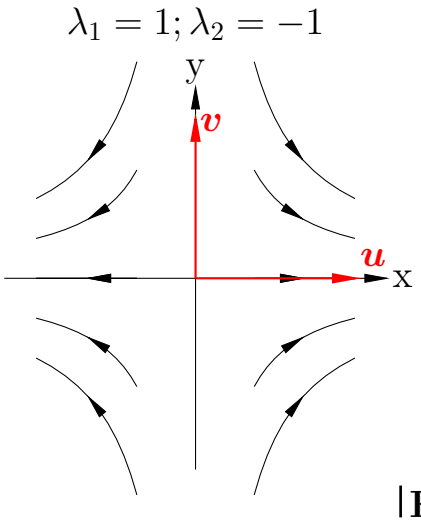


**Fig. 4.6**

You identify without much difficulty the stable and unstable manifolds.

Let us come back to our full system. The equation for $\dot{y}$ admits, as solution, $y(t) = C_2 e^{-t}$. Plugged into tho $\dot{x}$ equation, we have $\dot{x} = x + C_2^2 e^{-2t}$. The *homogeneous* equation $\dot{x} = x$ admits, as solution, $x^H(t) = C_1 e^t$. One approach for finding a particular solution to the inhomogeneous system is to make the constant variable, that is try $C(t)$ in lieu of $C_1$:

$$\begin{aligned} \dot{C}e^t &= C_2^2 e^{-2t}, \\ \Leftrightarrow C(t) &= -\frac{1}{3} C_2^2 e^{-3t}, \\ \Leftrightarrow x^I(t) &= -\frac{1}{3} C_2^2 e^{-2t}. \end{aligned}$$

The general solution is thus $x(t) = C_1 e^t - \frac{1}{3} C_2^2 e^{-2t}$.

Starting from any point $(x_0, y_0)$ at time $t = 0$, we have $C_2 = y_0$, $C_1 = x_0 - \frac{1}{3} y_0^2$.

In particular, if $y_0 = 0$, then $y(t) = 0$ and $x(t) = x_0 e^t$. Hence, along the $x$ axis, the system behaves *exactly* as the linear system (!). The

line $y = 0$ is the unstable (invariant) manifold.

Now, contrary to the linearised system, the line $x_0 = 0$ is *not* an invariant manifold, as, starting from $x_0 = 0$,

$$x(t) = -\frac{1}{3}y_0^2(e^t + e^{-2t}).$$

However, if we are a tiny bit smarter and arrange for $C_1$ to be 0, that is, $x_0 - \frac{1}{3}y_0^2 = 0$, then the system evolves as:

$$x(t) = -\frac{1}{3}y_0^2 e^{-2t},$$
$$y(t) = y_0 e^{-t},$$

on which the relationship $x_0 - \frac{1}{3}y_0^2 = 0$ is maintained. In other words, the curve defined by $x = \frac{1}{3}y^2$ is the stable invariant manifold.

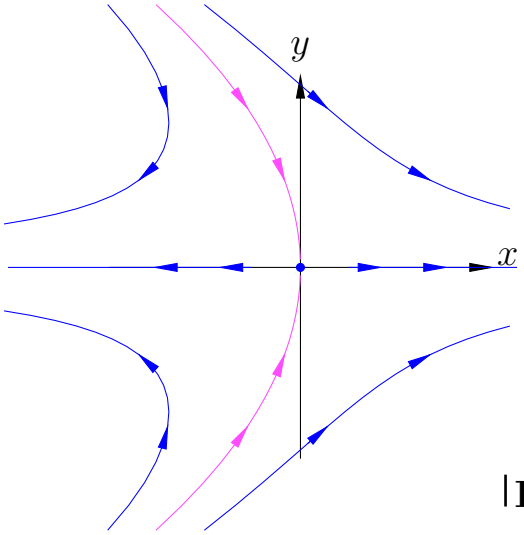


**Fig. 4.7**

With this particular non-linear system, about which we could find the analytical solution, we observe that the invariant manifolds of the

linear system are *tangent* and have the same stability characteristics as those of the linear tangent system. This is great news, because it suggests that we can learn quite a great deal about the non-linear system from inspection of the much simpler linear system, near the fixed point.

This is not *always* the case, as demonstrated by the following example:

$$\dot{x} = -y + ax(x^2 + y^2), \tag{9}$$
$$\dot{y} = x + ay(x^2 + y^2). \tag{10}$$

Lacking time, full inspection of the system is left as an exercise, but rushing through the lessons to be learned here, one would find that the *non-linear* system spirals downwards or upwards depending on the value of $a$ (negative or positive), while the *linear system* is the Hamiltonian system that we have already studied above and admits circular orbits.

So what is the trouble here? The key for establishing a qualitative equivalence between a linear and a non-linear system is the *hyperbolic* character of the fixed points, as established by the Hartman-Grobman theorem (1959 and 1960):

**THEOREM 7 Hartman-Grobman theorem**

Consider $p = (0,0)$ a *hyperbolic* fixed point of the ordinary differential equation $\dot{\boldsymbol{x}} = \boldsymbol{f}(\boldsymbol{x})$, $\boldsymbol{x} \in \mathbb{R}^2$, and $\boldsymbol{f} \in \mathbf{C}^k(\mathbb{R}^2), k \geq 1$. Then, there is a neighbourhood $B$ around $\boldsymbol{p} = (0,0)$ and a homeomorphism $h : B \to R^2$ with $h(0,0) = (0,0)$ such that, $\forall \boldsymbol{x} \in B$, there is an interval $I \subset \mathbb{R}$ such that:

$$h \circ \phi^t(\boldsymbol{x}) = \bar{\phi}^t \circ h(\boldsymbol{x}), \quad \forall t \in I, \boldsymbol{x} \in B,$$

where $\phi^t$ is the flow of $\dot{\boldsymbol{x}} = \boldsymbol{f}(\boldsymbol{x})$ and $\bar{\phi}^t$ is the flow of the linearised system $\dot{\boldsymbol{x}} = \mathrm{D}_{(f,g)}(\boldsymbol{p})\boldsymbol{x}$.

It is said that the flows $\phi^t$ and $\bar{\phi}^t$ are *topologically conjugate*.

The topological equivalence between linearised systems and non-linear systems around the *hyperbolic* fixed points imply that we can predict the existence of stable and unstable invariant manifolds and their tangent directions, from inspection of the eigenvalues and eigenvectors of the Jacobian.

We have a *sink* if all eigenvalues are negative real parts, a *source* if they all have positive real parts, and a *saddle point* if some are negative and negative, provided that none is null in which case the fixed point is no longer hyperbolic. This theory, including the Hartman-Grobman theorem, works also for $n \geq 2$.

Specifically, we define:

**DEFINITION 10 Stable local manifold**

The stable local manifold around $p$ in the neighbourhood $B$ is

$$S_B = \left\{ x \in B : \phi^t(x) \in B \forall t \geq 0 \right\}.$$

Similarly,

**DEFINITION 11 Unstable local manifold**

The unstable local manifold around $p$ in the neighbourhood $B$ is

$$U_B = \left\{x \in B : \phi^{-t}(x) \in B \forall t \geq 0\right\}.$$

Because of the way the definition is put, fixed points (even if they are saddle points or sources) belong to both the local stable and unstable manifolds. This is a bit counter-intuitive, so pay attention to this.

### 4.2.2 Stable-unstable manifolds theorem

Let us see one more consequence of the Hartman-Grobman theorem.

If $p$ is a (hyperbolic) sink, then there must be a neighbourhood $B$ around $p$ such that $S_B = B$ and $U_B = \{p\}$. Can you see this? Indeed, in this neighbourhood, the flow is topologically conjugate to that of the linearised system. We now that it is a *sink*, attracting from all directions. The stable manifold *is* the whole neighbourhood. But as we have just seen, $\{p\}$ must also belong to the unstable manifold.

If $p$ is a (hyperbolic) source, then, $U_B = B$ and $S_B = \{p\}$.

We will now formulate an important theorem, not demonstrated here, that will allow us to obtain more information about the shape of the stable and unstable manifolds around the fixed points.

**THEOREM 8 Stable and unstable manifolds theorem**

Consider $\boldsymbol{f} : \mathbb{R}^2 \to \mathbb{R}^2$, a diffeomorphism $\in \mathbf{C}^k$, $k \geq 1$, and $p = (0,0)$ a *hyperbolic* equilibrium of the ordinary differential equation $\dot{\boldsymbol{x}} = \boldsymbol{f}(\boldsymbol{x})$, such that

$$\mathrm{D}\boldsymbol{f}(p) = \begin{pmatrix} \lambda_1 & 0 \\ 0 & \lambda_2 \end{pmatrix}, \quad \text{with } \lambda_1 < 0 < \lambda_2.$$

Then, $\exists \varepsilon > 0$ and $B = ]-\varepsilon, \varepsilon[ \times ]-\varepsilon, \varepsilon[$ such that:

- $S_B = \{(x, s(x)) \text{with} x \in ]-\varepsilon, \varepsilon[\}$ where $s(x)$ is $\mathbf{C}^k$ and $s'(0) = 0$;
- $U_B = \{(u(y), y) \text{with} y \in ]-\varepsilon, \varepsilon[\}$ where $u(y)$ is $\mathbf{C}^k$ and $u'(0) = 0$;

Let us put this in plain text. If we have a hyperbolic saddle, then there is a neighbourhood where the stable manifold through the point has a functional form, tangent to the axis corresponding to the stable direction of the linearised system; and there is a *also* a neighbourhood where the unstable manifold has a functional form, tangent to the axis corresponding to the unstable direction of the linearised system. It results from this theorem that the stable and unstable manifolds are locally orthogonal to each other.

The consequences are pretty wild. Indeed, suppose again that the system has been put such that the eigenvectors correspond to the $x$ and $y$ axes (as above), with $x = 0$ (the $y-$axis) the unstable manifold through the origin.

Then, we can as we have done already linearise the system:

$$\begin{aligned} \dot{x} &= \lambda_1 x + N_x(x, y), \\ \dot{y} &= \lambda_2 y + N_y(x, y). \end{aligned} \tag{11}$$

The non-linear terms contain second-order terms and more, so by definition $\lim_{(x,y)\to(0,0)} \frac{N_{x,y}(x,y)}{x^2+y^2} = 0$.

So, consider now $(x(t), y(t))$ an orbit of the stable manifold that passes through $x, s(x)$. It must remain on the stable manifold, and we find that $y(t) = s(x(t))$. We can re-write system (11) as follows:

$$\begin{aligned} \dot{x} &= \lambda_1 x + N_x(x, s(x)), \\ \dot{x}s'(x) &= \lambda_2 s(x) + N_y(x, s(x)). \end{aligned} \tag{12}$$

Combining both equations to eliminate time (the $\dot{x}$ term), you get

$$s'(x)(\lambda_1 x + N_x(x, s(x))) = \lambda_2 s(x) + N_y(x, s(x)) \tag{13}$$

Similarly, for the unstable form, you would get:

$$(\lambda_1 u(y) + N_x(u(y), y)) = u'(y)(\lambda_2 y + N_y(u(y), y)) \tag{14}$$

We will now show how we can use these developments. Consider again the system that we have been playing with already, but we just swap the $x$ and $y$ directions to comply with the condition $\lambda_1 < 0 < \lambda_2$:

$$\begin{aligned} \dot{x} &= -x, \\ \dot{y} &= y + x^2. \end{aligned}$$

Thus, $N_x(x, y) = 0$, $N_y(x, y) = x^2$. We had the solution, and we know that $s(x) = -\frac{1}{3}x^2$, but as we said above, it is unusual to be able to find

it analytically. So suppose we don't know it. To this end, consider the differential equation for the stable manifold:

$$s'(x)(-x) = s(x) + x^2.$$

If we admit that $s$ is infinitely differentiable, and keeping in mind that its first-order derivative is null, then as a general rule we know that $s(x) = \sum_{k=2}^{\infty} s_k x^k$. Substituting in the differential equation, that makes

$$-x \sum_{k=2}^{\infty} k s_k x^{k-1} = x^2 + \sum_{k=2}^{\infty} s_k x^k.$$

Identifying terms for the different orders, one by one, we get $-2s_2 = s_2 + 1$ and $-ks_k = s_k$ for $k \geq 3$. The only solution is $s_2 = -\frac{1}{3}$ and $s_k = 0$ for $k \geq 3$.

As an exercise, you could find that, for

$$\dot{x} = x + y^3$$
$$\dot{y} = -y + 2xy + x^2,$$

we have:

$$u(x) = \frac{1}{3}x^2 + \frac{1}{6}x^3 + \frac{1}{15}x^4 + \mathcal{O}(x^5)$$
$$s(y) = -\frac{1}{4}y^3\mathcal{O}(y^5)$$

Attention, there is a small difficulty: the roles of $x$ and $y$ are inverted compared to the theory above (in other words: $\lambda_2 < 0 < \lambda_1$. The trick is just to rename $y^\star = x$ and $x^\star = y$ and then rename back when finished.

The graph below represents sample orbits (red) and the approximate stable and unstable manifolds (blue), the computed stable and unstable manifolds (green), and the flow direction (arrows)

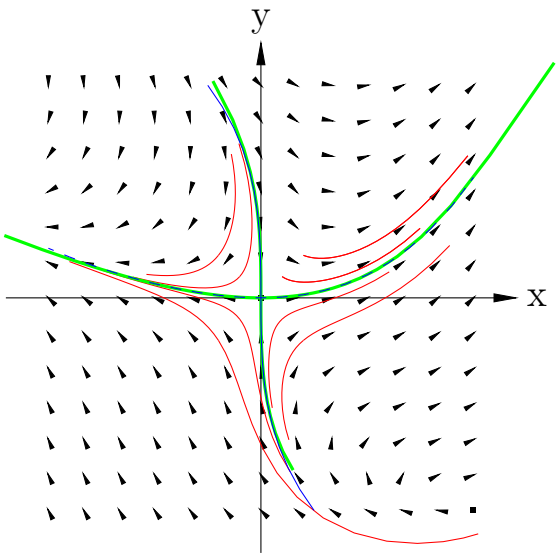


**Fig. 4.8**

# 5 Trapping regions, attracting sets and attractors



## 5.1 Lyapunov functions

The method of Lyapunov functions can be used to determine the stability of fixed points when the information obtained from the linearisation is inconclusive (e.g. non-hyperbolic fixed points). As noted by [Wig03, Chap. 2], the Lyapunov theory is a large area, and we examine here a very small part of it. Furthermore, while it is presented here in a chapter about vector fields in $\mathbb{R}^2$, it is in fact valid in any dimension, but so much easier to visualise on the plane.

The basic idea is to find, in a neighbourhood of the fixed point, a function of the state that is positive, zero at the fixed point, and known to decay strictly monotonously over time. In which case, quite intuitively, the fixed point is asymptotically stable.

More specifically, consider the following vector field:

$$\begin{aligned}\dot{x} &= f(x,y)\\ \dot{y} &= g(x,y), \quad (x,y) \in \mathbb{R}^2,\end{aligned}$$

with fixed point $(x_f, y_f)$. Let $V(x,y)$ a scalar-valued function on $\mathbb{R}^2$ that is at least $\mathbf{C}^1$, such that $V(x_f, y_f) = 0$.

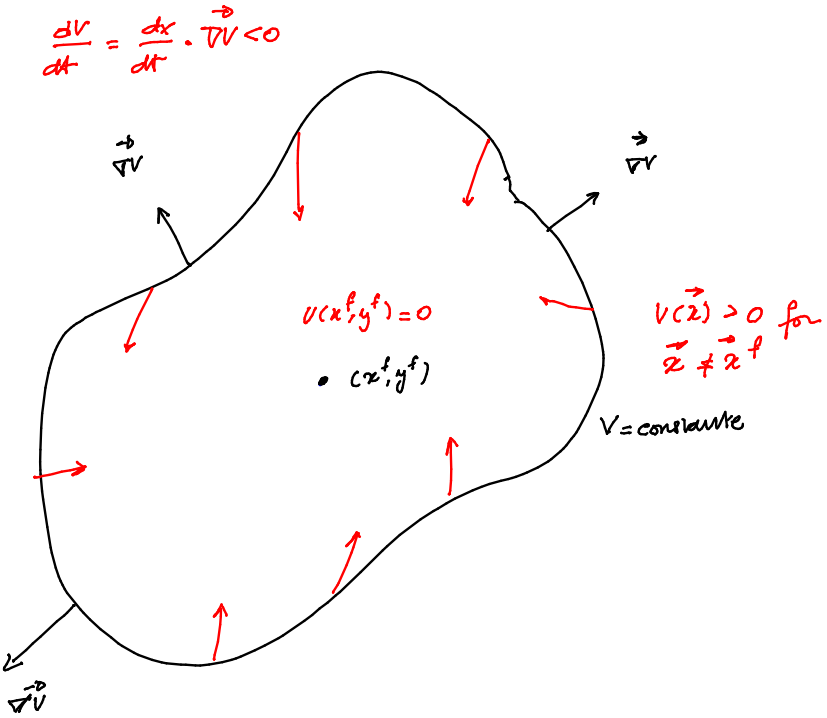


Suppose also that the locus of points satisfying $V(x, y) = C$ (constant) forms closed curves for different values of $C$ encircling $(x_f, y_f)$. Now, recall that the gradient of $V$, $\nabla V$, is a vector perpendicular to the tangent of the curves, pointing to the direction of increasing $V$. If this vector is always pointing outwards (decreasing values of $C$ as we get closer to $(x_f, y_f)$, then we get $\nabla V(x, y) \cdot (\dot{x}, \dot{y}) \leq 0$. Now we can state the general theorem

**THEOREM 9** **Existence of Lyapunov function implies stability**

In the conditions stated above, with $V(x_f, y_f) = 0$ and $V(x, y) > 0$ if $(x, y) \neq (x_f, y_f)$, there exists a neighbourhood $U$ around $(x_f, y_f)$ such that:

- ▷ $\dot{V}(x, y) \leq 0$ in $U \backslash \{(x_f, y_f)\}$ : $(x_f, y_f)$ is stable
- ▷ $\dot{V}(x, y) < 0$ in $U \backslash \{(x_f, y_f)\}$ : $(x_f, y_f)$ is *asymptotically* stable

Although quite intuitive, the proof is not quite straightforward and will only be discussed during the lecture time permitting. It is available in [Wig03], p. 24.

More insightful for the physicist is the physical meaning attached to $V$. In a conservative (Hamiltonian system), the Hamiltonian would actually satisfy the definition of a Lyapunov function, although this is a limit case, where $\dot{V}(x, y) = 0$. In a thermodynamic system, then the Free energy (at constant temperature) or the Gibbs free energy (at constant pressure) work as Lyapunov functions. In the simpler case of a near Hamiltonian system (e.g. pendulum with friction), then the potential + kinetic energy $V$ satisfy the definition of a Lyapunov function near the fixed point.

Hence, we seem to have a good method for proving the stability of a fixed point; in practice, finding $V$ is not always as straightforward as in the cases above. There is no miracle receipt.

## 5.2 Trapping regions and attracting sets

Again, the evolution of the Lyapunov function must be (strictly) monotonous in a neighbourhood of the fixed point. The latter may be arbitrarily small to satisfy the mathematical definition of an asymptotically stable fixed point, though of course, for physical significance, we might want a large neighbourhood !

Indeed, as we see it, a contour $C$ within which $\dot{V}(x, y) \leq 0$ will effectively define a *trapping region*, that is defined as a region that contains all its future states.

**DEFINITION 12 Trapping region**

A trapping region $U$ relative to a diffeomorphism is a compact [^2] set such that $\phi^t(U) \subset U \ \forall t > 0$.

[^2:] A compact set is closed (in contains the limit of its converging sequences), and bounded. A dense disc (with its boundary) and a ring are two examples of closed sets in $\mathbb{R}^2$.

The property $\phi^t(U) \subset U \ \forall t > 0$ is the property of *positive invariance*. Thus, a trapping region is a compact positive invariant set. As we move time forward, the trapping region, which keeps containing itself, can be made smaller and smaller until it asymptotically becomes the *attracting set*:

**DEFINITION 13 Attracting set**

An attracting set is a closed invariant set that can be defined as $\bigcap_{t>0}^{\infty} \phi^t(U)$.

3

On the other hand, the *basin* of attraction relative to the attracting set $A$ is the set of initial conditions that eventually falls into it, and it can be recovered by travelling backwards in time.

[3] Wiggins requires the set $U$ to be open but not Guckenheimer and Holmes 1983

**DEFINITION 14 Basin of attraction**

The basin of attraction (or *domain*) of an attracting set $A$ is $\bigcup_{t\leq 0}^{\infty} \phi^t(U)$, where $U$ is an open neighbourhood acting as a trapping region leading to $A$. The alternative (equivalent) definition is $\bigcup_{t\geq 0}^{\infty} \phi^{-t}(U)$.

Below is an example of basins of attractions of two sinks. The sinks act as two individual *attracting sets*. We will later identify this dynamical system as the Duffing oscillator.

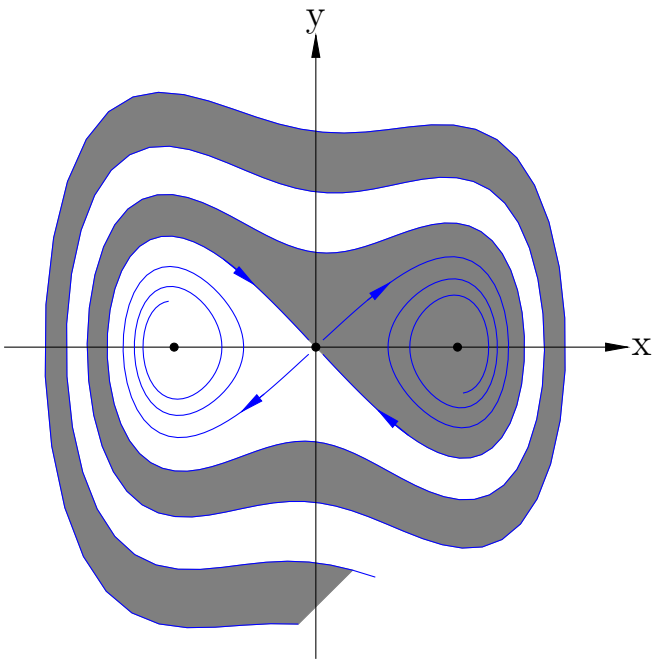


**Fig. 5.1**

## 5.3 The attractor as a topologically transitive attracting set



Intuitively, the attracting set is related to the asymptotic destination of orbits starting within its basin of attraction. But perversely, it does not quite work.

Consider the following system:

$$\dot{x} = x - x^3,$$
$$\dot{y} = -y.$$

We have a saddle at $(0, 0)$ and two stable fixed points at $(\pm 1, 0)$. We can define a trapping region as an ellipse encompassing the three fixed points. It turns out the whole compact interval $[-1, 1]$ on the $x$ axis is the attracting set obtained from that trapping region. Indeed, for any point $p$ on the segment, and for *any* time $t$, you can find an initial condition (close enough to the unstable fixed point, presumably) within the attracting set (it is indeed invariant) that reaches $p$ precisely at time $t$. So this interval is really the limit of self-evolving trapping regions. (see Figure)

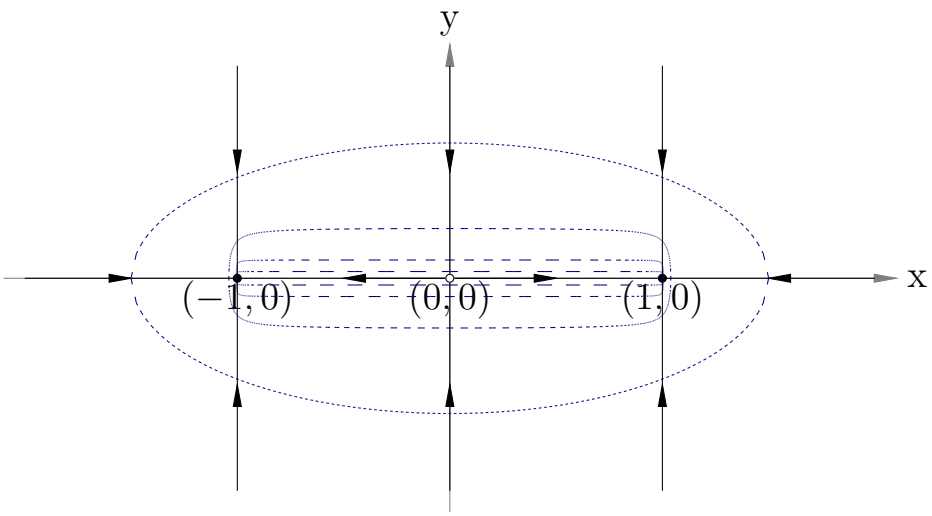


**Fig. 5.2**

But clearly this is not the idea that we might have of an attractor. Technically, we say that the attracting set that we obtained in the above example contains many "wandering points". Such point leave definitively their own neighbourhood as time continues, so we do not want to say that they are part of an "attractor". When you are on such points, you do not stay there.

There are different ways to mend the above definition and better capture the notion of attractor. The literature on this topic is not always very easy to follow. One approach is to require topological transitivity.

**DEFINITION 15 Attractor**

An attractor $A$ is an attracting set that is topologically transitive. In relaxed terms, it means that you always find an orbit that goes from one arbitrary (open) set of $A$ to another one.

In other words, and to make it short, when you are on the attractor, you will pass near all of its points in a finite amount of time.

Another approach is to require the attracting set to be *minimal*, i.e., it does not include any subset that is also an attracting set:

**DEFINITION 16 Attractor (alt.)**

An attractor is a minimal attracting set.

In the above example, both will generate the same result: we have two attractors, one on $(1, 0)$, and one on $(-1, 0)$. There is yet another approach, as we now see.

## 5.4 Limit set

The notion of attractor is very much linked to the notion of limit set, which considers the asymptotic behaviour of *individual* orbits.

**DEFINITION 17 $\omega$ limit points of a trajectory**

A point $x_0$ in the domain of dynamical system is called an $\omega$ *limit point* of $x$ if there exists a sequence $\{t_i\}$, $t_i \to \infty$, such that $\phi^{t_i}(x) \to x_0$.

In other words, there is a sequence of times, towards infinity, that brings asymptotically the state towards this limit point. If we reverse the direction, and flow backwards, then $x_0$ is called an $\alpha$ limit point.

We see the idea: a trajectory could flow asymptotically from the $\alpha$ (time $-\infty$) to the $\omega$ (time $+\infty$).

By extending the notation, we will note $\omega(p)$ as the set of limit points of orbits passing through $p$, and $\omega(U)$ the *limit set of* $U$ which contains the union of the $\omega(p)$ for all $p \in U$.

It can be proved (Wiggins, Proposition 8.1.3.) that within a trapping region, all points $p$ (thus, in the trapping region) can be attached to a limit set that is non-empty, closed, invariant under the flow, and connected.

Hence, we could also have defined an attractor as a topologically transitive set $A$ that admits a neighbourhood $U$ such that $\omega(U) = A$. This definition of the attractor can also be found in the literature, and I need more research to determine to what extent these different definitions overlap / are compatible / can contradict each other.

A final note about the notion of the Lyapunov function. We need to confess that we have been a little bit brutal. Indeed, we first defined the Lyapunov function as being defined on a *neighbourhood* around a fixed point. It had to be zero on the fixed point, and organised such that the flow points inwards the iso-contour of the Lyapunov function, in this neighbourhood.

Now, later in this chapter, we admitted that finding a Lyapunov function is also a good approach for determining a trapping region. To this end, we implicitly relaxed the condition that we have a fixed point. We just need iso-contours with the flow pointing inwards. As we will see, this helps us to see also the kind of solutions we expect within the trapping region.

## CLASS ROOM DISCUSSION 12

To anticipate a bit on what is coming, consider the following configuration:

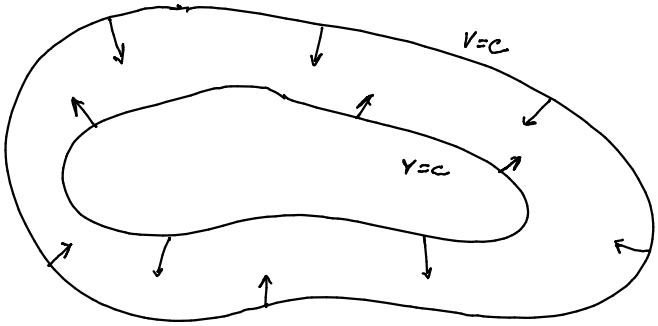


The two iso-contours, of same value, define a trapping region. What sort of scenario do we expect there? Perhaps your intuition already foresees some possibilities: either orbits land on a fixed point, either they keep looping around a so-called "limit cycle"... or ?

The Poincaré-Bendixson theorem, which we will see in section the possibilities

# 6 Periodic orbits

## 6.1 The van der Pol oscillator



Consider the following dynamical system.

$$\dot{x} = y$$
$$\dot{y} = \alpha(y - y^3/3 - x)$$

We consider first the regime $\alpha \gg 1$ (in the illustration below, we have used $\alpha = 10$). Defining $\varepsilon = 1/\alpha$, it is equivalent to write the second equation:

$$\varepsilon\dot{y} = (y - y^3/3 - x),$$

In the limit of small $\varepsilon$ the left-hand-side term vanishes, so that, to first approximation, $y$ behaves such as to satisfy the diagnostic equation $y - y^3/3 - x = 0$. This equation defines the nullcline. For any reasonable value of $x$, $y$ will run such as to satisfy this equation.

Hence, to get a first grasp on this system, we may consider that $x$ varies slowly, and $y$ equilibrates with respect to a slowly varying $x$, which effectively behaves as a parameter. We then recognise a first-order differential equation with, as we will show, two fold bifurcations with respect to $x$.
Indeed, the equation $y - y^3/3 - x = 0$ has three roots for $-1 \leq x \leq 1$, and only one out of this interval. Within the three-root regimes, the middle root corresponds to an unstable equilibrium and the upper and lower branches correspond to sinks of this fast system. Again, view $x$ as a parameter, and one will find two fold bifurcations for $x = \pm 1$.

Suppose that $x = 0$ and that the system is on the upper branch. The fast variable $y$ is positive, and because of the first equation of the full system ($\dot{x} = y$), $x$ must increase slowly. The fast variable $y$ keep tracking the upper branch, until it reaches the fold bifurcation. At this point $y$ runs away (it has lost its equilibrium), until it falls on the lower branch. Then $y < 0$, and $x$ reverses direction. The fast variable $y$ tracks the lower branch, until, again, it finds a fold bifurcation. We have just found an example of attractor that is a limit cycle, characteristic of a slow-fast *relaxation* oscillator.

It is a *stable* limit cycle in the sense that it is a periodic orbit, that is reached *asymptotically* as time moves forward, and which effectively acts (and is) an attractor.

The limit cycle persists outside the slow-fast regime, and $y$ then moves more softly from negative to positive values.

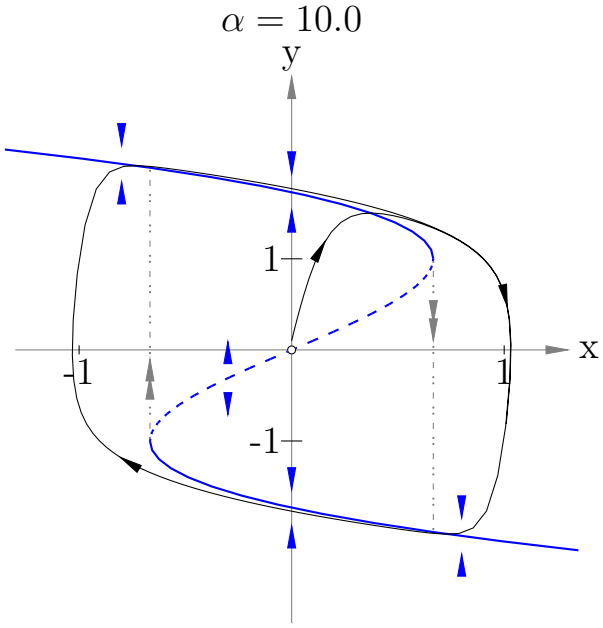


**Fig. 6.1**

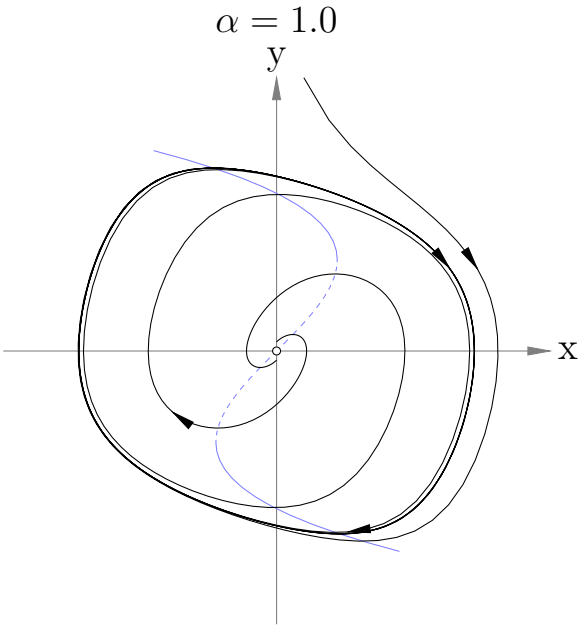


**Fig. 6.2**

## 6.2 Bendixson's criterion

Consider again a flow on the plane, defined by:

$$\begin{aligned} \dot{x} &= f(x,y), \\ \dot{y} &= g(x,y), \quad \text{with } f \text{ and } g \text{ at least } \mathbf{C}^1 : \end{aligned} \tag{15}$$

**DEFINITION 18 Periodic orbit**

A solution of (15) through the point $x_0$ is said to be periodic of period $T$ if there exists $T > 0$ such that $x(t) = x(t+T)$ (assuming the initial condition $x_0$), which is equivalent to saying $\phi^T(x) = x$ on this orbit.

**THEOREM 10 Bendixson's criterion**

If, on a simply connected region $\mathcal{D} \subset \mathbb{R}^2$, the expression $\frac{\partial f}{\partial x} + \frac{\partial g}{\partial y} := \boldsymbol{\nabla} \cdot (f, g)$ is not identically zero and does not change sign, then the system has no closed orbit lying entirely in $\mathcal{D}$.

This can be proved as a consequences of Green's theorem on the plane. Assume an orbit with contour $\Gamma$ actually exists in the domain $\mathcal{D}$.

Note then that the path integral $\int_\Gamma f\,\mathrm{d}y - g\,\mathrm{d}x = 0$:

$$\oint_\Gamma f\,\mathrm{d}y - g\,\mathrm{d}x = \int_0^T (f\dot{y} - g\dot{x})\,\mathrm{d}t = \int_0^T (fg - gf)\,\mathrm{d}t = 0.$$

On the other hand, because of the divergence theorem [4]

$$\oint_\Gamma \hat{\mathbf{n}} \cdot (f, g)\,\mathrm{d}s = \int_{\mathcal{S}} \left(\frac{\partial f}{\partial x} + \frac{\partial g}{\partial y}\right) \mathrm{d}\mathcal{S},$$

where $\hat{\mathbf{n}}$ is the normalised, outward pointing vector orthogonal to the path.

The left-hand-side term is the contour integral we just computed (you must use: $\hat{\mathbf{n}}\,\mathrm{d}s = (\mathrm{d}y, -\mathrm{d}x)$). It is zero. The second term can only be zero if the divergence is either identically null, or changes sign. □

The Bendixson theorem can be generalised so that is also works by monitoring $\frac{\partial(Bf)}{\partial x} + \frac{\partial(Bg)}{\partial y}$ for any $B(x, y)$ of class $\mathbf{C}^1$. The generalisation is due to Henri Dulac.

[4] The equivalent approach is to simply consider Green's theorem that states that $\oint_\Gamma \frac{\partial f}{\partial y} - \frac{\partial g}{\partial x}\,\mathrm{d}s = \int_{\mathcal{S}} \left(\frac{\partial f}{\partial x} + \frac{\partial g}{\partial y}\right) \mathrm{d}\mathcal{S}$.

## CLASS ROOM DISCUSSION 13

Check that the Duffing oscillator[a]

$$\begin{cases} \dot{x} = y, \\ \dot{y} = x - x^3 - \gamma y \end{cases}$$

has no closed orbit for $\gamma \neq 0$.

[a]The definition of the Duffing oscillator involves $\gamma \geq 0$, but this is not needed here.

The next example (taken form Wiggins, sect. 4.1) shows how the Bendixson' criterion allows us to restrict regions in the plane where closed orbits *might* exist. Consider this modification of the Duffing oscillator:

$$\begin{cases} \dot{x} = y \\ \dot{y} = x - x^3 - \gamma y + x^2 y, \quad \gamma \geq 0. \end{cases}$$

The equation has three fixed points at $(x, y) = (0, 0)$, $(\pm 1, 0)$, with the eigenvalues $\lambda_{1,2}$ given by the following expressions:

$$\begin{aligned} (0,0) \Rightarrow \lambda_{1,2} &= \frac{-\gamma}{2} \pm \frac{1}{2}\sqrt{\gamma^2 + 4}, \\ (1,0) \Rightarrow \lambda_{1,2} &= \frac{-\gamma + 1}{2} \pm \frac{1}{2}\sqrt{(-\gamma + 1)^2 - 8}, \\ (-1,0) \Rightarrow \lambda_{1,2} &= \frac{-\gamma + 1}{2} \pm \frac{1}{2}\sqrt{(-\gamma + 1)^2 - 8}. \end{aligned}$$

Thus, $(0, 0)$ is a saddle, and $(\pm 1, 0)$ are sinks for $\gamma > 1$ and sources for $0 \leq \gamma < 1$. Furthermore, we find

$$\frac{\partial f}{\partial x} + \frac{\partial g}{\partial y} = -\gamma + x^2.$$

Thus, the divergence vanishes on the lines $x = \pm\sqrt{\gamma}$. These two lines divide the plane into three regions which we label $R_1$, $R_2$ and $R_3$. We cannot have any closed orbit in this regions, but we *cannot* rule out orbits which would overlap these regions.



It is possible to restrict the possibilities further with the *index theory* but at this point of writing the notes, it is not yet clear we have time to cover this theory in the context of this course.

## 6.3 The Hopf bifurcation

We will now explore *one* mechanism by which orbits emerge. Consider again the van der Pol oscillator, in the regular regime (not slow fast), but with an extra bifurcation parameter called here $\beta$ (and $\alpha = 1$):

$$\dot{x} = y - \beta$$
$$\dot{y} = (y - y^3/3 - x)$$

We study the stability of the fixed point $(\beta - \beta^3/3, \beta)$ with the Jacobian:

$$D_{f,g}(\beta - \beta^3/3, \beta) = \begin{pmatrix} 0 & 1 \\ -1 & 1 - \beta^2 \end{pmatrix}$$

which admits, as eigenvalues

$$\lambda_{\pm} = \frac{1 - \beta^2 \pm \sqrt{\beta^4 - 2\beta^2 - 3}}{2};$$



as we see it, the real part of the eigenvalues vanish for $\beta = \pm 1$, at which point $\lambda_{\pm} = \pm i$.

In summary, we have three regimes:

- ▷ for $|\beta| \geq \sqrt{3}$: two negative, real eigenvalues;
- ▷ for $1 < |\beta| \leq \sqrt{3}$: two complex-conjugate eigenvalues with negative real part;
- ▷ for $|\beta| < 1$: two complex-conjugate eigenvalues with positive real part.

The fixed point is a source in the third regime, which generates trajectories spiraling outwards, and reaching the limit cycle described in the first section.

The transition from negative to positive real values with imaginary parts is the signature of a Hopf (or Andronov-Hopf) bifurcation.

Rushing through the theory, it may be shown that if some generic non-degeneracy conditions are met (specifically, the first Lyapunov exponent near the limit cycle is non-zero [5], and the derivative of the real part of the eigenvalue is non-zero at the equilibrium), it may be shown that systems with a Hopf bifurcation are locally topologically equivalent to the following normal form, with $\sigma$ either equal to 1 or $-1$ (topological equivalence may imply a rescaling of time):

[5] but we haven't defined it, yet; no panic

$$\dot{x} = \beta x - y + \sigma x(x^2 + y^2)$$
$$\dot{y} = x + \beta y + \sigma y(x^2 + y^2)$$

The bifurcation is found at $\beta = 0$.

The system of equations may be rewritten in polar coordinates[6]% , in which case we find

$$\dot{r} = \beta r + \sigma r^3,$$
$$\dot{\theta} = 1.$$

The equation for $r$ is the normal form for the pitchfork bifurcation on the line. Consider first the trivial fixed point for $r$, $r = 0$. It is stable for $\beta < 0$. The zero fixed point is stable for $\beta < 0$. The radius $r$ admits a second fixed point when the sign of $\sigma$ and $\beta$ are opposite to each other.

- ▷ ( $\sigma = -1$) : In the *supercritical* bifurcation, one finds a stable limit cycle (fixed point for $r$) for positive values of $\beta$, and growing as $(\sqrt{\beta})$. In other words, the limit cycle grows from zero and reaches a finite amplitude as $\beta$ increases.
- ▷ ( $\sigma = 1$) : In the *subcritical*, an *unstable* limit cycle exists in the negative domain of $\beta$, and then disappears as $\beta$ is positive. That is, for positive $\beta$, the only invariant form is the unstable fixed point.

As we see it, the Hopf bifurcation is a *local* mechanism for the generation of a limit cycle. It is local, because it emerges out of the loss of

[6]Conversion in polar coordinates is covered in the exercises. If $x = r\cos\theta$, $y = r\sin\theta$, then $r^2 = x^2 + y^2$ and $\tan\theta = y/x$, from which it follows that $2r\dot{r} = 2y\dot{x} - 2x\dot{y}$ and $\dot{\theta}/\cos^2\theta = x\dot{y} - y\dot{x}/(r^2\cos\theta)$.

(local) stability of a fixed point. The imaginary part of the eigenvalue are finite, so that the new born orbit, near the bifurcation point, is generally associated with a finite period. It will definitely be associated with a finite period if the bifurcation is supercritical; what happens with a subcritical bifurcation is less certain because the system moves out of the domain of fixed point. What happens is not predicted by the normal form: higher order terms must be taken into account. It may land on a fixed point or, more likely, on another limit cycle. A typical scenario is obtained when the unstable limit cycle for negative $\beta$ regains stability and continues towards positive values of $\beta$, in which case the period of the stable limit cycle is often not very different from that of the unstable limit cycle near the bifurcation point.

Similar to what we have found when studying pitchfork bifurcations (section 3.4.2), adding a fourth-order term produces stable limit cycles to land on:

$\dot{r} = \beta r + r^3 - r^5$.

Determining whether a given Hopf bifurcation is subcritical or supercritical can be a tedious process, especially if you can't find a polar-coordinate expression that can then be transformed into a normal form. In practice, bifurcation software (AUTO, MATCONT) can do this for you. Furthermore, criteria have been worked out for specific dynamical systems [e.g. Kuz23, section 3.5].

For example, it may be shown that for the generic form :

$\dot{x} = a(y - b)$
$\dot{y} = F(y) - x$

the sign of $\sigma$ is given by $F'''$ at the bifurcation point. It is here *negative*, so we have a *supercritical* Hopf bifurcation. The above equation gives the FitzHugh-Nagumo equation ($\alpha = 1$) with $F(y) = y - y^3/3$, and

the van der Pol oscillator by furher setting $b = 0$.

Below the limit cycles found in the van der Pol oscillator with $\alpha = 1$, for $\beta = 0.98$ (grey), $\beta = 0.95$ (black), $\beta = 0.9$ (blue) and $\beta = 0.8$ (green). We recognise the (reasonably) smooth growth of the cycle as $\beta$ gets away from the bifurcation point, as predicted by the theory.



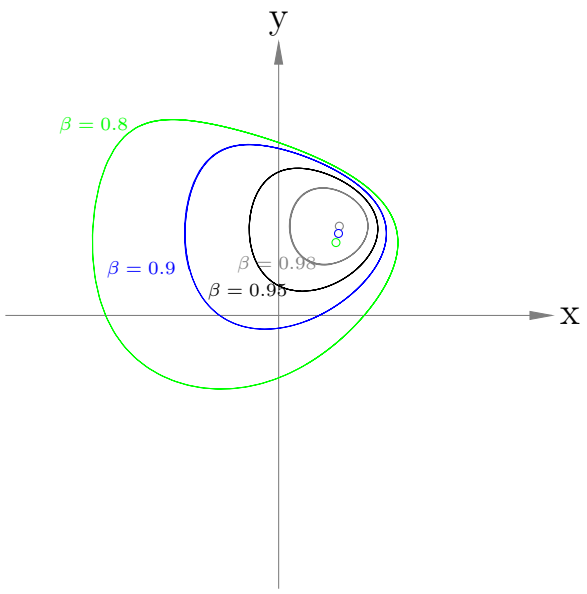


**Fig. 6.3**

In some more pathological cases, however, the limit cycle may grow quite quickly and reach saturation, even though the bifurcation is supercritical. This is a case of supercritical, explosive Hopf bifurcation. This is found in the above case, but in the slow-fast regime, with $\alpha \gg 1$. The behaviour of Hopf bifurcations is slow-fast systems is a field of research on its own, and gives rises to curious orbits termed "Canard".

The case for $\beta = 0.98$, $\alpha = 10$ is shown below, for illustration

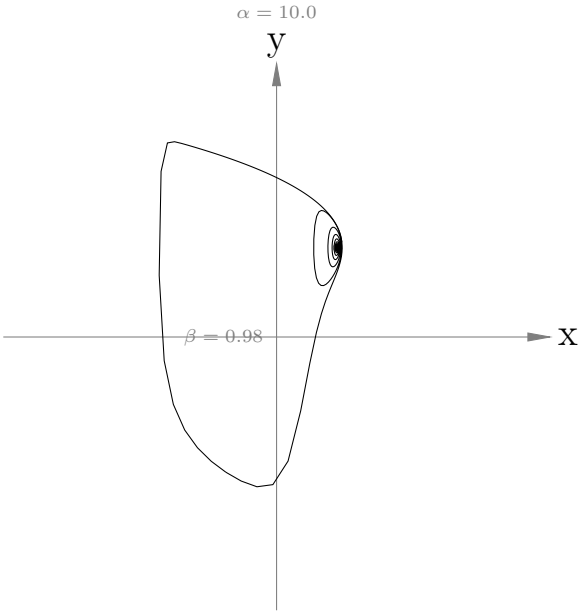


**Fig. 6.4**

# 7 Still on the plane: Beyond periodic orbits

## 7.1 The Poincaré - Bendixson theorem



Remember that we have defined the limit set of an orbit (more precisely, the limit set of a point of an orbit, but that is equivalent) as the set of points that are asymptotically reached as time goes forward ($\omega$-limit set), or backwards ($\alpha$-limit set).

So far we have met two types of limit sets in the plane: fixed points (if it is a $\omega-$fixed point, it is also an attractor), and limit cycles (think of the van der Pol oscillator which we have seen). We have defined the limit set of a whole region $U$, as the union of all limit sets associated with all points in this region. On the other hand, we have defined the attractor as a minimal attracting set: the notion of "attraction" is very much focused on the idea of a neighbourhood that get smaller and smaller as times goes by.

So we could reasonably guess that the notion of limit cycle and the notion of *attractor* are similar. In fact, attractors *are* limit sets. However the reverse may not necessarily be true. Hence, we need a strategy: an approach that allows us to make an account of all possible limit sets. In this enterprise, we have two friends. The first one is the concept of trapping region, that is closely related to the Lyapunov function. If there is a Lyapunov function — if we can draw isocontours (so called: level sets) that upper-bound the flow — then we know we have a trapping region. The second is a theorem: the Poincaré-Bendixson theorem.

In these notes, we will only provide the theorem result, and some elements of the proof will be given during the lecture. The proof is not exam material.

**THEOREM 11 Poincaré - Bendixson theorem**

Let $U$ a trapping region in the plane, containing a finite number of fixed points (it may be zero). The limit set of any point $p$ in $U$ is either

- ▷ one fixed point
- ▷ a closed orbit
- ▷ a finite number of fixed points $p_1 \dots p_n$ and orbits $\gamma$ linking these fixed points with $\alpha(\gamma) = p_i$ and $\omega(\gamma) = p_j$, $i, j \in 1 \dots n$.

A few observations before we get some ideas about how this theorem works. Observe first that it requires very few assumptions. All what we need is a trapping region in the plane, and not a infinite number of fixed points (we don't want a whole region or even a segment where $f(x, y) = 0$). The theorem tells us about limit sets, and it restricts the possible behaviours: we have either attractor points, limit cycles, or (that is the new stuff) homoclinic or heteroclinic orbits. The *homoclinic* orbit is one that links a fixed point to itself (asymptotically); the *heteroclinic* orbit links two fixed points. We will speak about those a bit later, and let us briefly explore the mechanics of the proof without, again, considering the details.

Two prove the Poincaré-Bendixson theorem, you need the concept of a *transverse* $\Sigma$ of the field. Think of it as a one-way section, with the flow crossing the transverse always from, say, the left to the right, without being ever tangent to the transverse. The transverse may not have any hole. Technically, it is defined a continuous, connected arc. We also use the concept of *positive* orbit through $p$, which is the set of points met by the trajectory after it has gone through $p$.

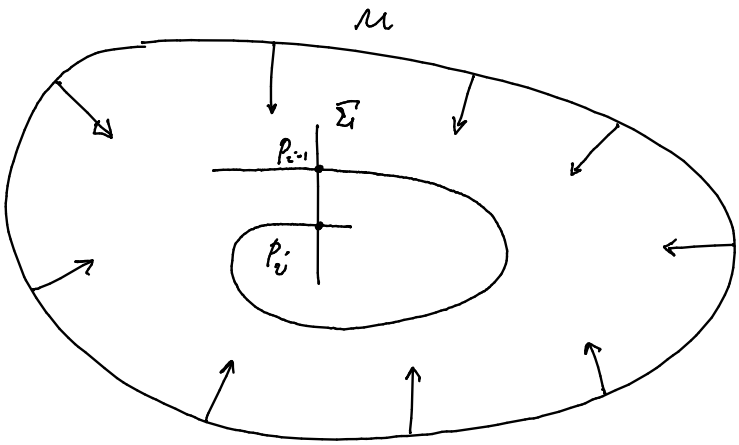


Then, the proof goes on by steps:

- ▷ *Lemma 1*: the positive orbit through $p$ cuts the transverse $\Sigma$ in a monotone sequence of $p_i$ (the points of the intersection are ordered on the sequence). (The Lemma is proved by constructing a positively invariant region)
- ▷ *Lemma 2*: The limit set of $p$ crosses $\Sigma$ at at most one point. (this is a consequence of the monotonous character of the sequence of $p_i$)
- ▷ *Lemma 3*: If $\omega(p)$ contains *no* fixed point, then it is a closed orbit. This is the vanilla-version of the Poincaré-Bendixson theorem. It is proved by contradiction. To make it short and a bit rough, we take $q \in \omega(p)$ and draw a section such that $q$ is on it. Given that $q$ is *not* a fixed point, it crosses the section, and it has a positive orbit that will cut the section through a monotone sequence. But

as we now that $\omega(p)$ crosses the section at only one point, the monotone sequence is made of $q$ only. This is a closed orbit.

- ▷ *Lemma 4* : if $p_1$ and $p_2$ are distinct fixed points contained in $\omega(p)$; then there exists at most *one* orbit linking asymptotically $p_1$ ($\alpha$-point) from $p_2$ ($\omega$-point). The proof is made by contradiction. The idea is that the orbit passing by $p$ would need to pass nearby $\gamma_1$ and $\gamma_2$, two hypothetical distinct orbits. We consider two transverses that are linking our hypothetical orbit with $\gamma_1$ and $\gamma_2$ and observe that it produces a topological absurdity (you can't both get nearby the two orbits at two distinct times, and have both of them as limit sets).



We now show how to use this theorem, with examples.

## 7.2 The Duffing Oscillator

$$\begin{aligned} \dot{x} &= y \\ \dot{y} &= x - x^3 - \gamma y \end{aligned} \tag{16}$$

A perhaps more intuitive way to view it is to substitute the first equation into the second, that is:

$$\ddot{x} = x - x^3 - \gamma \dot{x};$$

We see then a down-potential movement with friction coefficient $\gamma$, with the potential $V = x^4/4 - x^2/2$. We have quite obviously a good starting point for a Lyapunov function. The equivalent of the Hamiltonian, in this system, would be $H = V + y^2/2$ and, indeed, we have:

$$\begin{aligned}\dot{x} &= \frac{\partial H}{\partial y} \\ \dot{y} &= -\frac{\partial H}{\partial x} - \gamma y\end{aligned} \tag{17}$$

- ▷ In the frictionless case $\gamma = 0$, $\dot{H} = 0$. All solutions are iso-curves of $H$.
- ▷ In the friction case, $\dot{H} = -\gamma \dot{x}^2$. It is monotonously decaying, indicating that the constant-$H$ orbits defined in the frictionless case have become trapping regions.



**CLASS ROOM DISCUSSION 14**

Draw the graph of $H$ and discuss the implications of the Poincare-Bendixson theorem

## 7.3 An example showing the existence of periodic orbits

Consider now:

$$\begin{aligned}\dot{x} &= y + \frac{1}{4}x(1 - 2r^2); \\ \dot{y} &= -x + \frac{1}{2}y(1 - r^2), \quad \text{with } r^2 = x^2 + y^2.\end{aligned} \tag{18}$$

Equilibria impose, by the equation for $\dot{y}$, $x = \frac{1}{2}y(1 - r^2)$, which, after substitution in the equation for $\dot{x}$ gives

$$0 = y(9 - 3r^2 + 2r^4)$$

As the polynomial $(9 - 3r^2 + 2r^4)$ has no real root, $(0, 0)$ is the only equilibrium. On the other hand, if we transform the equation into the polar coordinates $(x, y) = r(\cos\theta, \sin\theta)$, and compute $\dot{r} = \frac{1}{r}(\dot{x}, \dot{y}) \cdot (x, y)$, we find:

$$\dot{r} = \frac{1}{4}r(1 + \sin^2\theta) - \frac{1}{2}r^3.$$

As $0 \leq \sin^2\theta \leq 1$, we have the order relationship

$$\frac{1}{4}r - \frac{1}{2}r^3 \leq \dot{r} \leq \frac{1}{2}r(1 - r^2).$$

In other words,

- $\dot{r} > 0$ (for any $\theta$) for $\frac{1}{4}r - \frac{1}{2}r^3 > 0$, that is, $r < \sqrt{2}/2$, and
- $\dot{r} < 0$ (for any $\theta$) for $r(1 - r^2) < 0$, that is, $r > 1$.

Can you see that we have defined a trapping region without any fixed point?

## 7.4 Periodic orbits in the Liénard systems

Liénard systems are named according to Anne-Marie Liénard, 1869–1958, and can be seen as a generalisation of the Van der pol oscillator:

$$\ddot{y} + f(y)\dot{y} + y = 0,$$

which appears as a harmonic oscillator under a friction $f(y)\dot{y}$. We further assume that $f(y) = F'(y)$ with $F'(0) = 0$.

- ▷ $F(-y) = -F(y)$, equivalent to $f(-y) = f(y)$
- ▷ $\lim_{y\to\infty} F(y) = \infty$, and $\exists\beta : F(y)$ is strictly growing for $y > \beta$;
- ▷ $\exists\alpha : F(y) < 0$ for $0 < y < \alpha$

The system is equivalently written as $\ddot{y}+\dot{F}(y)+y = 0$. Further defining $x \stackrel{\text{def}}{=} \dot{y} + F(y)$, we find the first-order system:

$$\dot{x} = -y$$
$$\dot{y} = x - F(y)$$

so that we recover the Van der pol system for $F(y) = y^3/3 - y$ (compared to the definition we have given in section 6.1 the sign of $y$ is inverted). We now consider the Lyapunov function candidate $H(x, y) = \frac{1}{2}(x^2 + y^2)$. We find that

$$\dot{H} = -yF(y)$$

Remember that iso-contours of $H$ are circles. It is reasonably clear that any iso-$H$ with a radius $r < \alpha$ ejects trajectories out of that circle, since $\dot{H}$ will be positive.

Finding a *trapping region* is a much more difficult exercise. The demonstration, e.g., available in [Per01], sect. 3.8 is quite accessible but requires attention. The demonstration below is based on [Per01] with some variations.

First, observe that the differential for $H$ can be written in different equivalent forms:

$$\mathrm{d}H = -yF(y)\,\mathrm{d}t, \tag{19a}$$
$$\mathrm{d}H = F(y)\,\mathrm{d}x, \tag{19b}$$
$$\mathrm{d}H = \frac{-yF(y)}{x - F(y)}\,\mathrm{d}y \tag{19c}$$



Next, we construct an orbit (call it $\gamma(x_0)$) that starts somewhere from the right hand side of $x-$axis, at $x = x_0$. Call this starting point $p_1$. Given the Liénard equations, we know that at its starting point, $\dot{x} = 0$, thus it is tangential to the orbit, and it will remain negative as long as $y$ is positive. For visual aid, we also draw the $x = F(y)$ curve. On this curve, $\dot{y} = 0$, so the path must be horizontal when it crosses it. These observations make it necessary that the orbit will cross again the $x$ axis on the left-hand-side. Call it $p_4$. Because of the symmetry of the equations with respect to $y$, a mirrored orbit exists on the negative side of $y$.

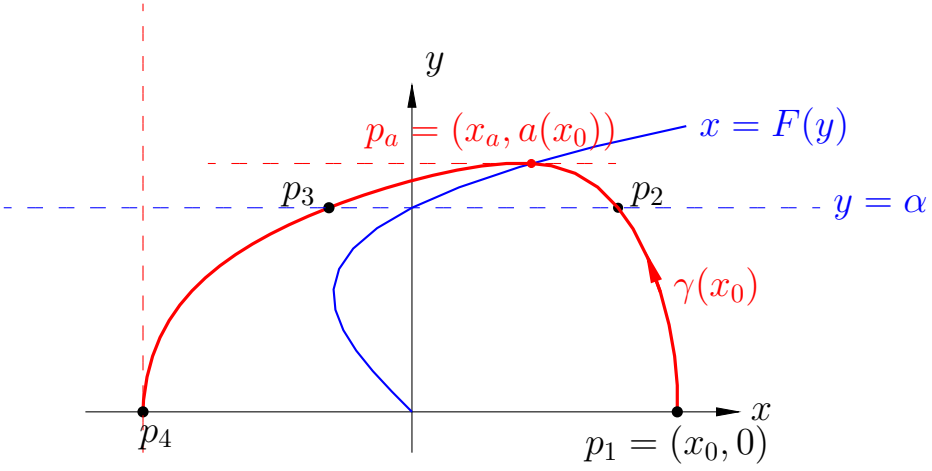


**Fig. 7.1**

Because of this, if $H(p_4)$ was equal to $H(p_1)$, then we would have a closed orbit. But this is generally not the case.

We call the point at which the orbit intersects the $x = F(y)$ curve $p_a$

and its $y-$value $a(x_0)$. We make it explicit that $a$ depends on the initial condition $x_0$. We further expect $a(x_0)$ to depend monotonously on $x_0$ because different orbits cannot cross each other. We are interested in the quantity $\Delta H(x_0) := H(p_4) - H(p_1) = \int_{\gamma(x_0)} \mathrm{d}H$. This is where we will be able to exploit the different differential forms of $H$. Remember that we have imposed $F(\alpha) = 0$, with $F$ negative below, and positive above $\alpha$ (and $F$ is anti-symmetric).

First, if $a(x_0) < \alpha$ (the horizontal red curve below the horizontal blue curve on the Figure), then the path $\gamma$ remains in the negative domain for $F$. Exploiting the differential form (19b) (and $\mathrm{d}x < 0$), it comes out that $\Delta H$ is positive. This is consistent with the ejecting character of iso-$H$ curves of small radius. We had already noted this.

For $x_0$ large enough (that is, $a(x_0) > \alpha$), we are able to decompose the path in 3 chunks, $\gamma_{p_1p_2}$, $\gamma_{p_2p_3}$ and $\gamma_{p_3p_4}$, defined by the intersection with the $y = \alpha$ curve. Exploiting again the differential form (19b), the $\Delta_{p_1p_2} = \int_{\gamma_{p_1p_2}} \mathrm{d}H$ and $\Delta_{p_3p_4} = \int_{\gamma_{p3p4}} \mathrm{d}H$ are both positive. We are interested in knowing how $\Delta_{p_1p_2}$ and $\Delta_{p_3p_4}$ evolve as $a(x_0)$ increases. When $a(x_0)$ increases, both paths $\gamma_{p_1p_2}$ and $\gamma_{p_3p_4}$ are shifted towards the exterior. We now exploit the differential form (19c). Within $p_1p_2$, the range of $y$ is not affected by the change in initial condition $x_0$, so that all terms in $y$ remain the same. But the denominator $x - F(y)$ has become, in absolute value, bigger, on both sides. So, both $\Delta_{p_1p_2}$ and $\Delta_{p_3p_4}$ *decrease* with $a$, but will never be negative.

Now, let us come to $\Delta_{p_2p_3}$. Exploiting differential form (19b) makes it clear that that integral $\Delta_{p_2p_3}$ is negative. What happens when $a(x_0)$ grows? The path $\gamma_{p_2p_3}$ grows bigger, with its lateral boundaries $p_2$ and $p_3$ shifted towards the exterior, and the path $\gamma_{p_2p_3}$ lies entirely in the $F(y) > 0$ domain. Exploiting the differential form (19b) shows that $\Delta_{p_2p_3}$ must *decrease* (increase, in absolute value) at least with order $\mathrm{d}x_0$. In other words, we expect $\Delta_{p_2p_3}(x_0)$ to decrease monotonously towards $-\infty$ as $x_0 \to \infty$. On the other hand, $\Delta_{p_1p_2}$ and $\Delta_{p_3p_4}$ decrease monotonously with $x_0$ but are bounded by zero.

In summary, $\Delta H(x_0)$ is positive for $a(x_0) < \alpha$. It decreases monotonously towards minus infinity as $a(x_0)$ increases. Thus, it *must* pass through one, single root. This is that root that *defines* the (unique) circular orbit. Call this critical point $x_0 = x^\star$.

Remember that the path we have constructed in the positive $y-$axis domain can be mirrored in the negative domain. For that reason, we can define an ejecting region by choosing $x_0$ such that $a(x_0) < a_0$, and a trapping region by choosing $x_0$ such that $a(x_0) > a_0$, and connecting paths such as shown on the graph below. We have demonstrated that the Liénard system admits one single attractor that is a closed orbit.

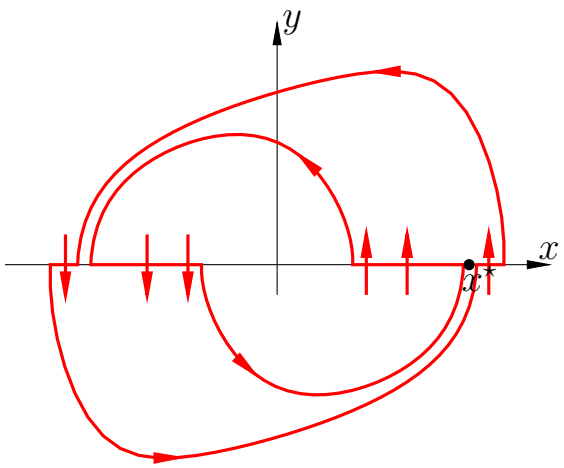


**Fig. 7.2**

## 7.5 Homoclinic orbits in the modified Duffing oscillator

We now consider the (somewhat artificial) system:

$$\begin{aligned} \dot{x} &= \frac{\partial H}{\partial y} + \lambda H \frac{\partial H}{\partial x}, \\ \dot{y} &= -\frac{\partial H}{\partial x} + \lambda H \frac{\partial H}{\partial y}. \end{aligned} \tag{20}$$



This time, $\dot{H} = \lambda H((\frac{\partial H}{\partial x})^2 + (\frac{\partial H}{\partial y})^2)$, still with $H = V(x) + y^2/2$, $V(x) = x^4/4 - x^2/2$ (do not confuse with the $H$ we used for Liénard systems). We have already studied the (conservative) $\lambda = 0$ case. If $\lambda \neq 0$, the fixed points $p(\pm 1, 0)$ and $p(0, 0)$ persist. The first two points are centres; the $p(0, 0)$ is a saddle. The iso-contours $H = C$ are generally not orbits, *except* the very particular case $H = 0$.

We now concentrate on the curves defined by $H = 0$, which separate negative (inside) from positive (outside) values.

- ▷ For $\lambda < 0$, we have trajectories reaching asymptotically one of the two homoclinic loops if they start *inside*, and revolve (slowly) around the homoclinic loops if they start outside. Homoclinic loops act as attractors. The period of the oscillation will increase to infinity as the trajectory approaches the homoclinic attractor.
- ▷ For $\lambda > 0$, we have trajectories reaching asymptotically one of the two centers if they start *inside*, and diverging if they start outside. Homoclinic loops act as repellers.

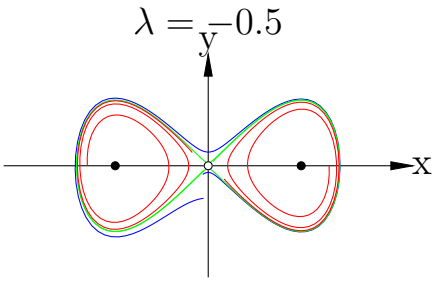


Fig. 7.3

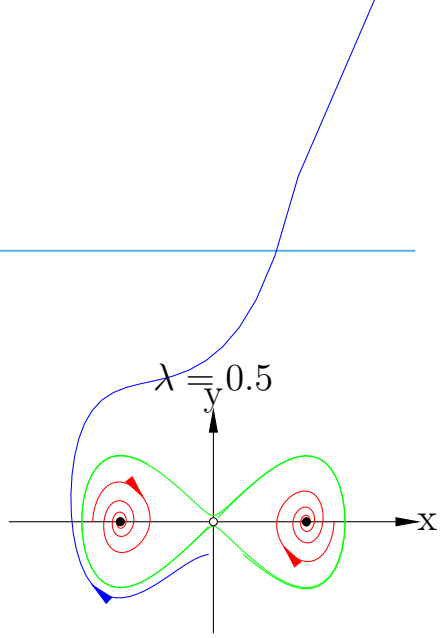


Fig. 7.4

## 7.6 Further remarks about periodic orbits

(these notes are for information only and not study material).

- A stable limit cycle is stable with respect to deviations orthogonal to the orbit, and neutrally stable in the direction of the orbits. This means that, for example if a particle which follows an orbit is suddenly slightly advanced with respect to its trajectory, it keeps its advance; the latter doesn't grow or shrink, on average, over time (the Lyapunov exponent is zero along the orbit). However, in certain cases, periodic orbits provide a structure to emerging chaotic behaviours. The Lorenz model seen in the next section can be, depending on the parameters, chaotic with an attractor made of 2 "wings" and within each wing 1 recognise almost-periodic behaviours. Before the transition to chaos, the attractor of the system is a periodic limit cycle. It can also be shown that after the transition to chaos, the attractor is structured around a large number of unstable periodic orbits. It is believed that unstable periodic orbits play a large role in the structure of the behaviour of some chaotic dynamical systems. The PhD theses if Oisin Hamilton is focused on these unstable periodic orbits in the atmosphere.
- Dynamical systems presenting periodic orbits are used to study a

large variety of natural phenomena: cycles in population dynamics and ecosystems, glacial-interglacial cycles, lasers... The study of bifurcations in such systems gives insight about how, qualitatively, cycles appear in nature and whether their appearance is expected to be explosive (sudden) or more gradual. There is also a vast field of study about how these phenomena behave when submitted to a periodic or a quasiperiodic forcing. Different phenomena may occur, including synchronisation and non-linear resonance. Coupled dynamical systems presenting periodic orbits with slightly different periods may also synchronise each other. A periodic forcing may also, if sufficiently large, cause a transition towards a chaotic behaviour (the Duffing oscillator can also easily be brought to chaos). All these behaviours are relevant for the study of natural phenomena.

- ▷ To study synchronisation and transitions to chaos caused by an external forcing, mathematicians have developed paradigmatic model of the limit cycle: circle flows [Str14] and circle maps [Hil00, sect 6.7], which brings points on the unit circle to points on the same unit cycle. The great advantage of the circle flow is to produce the idea of a limit cycle with only one equation, thus one degree of freedom, which allows to use all the methods and bifurcation theory valid on the line. The pattern of synchronisation of the limit cycle to an external forcing is associated with a diagram called the Arnold tongue diagram [Hil00, fig 6.9]. Circle maps have been used to study the synchronisation of glacial-interglacial cycles in [MCA15].
- ▷ Another paradigmatic model for the study of limit cycle is the delay equation. In this case, we have only one differential equation, but which bears the characteristic of using information of the system at the time $t$ minus a delay — which can make its resolution hard. This is this a quite specific kind of equation which has the property of generating periodic or quasiperiodic behaviours, and which has been used to study phenomena involved in lasers but also in climate science to study El-Nino phenomenon. Again,

complex behaviours are obtained because they do not require some many equations. There is a Wikipedia page on the subject.

- As the periodic limit cycle is so important in the study of natural phenomena, there is also field of study which attempts to construct attractors based on empirical timeseries. This approach falls into the domain of nonlinear time series analysis and it is partly justified by a theory called the embedding theorem of Takens [GAD+02].

# 8 Leaving the plane: The Lorenz model

## 8.1 The origins of the Lorenz 63 model



We will now meet the celebrated Lorenz attractor. The original article by [Lor63] is a follow up of a model of atmospheric convection written by [Sal62]. This original model of "Finite amplitude free convection" was used to solve an initial value problem to demonstrate the formation of "roll" convection between two free surfaces maintained at a constant temperature difference. Saltzman started from the so-called Oberbeck and Bussinesq equations to generate a set of *52* (!) ordinary differential equations of quadratic form (i.e., $\dot{X}_i = \sum_{j,k} C_{ijk} X_j X_k$). Saltzman viewed it as a *highly idealised model* meant to study the development of turbulence in the atmosphere.

This is an approach that has been generalised to different problems, for example accounting for Earth rotation and the interface between the oceans and the atmosphere. The PhD thesis of Oisin Hamilton, co-supervised by Stephanne Vannitsem at the Royal Meteorological Institute, and myself, uses a model of that sort of complexity.

However, 52 equations is still a lot for a qualitative analysis and Ed Lorenz proposed a further idealised version, with three equations only:

$$\begin{aligned} \dot{X} &= -\sigma X + \sigma Y, \\ \dot{Y} &= -XZ + \rho X - Y, \\ \dot{Z} &= XY - bZ. \end{aligned} \tag{21}$$

The system is presented as $X$ proportional to the intensity of convective motion, $Y$ proportional to the temperature difference between the ascending and descending currents, and $Z$ to the distortion of the temperature profile with respect to linearity, "a positive value indicating

that the strongest gradients occur near the boundaries".

The parameters $\sigma$ is the Prandtl number defined as the ratio of momentum diffusivity to thermal diffusivity; $b$ is related to the motion wavenumber, and $\rho$ is the ratio between the Rayleigh number and the *critical* Rayleigh number. In short, the higher $\rho$, the more turbulent we expect the flow to be.

Whether this highly truncated model keeps producing realistic results for $\rho > 1$ is contentious and might have been a moot point between Saltzman and Lorenz. Lorenz claimed that [his] "Equations may give realistic results when the Rayleigh number is slightly supercritical, but their solutions cannot be expected to resemble those of [Saltzman's] when strong convection occurs, in view of the extreme truncation".



This is a fascinating case where a model that is too idealised to still be realistic, proved to be highly insightful. In his acknowledgements, Ed Lorenz writes: "The writer is indebted to Dr. Barry Saltzman for brining to his attention the existence of nonperiodic solutions". This is a big statement, because this is the core of the paper. Yet, Saltzman may have done even more, as explained by [MOF05]:

> Lorenz (1993) recalls that he had "tried to simplify the model ... with no luck" and so he was "indebted to Dr. Barry Saltzman for bringing to his attention the existence of nonperiodic solutions of the convection equations" (Lorenz 1963). Indeed, with Saltzman providing such a low-order system ["whose existence Lorenz had begun to doubt" (Lorenz 1993)]

So, Lorenz' model should duly be called the Saltzman-Lorenz model.

[Lor63] provides a qualitative analysis of the model, which we will partly follow here, with some complements.

## 8.2 Fixed point analysis

The linearised model reads:

$$\begin{pmatrix} \dot{X} \\ \dot{Y} \\ \dot{Z} \end{pmatrix} = \begin{pmatrix} -\sigma & \sigma & 0 \\ (\rho - Z) & -1 & -X \\ Y & X & -b \end{pmatrix} \tag{22}$$

The trace of the Jacobian is $-(\sigma + b + 1)$, indicating that a *small* volume in phase space will shrink (wherever the position in the state space) for any combination of positive (thus, physical) parameters.

Furthermore, the equation system is invariant to the transformation $(X, Y, Z, t) \to (-X, -Y, Z, t)$. We therefore expect solutions (and attractor geometries) to be symmetric along the $Z-$axis.

The (not quite formal from a mathematical point of view) consequence is that each small volume shrinks to zero as $t \to \infty$. Quite informally, we deduce that the volume contained in a trapping region shrinks to zero at the same rate. It does not mean that it shrinks to a point. It technical terms, it shrinks to a variety of *zero measure*, which may be a surface or, as we will see, a variety of strange character. But in any case, we have a dissipative system and we expect at least one attractor, but that is not enough to guarantee that trajectories will not fly to infinity.

To this end, consider the fixed points. They obey $X_0 = Y_0$, $X_0^2 = bZ_0$ and, hence, we find either the fixed point $(X_0, Y_0, Z_0) = (0, 0, 0)$ or $X_0$ satisfies $X_0^2 = b(\rho - 1)$.

8.3

## 8.3 Subcritical flow ($\rho < 1$)

Only the trivial fixed point exists. Its eigenvalues satisfy

$$(\sigma + \lambda)(1 + \lambda)(b + \lambda) = \sigma\rho(b + \lambda),$$

giving $\lambda_0 = -b$ and

$$\lambda_\pm = -\frac{1+\sigma}{2} \pm \sqrt{\left(\frac{1+\sigma}{2}\right)^2 + \sigma(\rho - 1)}.$$

The subcritical case has all eigenvalues negatives. The trivial fixed point is an attractor, as can be shown by considering the Lyapunov function $V = X^2 + \sigma Y^2 + \sigma Z^2$.

## 8.4 Supercritical flow ($\rho > 1$)

Consider again the trivial solution. We find $\lambda_+$ becomes positive; the fixed point has become a saddle-point, so that in general (except along the stable manifold), trajectories will be *ejected* out of the fixed point. Where do they go ?

We also have new solutions at $X_0 = Y_0 = \pm\sqrt{b(\rho - 1)}$, which we expect to behave similarly given the symmetry of the system. With some algebra, it can be shown that they are attracting for $1 < \rho < \rho_H = \sigma\frac{\sigma+b+3}{\sigma-b-1}$. (cf. Appendix A)

More precisely, they are sinks for $\rho < \rho_1 < \rho_H$, and sinking spirals (sinks with imaginary parts) for $\rho_1 \leq \rho < \rho_H$. In may be shown (specialised work!) that there are unstable periodic orbits for $\rho_1 < \rho < \rho_H$.

Yet, trajectories are bounded for all $\rho > 1$ To show this, define $U = \rho X^2 + \sigma Y^2 + \sigma(Z - 2\rho)^2$. Observe that this time derivative satisfies:

$$\dot{U} = -2\sigma(\rho X^2 + Y^2 + (Z - \rho)^2 - b\rho^2).$$

In other words $\dot{U}$ is strictly negative for $\rho X^2 + Y^2 + (Z - \rho)^2 - b\rho^2 > 0$, that is, any point outside the ellipsoid defined by $\rho X^2 + Y^2 + (Z - \rho)^2 = b\rho^2$. Outside that ellipsoid, any isocontour of $U$ acts as a trapping region. Trajectories will not fly to infinity as time goes by.



## 8.5 The Lorenz attractor

An animation of the Lorenz attractor with the canonical parameters $\sigma = 10$, $\rho = 28$, $\beta = 8/3$ is available on Moodle. Demonstrating the "strange" character of the geometry was considered as one of the great challenges of the mathematics and was formally achieved by [Tuc02]. However, Lorenz already provided an intuitive approach for showing the chaotic character of his system by constructing a tent map, as shown in Appendix B.

The chaotic character may be defined as the sensitive dependence on initial conditions, and expressed by the mean value of the greatest Lyapunov exponent along the trajectory to be positive. The Benettin algorithm ([BGGS80], see also [RS00]) for the computation of the mean value of the greatest Lyapunov exponent, and its dependency on $\rho$ is provided in Appendix C. As can be seen, chaos emerges for $\rho > \rho_H$.

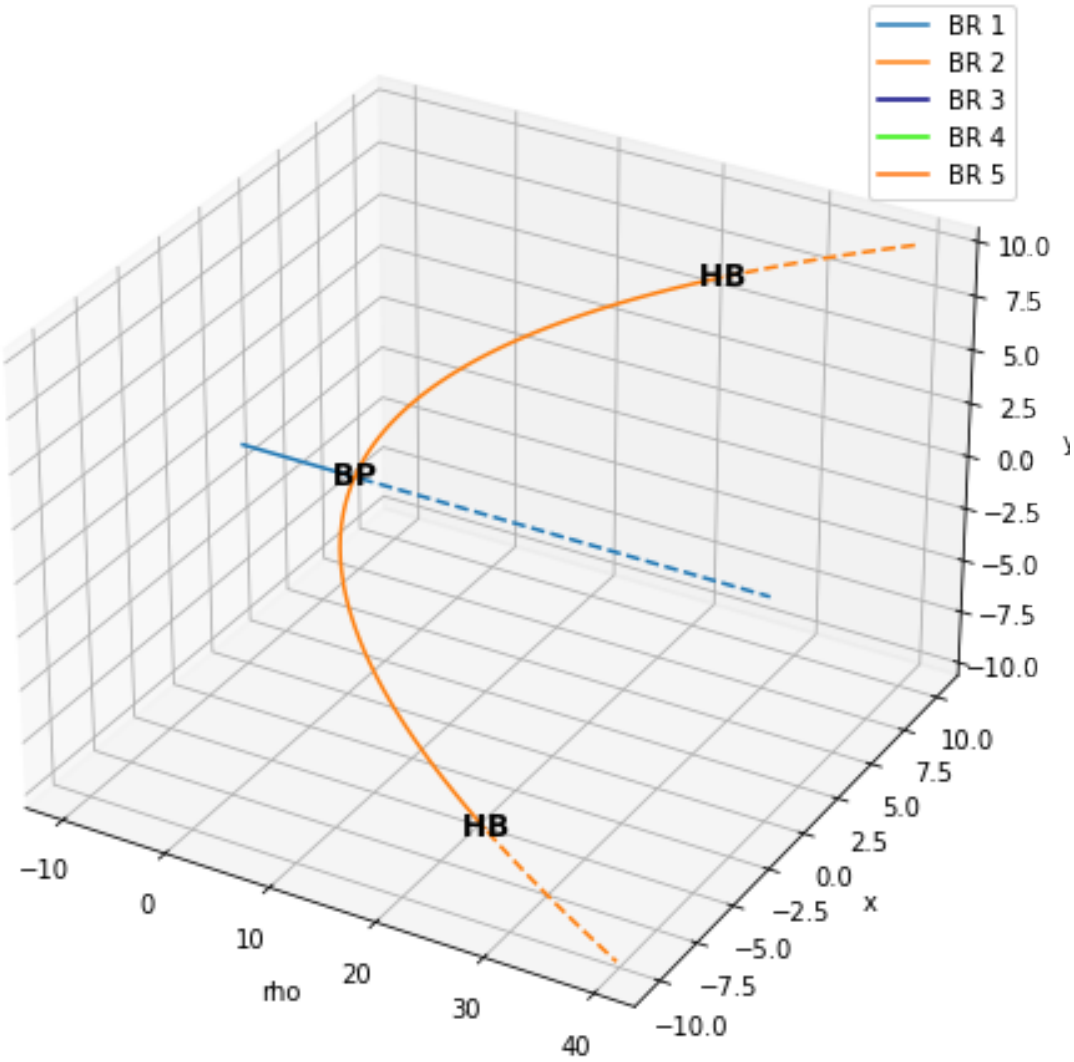


Figure 8.1: This bifurcation diagram was generated using the continuation software "auto" https://github.com/auto-07p/auto-07p, with the Python interface "auto2" https://oisinhamilton.com/_publications/2025-02-28_auto-AUTO. It shows, for standard parameter $\beta = 8/3$ and $\sigma = 10$, the bifurcation point at $\rho = 1$ in which the center point loses its stability, and the two Hopf bifurcation at $\rho = \rho_H$.

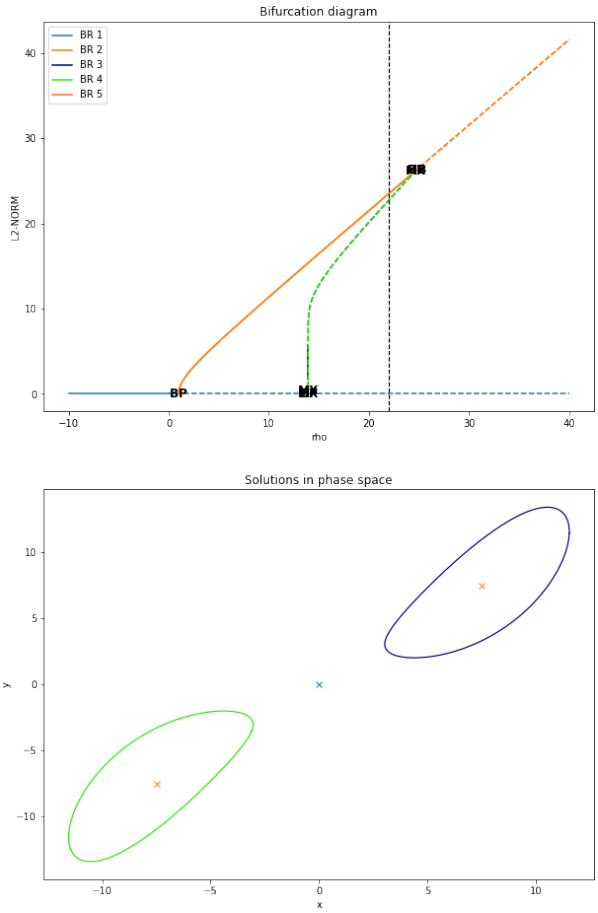


Figure 8.2: On both sides of the Hopf bifurcation accurring at $\rho_H$ auto allows to follow the unstable periodic orbits (the "L2-norm" is $X^2 + Y^2 + Z^2$, and the unstable periodic orbits are those represented by the dashed lines in the bifurcation diagram (top). The unstable periodic orbit for $\rho_H$ terminates as a *homoclinic bifurctation* for $\rho \simeq 13.29$. This is a new type of bifurcation that we haven't met so far, in which the orbit has as infinite period, and touches the center point (which is then acts both as as $\alpha-$ and $\omega-$ point. Homoclinic orbits can also be found by varying $\sigma$. The full demo is available at 09˙lrz˙auto˙auto.html. The lower figures show the unstable periodic orbits for $\rho = 22$.

.

## 8.6 The Rössler system

The Saltzman-Lorenz '63 is paradigmatic for showing how chaos emerges out of unstable periodic orbits. It may be further be shown that it displays intermittent behaviour, or "transient chaos" for $24.06 < \rho < \rho_H$, a regime for which it oscillates between the strange attractor and the two unstable periodic orbits. This occasional activity is called *intermittency* (see further at https://www.math.fsu.edu/~bertram/lectures/Chaos.pdf).

In order to better understand this "intermittency route" to chaos, Otto Rössler published in 1976 a simpler model which, as we will see, clearly demonstrates the intermittency route to chaos.

$$\begin{aligned} \dot{X} &= -Y - Z \\ \dot{Y} &= -X + aY \\ \dot{Z} &= b + Z(X - C) \end{aligned} \tag{23}$$

The equations have some similarity with the Lorenz '63, but there is only one non-linear system. The $x$ and $y$ components are determined by linear equations.

Let us briefly introduce here the principle of a Poincaré section : every time the system crosses the line $y = 0$, we record the values of $x$ and $z$. The diagram below shows the gradual complexification of the Poincaré section as $c$ increases. It follows a "period-doubling" route to chaos with *intermittent* zones of order, until fully-developed chaos.

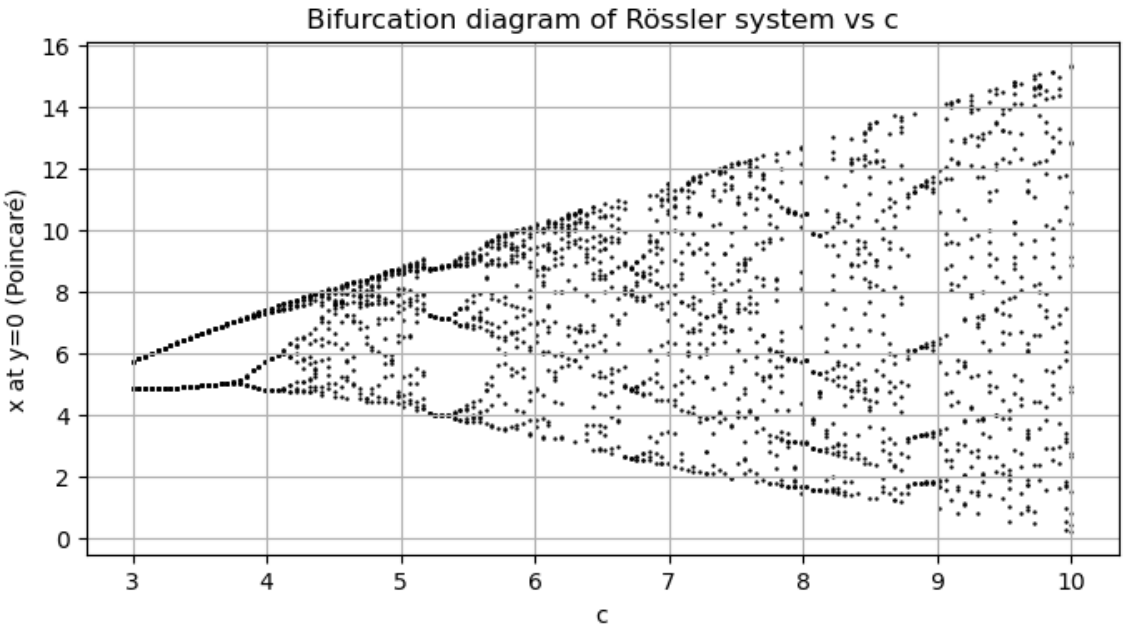


Figure 8.3: Poincaré section of the $x, z$ plane (showing $x$), as a function of $c$.

For those having a `jupyter-notebook` installation with working Python and `sci-py`, a notebook featuring some aspects of the Rössler attractor are available at 08˙rossler.ipynb.

This figure is intriguingly similar to the period-doubling route which we will discover in the logistic equation model section 9.2.1. This is a clue to the existence of a limited number of possible *routes to chaos*.

# 9 Iterations: definitions and examples

## 9.1 Positive, negative and full orbit

The *map* or *discrete dynamical system* is defined by an iteration. We define $x_i \in \Omega \subseteq \mathbb{R}^n$, and the iteration $f : \Omega \to \Omega$ such that:

$$x_{i+1} = f(x_i).$$

Thus,

$$x_i = \underbrace{f \circ f \circ f \ldots \circ f}_{i \text{ times, noted } f^i}(x_0).$$

**DEFINITION 19 Positive orbit**

The *positive* orbit of $x \in \Omega$, noted $\theta^+(x)$ is defined by $\theta^+(x) = \{f^i(x) | i \geq 0\}$.

If $f$ is invertible, then one can go backwards using $f^{-1}$. One can then define the negative orbit and the full orbit:

**DEFINITION 20 Negative and full orbit**

- ▷ The *negative* orbit of $x \in \Omega$, noted $\theta^-(x)$ is defined by $\theta^+(x) = \{f^{-i}(x) | i \geq 0\}$;
- ▷ The *full* orbit of $x \in \Omega$, noted $\theta(x)$ is defined by $\theta(x) = \{f^{-i}(x) | i \in \mathbb{Z}\}$.

## 9.2 Motivating examples

### 9.2.1 The logistic growth

A simple model for, e.g., demographic growth is defined as $f(x) = rx$. Quite obviously the positive orbits diverge to $+\infty$ for positive $r$ ($\lambda = r$). The idea of *limiting growth* by a competition or limiting resource argument bringing a demographic limitation is the basis of the *logistic growth* model:

$$f(x) = rx(1 - \frac{x}{N}),$$

or, rescaling the population mass by $N$, $f(x) = rx(1 - x)$.

This *logistic* equation can be interpreted as a *discrete* version of the Verhulst model for population growth, developed under the influence of Adolphe Quetelet (both Belgian Mathematicians). Its behaviour can be surprisingly complex depending on the value of $r$ and we will explore some of it later on.

The Cobweb construction provides a insightful approach to construct the orbits. It consists in iterating using by reporting the iteration $x_{i+1}$, found on the $y-$axis, to the $x-$axis using the $x_i = x_{i+1}$ line.

[1]:
```
# using InteractiveDynamics, GLMakie
using DynamicalSystems
using Plots

r=3.2
lo = Systems.logistic(0.1; r=3)

# interactive_cobweb(lo, rrange, 5)
```

```
ArgumentError: Package Plots not found in current path.
- Run `import Pkg; Pkg.add("Plots")` to install the Plots package.

Stacktrace:
```

```
[1] macro expansion
  @ ./loading.jl:2375 [inlined]
[2] macro expansion
  @ ./lock.jl:376 [inlined]
[3] __require(into::Module, mod::Symbol)
  @ Base ./loading.jl:2358
[4] require(into::Module, mod::Symbol)
  @ Base ./loading.jl:2334
[5] eval(m::Module, e::Any)
  @ Core ./boot.jl:489
```

[2]:
```
N=30;
traj=vec(trajectory(lo,N)[1]);
```

[3]:
```
tt=zip(traj[1:(N-1)],traj[2:(N)]);
```

[4]:
```
Cobweb = collect(Iterators.flatten(map(x -> [[x[1][1],x[1][1]],[x[1][1],x[2][1]]], tt)));
```

[5]:
```
f(x) = x*(1-x)*r; id(x)=x;
```

[6]:
```
using LaTeXStrings
plot!(vec(map(x->x[1],Cobweb)), vec(map(x->x[2], Cobweb))) # , xlabel=L"x_i",␣
↪ylabel=L"x_{i+1}");
print(vec(Cobweb)[1])
```

```
[0.1, 0.1]
```

[7]:
[7]:
```
plot!(f, 0,1); plot!(id,0,1)
```

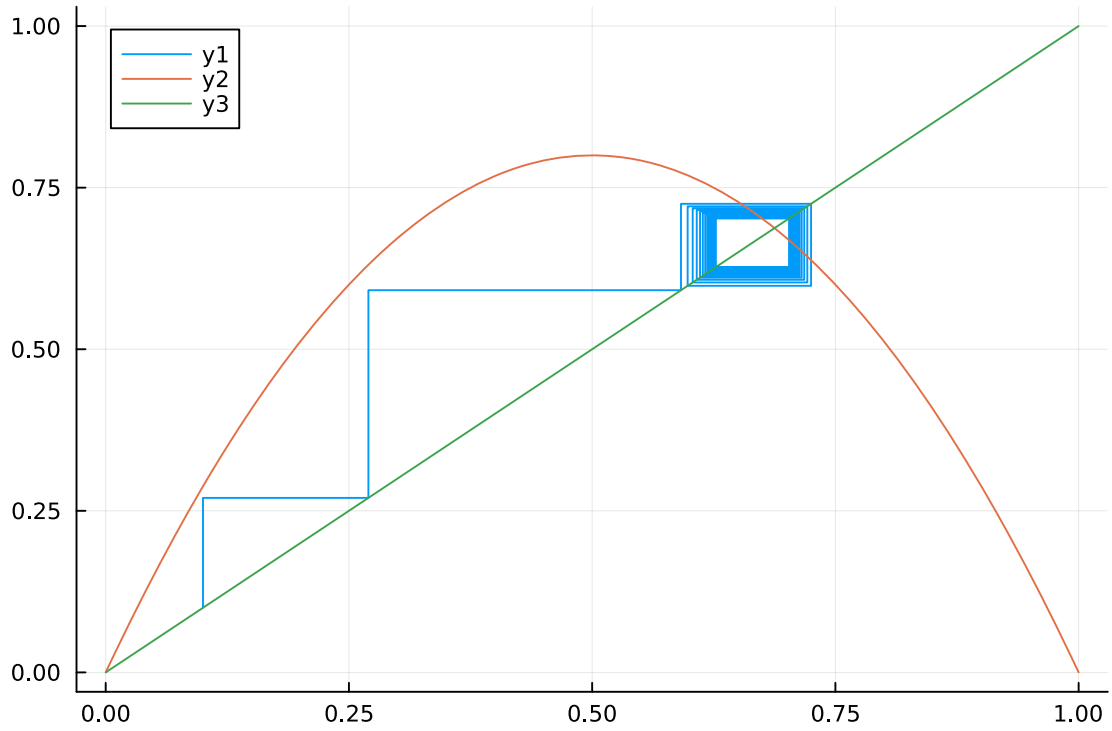


[ ]:

We have here an example ($r = 3.2$) where the map converges to a limit cycle attractor. For low-enough $r$, the attractor is a fixed point; for high $r$, the solution is a-periodic and chaotic (will still need to define chaos in this case). These behaviours can be visualised with the so-called *orbit diagram*, which may be understood as the equivalent of the bifurcation diagram in the continuous domain.

[4]:
```
# Example taken from https://juliadynamics.github.io/DynamicalSystems.jl/latest/chaos/
↪orbitdiagram/
using DynamicalSystems, CairoMakie

ds = Systems.logistic()
i = 1
pvalues = 2.7:0.003:4
ics = [rand() for m in 1:10]
```

[4]:
```
n = 2000
Ttr = 2000
p_index = 1
output = orbitdiagram(ds, i, p_index, pvalues; n = n, Ttr = Ttr)

L = length(pvalues)
x = Vector{Float64}(undef, n*L)
y = copy(x)
for j in 1:L
    x[(1 + (j-1)*n):j*n] .= pvalues[j]
    y[(1 + (j-1)*n):j*n] .= output[j]
end

fig, ax = scatter(x, y; axis = (xlabel = L"r", ylabel = L"x"),
    markersize = 0.8, color = ("black", 0.05),
)
ax.title = "total points: $(L*n)"
xlims!(ax, pvalues[1], pvalues[end]); ylims!(ax,0,1)
fig
```

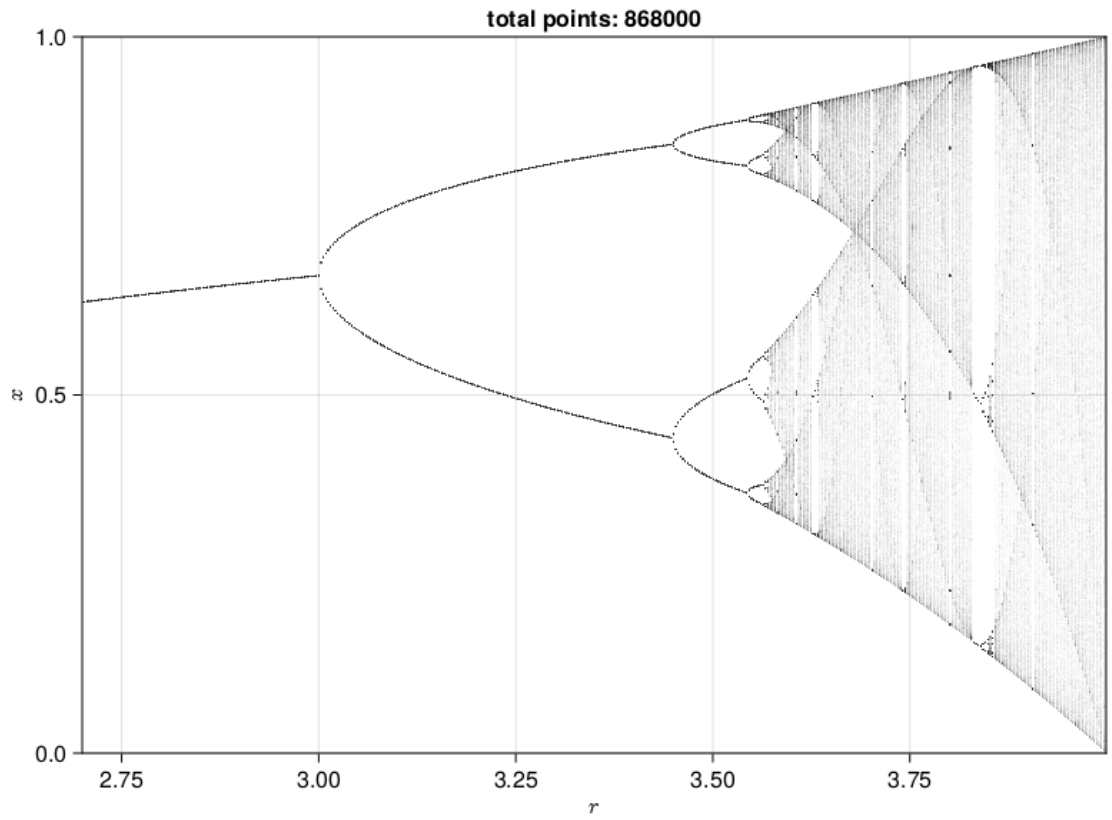

The orbit map of the logistic model is a *fractal* : it reproduces itself by zooming over it again and again.

### 9.2.2 The tent map

The tent map is defined as

$$x_{i+1} = \begin{cases} 2x_i \text{ for } x_i < \frac{1}{2}, \\ 2 - 2x_i, \text{ otherwise} \end{cases} \tag{24}$$

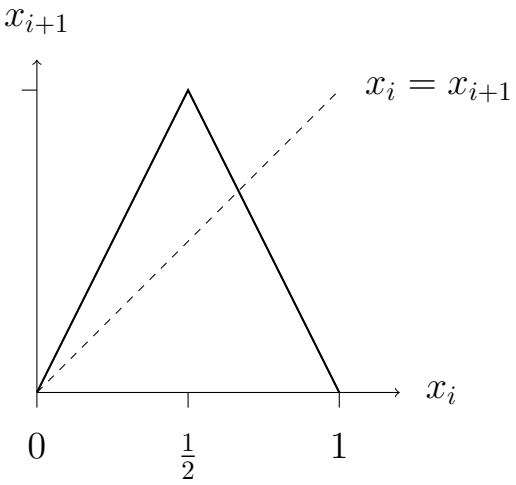




**CLASS ROOM DISCUSSION 15**

By reasoning in base 2 (as computers do), one can see that the tent map produces *periodic* solutions for all rational numbers, and *aperiodic* solutions for all irrational initial conditions. For that reason, computing the tent map with a digital computer gives you almost surely the wrong solution, because $\mathbb{Q}$ is a set of measure zero in $\mathbb{R}$. *Hint*: multiplying by 2 in base 2 is equivalent to shifting all digits leftwards.

### 9.2.3 Getting iterations from continuous dynamical systems

It is common to map a continuous dynamical system on an iteration to understand its properties, at the cost of some information loss:

- ▷ *Numerical iteration* is perhaps the most common case. The *Euler*, *Runge Kutta* schemes are example of iterations extracted from a continuous dynamical system.
- ▷ The *Poincaré* map is the cross section of a n-dimensional continuous orbit onto a lower-dimensional section, typically a plane. For example, the Poincaré map of a limit cycle is a point; that of a torus: a circle.
- ▷ The *stroboscopic map* is obtained as the sample of a continuous orbit at fixed intervals $T$. It is particularly useful to study synchronisation in forced systems with period $T$.

- ▷ In some cases, authors have been more creative. We have seen how Lorenz interpreted the behaviour Saltzman-Lorenz by plotting successive local maxima in the $z-$coordinate with the tent map. We come now to another example.

### 9.2.4 The Hénon map

The Hénon map (Michel Hénon, Communications in Mathematical Physics, 1976) was introduced as a minimalist dynamical system presenting a strange attractor, reminiscent of a cross section of the Lorenz system.

$$\begin{aligned} x_{i+1} &= 1 - ax_i^2 + y_i, \\ y_{i+1} &= bx_i. \end{aligned} \tag{25}$$

We use the powerful package DynamicalSystems.jl package for genereating 1 million points with the Hénon

map and show the graphical result.

[1]:
```
using DynamicalSystems
using PredefinedDynamicalSystems
using StaticArrays # only necessary when defining a system

he = PredefinedDynamicalSystems.henon([0.,0.0]; a = 1.4, b = 0.3)
```

```
[ Info: Precompiling DynamicalSystems
[61744808-ddfa-5f27-97ff-6e42cc95d634]
```

[1]:
```
2-dimensional DeterministicIteratedMap
 deterministic: true
 discrete time: true
 in-place:      false
 dynamic rule:  henon_rule
 parameters:    [1.4, 0.3]
 time:          0
 state:         [0.0, 0.0]
```

[12]:
```
traj = trajectory(he, 100000);
```

[11]:
```
using GR
shade(traj[1][:,1],traj[1][:,2], colormap=-2, xlabel="x", ylabel="y")
```

[11]:

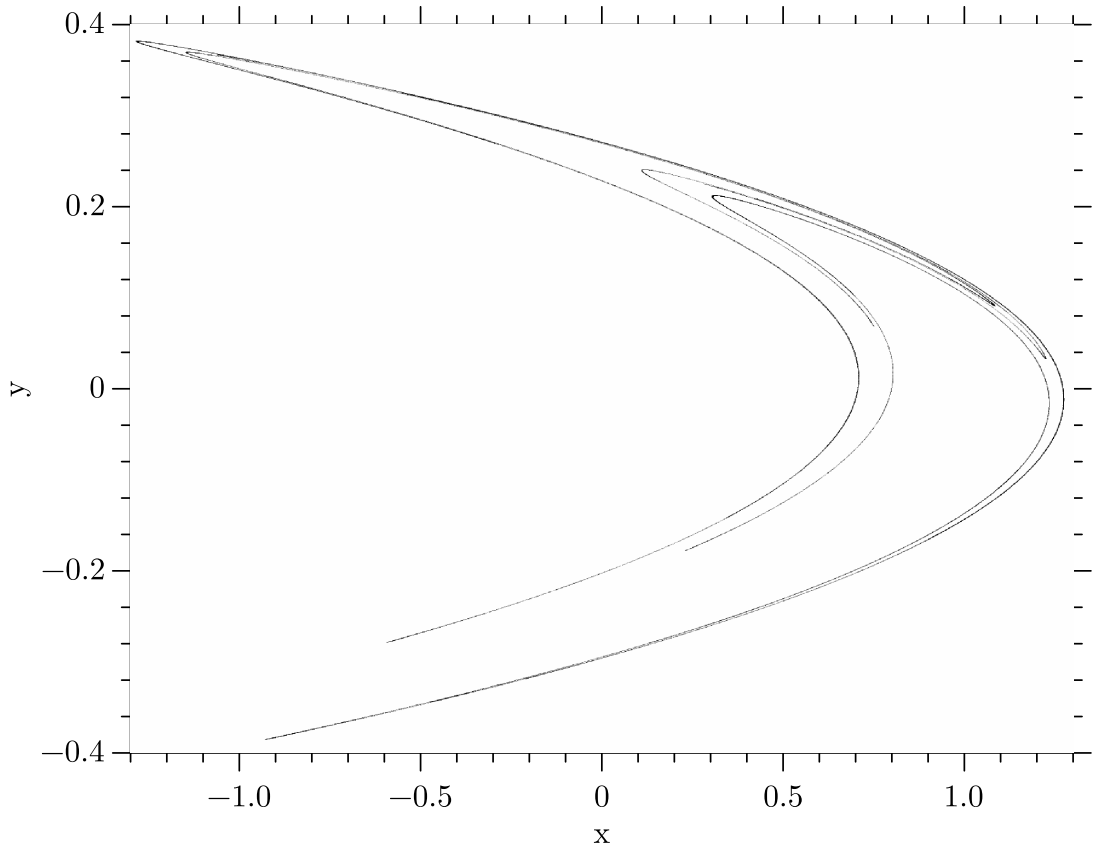




[ ]:

The *strange* character of the attractor is related to the fact the way the number of pixels you need to cover it scales with the dimensions of the pixels.

For a example, for a line segment, the number of pixels grows linearly with the inverse of the size of the pixels. The dimension is 1.

For a square or a rectangle, the number of pixels needed grows with the *square* of the inverse of the size of the pixels. Dimension is 2.

The *Hausdorff* dimension quantifies this scale relationship.

In the Hénon attractor, this number is about 1.261. This is *strange* in that sense.

## 9.3 Fixed points and periodic orbits

### 9.3.1 Definition

Similarly to diffeomorphisms, we can define fixed points, periodic orbits, sinks and sources.



**DEFINITION 21** $k-$**periodic points**

Given the iteration $f$, a point in the domain $\Omega$ is said to be $k-$periodic, or periodic with period $k$, if $f^k(p) = p$, and $f^j(p) \neq p$ for $j = 1 \dots k-1$.

A fixed point is a 1-periodic point, $f(p) = p$.

The positive orbit $\theta^+$ of a $k-$periodic point is thus an ensemble of $k$ points $\{f(p) \dots f^k(p)\}$. It happens that the $k-$periodic character of an orbit develops after a finite number of iterations given an initial condition. This will be the case, for example, for $f(x) = 2x \, mod \, x$ ($mod$ is the modulus).

The initial condition $\frac{1}{14}$ ends up in a periodic orbit (show this).

**DEFINITION 22** **Finally periodic points**

A point $p \in \Omega$ in the domain of the iteration $f$ is said to be *finally* $k-$periodic if $\exists m \in \mathbb{N}_0$ such that $f^m(p)$ is $k-$periodic.

### 9.3.2 Stability

Given a metric in domain $\Omega$ (usually $\Omega = \mathbb{R}^n$), we can characterise the stability property of a $k-$periodic orbit. To proceed by steps, we first consider the case of a fixed point.

**DEFINITION 23 Attractor and repeller of an iteration**

- ▷ A fixed point $p$ is locally attracting (it is a *sink*) if $\exists \delta > 0$ such that $\forall x \in \Omega$ with $|x - p| < \delta$, $\lim_{i\to\infty} f^i(x) = p$.
- ▷ A fixed point $p$ is *repelling* (it is a *source*) if $\exists \delta > 0$ such that $\forall x \in \Omega$ with $|x - p| < \delta$ and $x \neq p$, $\exists i \geq 1$ such that $|f^i(x) - p| \geq \delta$.

Again, similarly to the *hyperbolic* character of a fixed point in a flow:

**DEFINITION 24 Hyperbolic fixed point**

The fixed point of an iteration is *hyperbolic* if none of the eigenvalues of its Jacobian is on the unit circle.

We anticipate a similar connection between eigenvalues of the Jacobian and the locally attracting - repelling properties of the fixed point, but we leave the demonstration for the next section.

We just proceed a bit more with our enthusiasm for definitions to define the stability of a periodic orbit:

**DEFINITION 25 Stability of periodic orbits**

For $k \geq 1$ and $p$ a point of the $k-$periodic orbit of $f$, the latter is said to be - attracting if $p$ is a sink of $f^k$, and - repelling if $p$ is a source of $f^k$.

Similarly, we will characterise the hyperbolic character of $p$ by considering the $f^k$ iteration.

Finally, we consider the *basin* of attraction of a fixed point or a $k-$periodic fixed point:

**DEFINITION 26 Basin of attraction**

For an iteration $f$ on $\Omega$, given a $k-$periodic fixed point, locally attracting (a sink), the basin of attraction is the set of all points $x$ such that

$$\lim_{i\to\infty} |f^i(x) - f^i(p)| = 0.$$

The basin of attraction of the *positive orbit* $\theta^+(p)$ is the union of the basins of attractions of all points of the positive orbit, thus the $f^j(p)$, $j = 1 \dots k$.

# 10 Stability of periodic orbits in 1-d iterations

## 10.1 Stability of iterations

We consider iterations mapping $\mathbb{R}$ on itself, that is: $f : \mathbb{R} \to \mathbb{R}$.

The cobweb construction makes it reasonably intuitive that the stability of a fixed point is linked to the first-order derivative of $f$



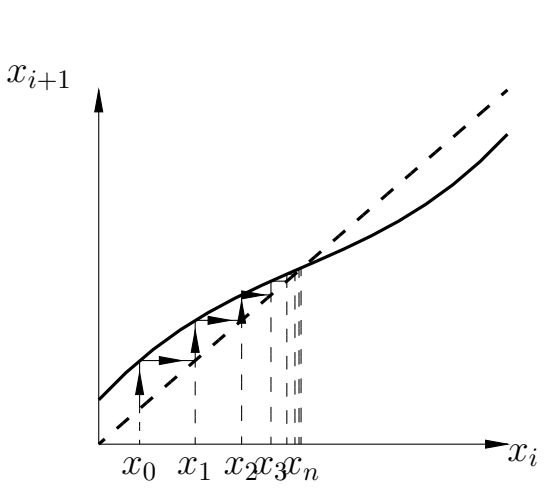


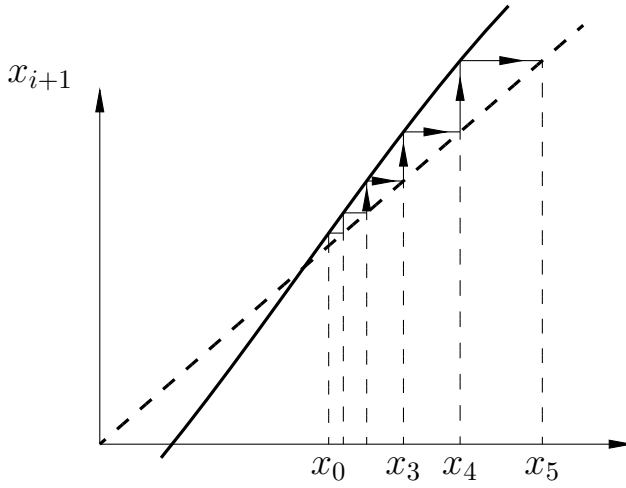


**Fig. 10.1**

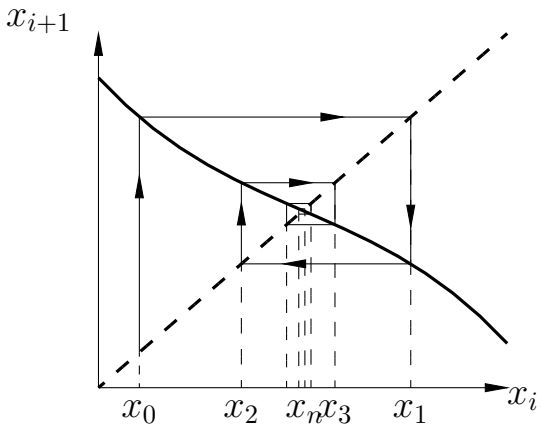


**Fig. 10.3**



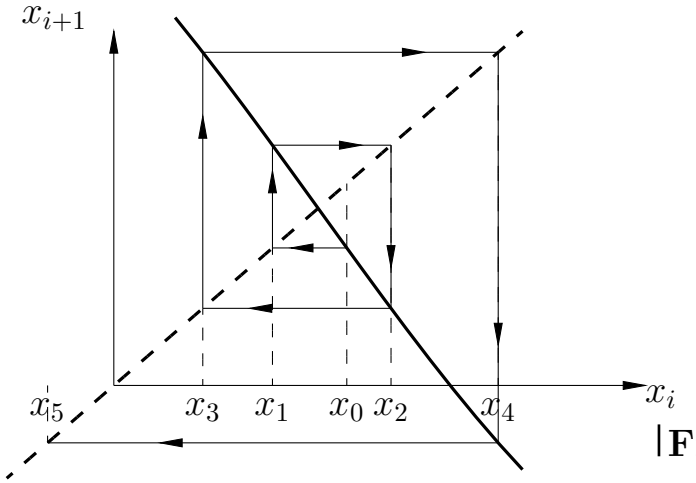


**Fig. 10.4**

More specifically, we prove:

**THEOREM 12 Stability of hyperbolic fixed points**

Let $p$ a hyperbolic fixed point of $f$.

- ▷ $p$ is a *sink* if $|f'(p)| < 1$,
- ▷ $p$ is a *source* if $|f'(p)| > 1$.

We first proceed by proving that for any $\epsilon > 0$, there is $\delta > 0$ such that, for $|x - p| < \delta$:

$$|f'(p)| - \varepsilon < \left| \frac{f(x) - p}{x - p} \right| < |f'(p)| + \epsilon.$$

This relationship emerges from the definition of the derivative, and the definition of the fixed point. Indeed, from:

$$f'(p) = \lim_{x \to p} \frac{f(x) - f(p)}{x - p} = \lim_{x \to p} \frac{f(x) - p}{x - p},$$



we find, by definition of the limit that, for any $\epsilon$ we can find a $\delta$ such that: $\left| f'(p) - \frac{f(x)-p}{x-p} \right| < \epsilon$.

It comes up that the distance between $f'(p)$ and $\frac{f(x)-p}{x-p}$ is less that $\epsilon$, that is:

$$-\epsilon < f'(p) - \frac{f(x) - p}{x - p} < \epsilon.$$
$$-\epsilon - f'(p) < -\frac{f(x) - p}{x - p} < \epsilon - f'(p)$$

If $f'(p) < 0$, this inequality becomes ($f(x) - p$ and $(x - p)$ have opposite signs)

$$-\epsilon + |f'(p)| < \frac{|f(x) - p|}{|x - p|}| < \epsilon + |f'(p)|,$$

which we rewrite, for clarity

$$|f'(p)| - \epsilon < \frac{|f(x) - p|}{|x - p|}| < |f'(p)| + \epsilon.$$

Now, if $f'(p) > 0$, this inequality becomes ($f(x) - f(p)$ and $(x - p)$ have the same sign)

$$-\epsilon - |f'(p)| < -\frac{|f(x) - p|}{|x - p|} < \epsilon - |f'(p)|.$$



We turn the sign to obtain:

$$|f'(p)| - \epsilon > \frac{|f(x) - p|}{|x - p|} > |f'(p)| + \epsilon,$$

so that both positive and negative $f'(p)$ will satisfy the inequality

$$(|f'(p)| - \epsilon)|x - p| < |f(x) - p| < (|f'(p)| + \epsilon)|x - p|$$

Now, we consider separately the attractor and the sink.

If $|f'(p)| < 1$, we can find $\epsilon$ such that $|f'(p)| + \epsilon < 1$, and we can find $\delta$ with $|x - p| < \delta$ such that

$$|f(x) - p| < (|f'(p)| + \epsilon)|x - p| < 1\delta = \delta. \tag{26}$$

We proceed by successive iterations. Indeed, we now know that the point $f(x)$ is also close to $p$, with a distance less than $\delta$. Hence, the

above relationship also applies to this point, i.e., we may substitute $f(x)$ to $x$, to find:

$$|f(f(x)) - p| < (|f'(p)| + \epsilon)|f(x) - p| < \delta$$

and then substitute the result of (26). Iteration after iteration we eventually find

$$|f^n(x) - (p)| < (\underbrace{|f'(p)| + \varepsilon}_{<1})^n |x - p| < \delta,$$

and this is true for $\forall n > 0$. We can thus find a $\delta$ such that $\lim_{n\to\infty} |f^n(x) - p| = 0$, and this is exactly the attractor property.

Now, we consider the source case. We know that we can find $\epsilon > 0$ such that $|f'(x)| - \epsilon > 1$. But from what we have already learned, there is also a $\delta$ such that, for $|x - p| < \delta$,

$$|f(x) - p| > (|f'(p)| - \varepsilon)|x - p|, \tag{27}$$

By iteration of (27):

$$|f^n(x) - p| > (|f'(p)| - \varepsilon)^n |x - p|.$$

As $(|f'(p)| - \varepsilon) > 1$ one can find a $n$ such that, given $|x - p|$, the right-hand-side as big as one wants. We have therefore found a $\delta$ such that $|f^n(x) - p| > \delta \ \forall n \geq 1$. □.

## 10.2 Linearised system

If $f(x)$ is $C^\infty$, we can also proceed by Taylor expansion, writing, around a fixed point $p$, if $x_n = p + \xi_n$,

$$\begin{aligned} p + \xi_{n+1} = f(p + \xi_n) &= f(p) + f'(p)\xi_n + \frac{1}{2}f''(p)\xi_n^2 + \mathcal{O}(\xi_n^3) \\ &= p + f'(p)\xi_n + \frac{1}{2}f''(p)\xi_n^2 + \mathcal{O}(\xi_n^3) \end{aligned}$$

Hence,

$$\xi_{n+1} = f'(p)\xi_n + \frac{1}{2}f''(p)\xi_n^2 + \mathcal{O}(\xi_n^3)$$

From this it is clear around a *hyperbolic* fixed point, the linearised system evolves, near the fixed point, as a geometric convergence towards the fixed point if $|f'(p)| < 1$, and geometric for $|f'(p)| > 1$:

$$\xi_n \sim f'(p)^n \xi_0$$

A bit abusively, we sometimes speak of exponential divergence or convergence but cleary what we have here is a power law. It dictates the behaviour of the system in a neighbourhood of a non-hyperbolic fixed point as long as $f'(p)$ is non-zero.

The particular case $|f'(p)| = 0$ merits some mention. The fixed point is said to be *superstable*. The second-order approximation is

$$\xi_{n+1} = \frac{1}{2}f''(p)\xi_n^2.$$

The convergence (we have convergence since $|f'(p)| < 0$) is supergeometric:

$$\begin{aligned}\xi_n &\simeq \frac{1}{2}f''(p)\xi_{n-1}^2 \\ &\simeq \frac{1}{2}\frac{1}{2}^2 f''(p)f''(p)^2\xi_{n-2}^4 \\ &\simeq \left(\frac{1}{2}f''(p)\right)^{1+2+\ldots+n}\xi_0^{2n} \\ &\simeq \left(\frac{1}{2}f''(p)\right)^{\frac{1}{2}(n)(n+1)}\xi_0^{2n}\end{aligned}$$



**DEFINITION 27 superstable point**

A point with $f'(p) = 0$ is said to be superstable.

It may be shown that the root found by a Newton-Raphson iteration is superstable.

Quite naturally, the stability of $k-$periodic orbit may be assessed considering the iteration $f^k$ and its derivatives.

## 10.3 Analysis of the logistic equation

We come back to the logistic iteration $f(x) = rx(1-x)$,and examine some of its properties:

### 10.3.1 Diverging orbits outside $[0,1]$ for $r > 1$.

For $r > 1$, orbits are diverging towards $-\infty$ for $x_0 \notin [0,1]$. We proceed separately for $x_0 < 0$ and $x_0 > 1$.

For $x_0 < 0$, the definition of the iteration makes it clear that $x_{n+1} < x_n$

(tip: write it as $rx - rx^2$), and there cannot be any fixed point $p$ towards which the iteration converges. Indeed, this would imply

$$p = \lim_{n\to\infty} x_{n+1} = \lim_{n\to\infty} f(x_n) = f(\lim_{n\to\infty} x_n) = f(p) < p.$$

If $x_0 > 1$, then $f(x_0)$ is negative, and we are back to case one.

### 10.3.2 Fixed points

The fixed points satisfy $p = f(p) = rp(1-p)$. The two roots are $p = 0$ and $p = 1 - \frac{1}{r}$. The second root $p = 1 - \frac{1}{r}$ exists even for $r < 1$ but it is negative, and unstable.

Inspection of the derivative shows that:

- $p = 0$ is a sink for $r < 1$ and a source for $r > 1$ (assuming $r$ positive);
- $p = 1 - \frac{1}{r}$ is a hyperbolic sink for $1 < r < 3$ and a source for $r > 3$.

The paramater $r = 1$ corresponds to a *transcritical* bifurcation, where both fixed points exchange their stability. Above $r > 3$, both fixed points become unstable, so that we have another kind of bifurcation that is now investigated.

### 10.3.3 Existence of 2-periodic points for $r > 3$.

The existence of a 2-periodic point is conditioned by the equation

$$r^2 p(1-p)(1 - rp(1-p)) = p.$$

Having the $p$ of the right-hand-side in the left-hand-side and some algebra genie would show that this is equivalent to

$$rp(p-(1-\frac{1}{r}))(r^2p^2-r(r+1)p+r+1)=0.$$

This form has the merit to make it clear that we have a fixed point for $p=0$ and $p=1-\frac{1}{r}$ but these are the fixed points of the iteration (period 1) so they can't count as a solution for period-2 orbits. The period-2 points are hidden in the third factor. There must be 2 roots, which are real for $r>3$, and which correspond to the 2 distinct points ($p_1$ and $p_2$) that form the orbit.



Further analysis shows that the $2-$periodic orbit is attracting for $3<r<1+\sqrt{6}$, and repulsive for $r>1+\sqrt{6}$. This requires inspection of $(f^2)'=f'(p_2)f'(p_1)$.

In summary, we have a *period doubling* bifurcation at $r=3$ and we anticipate a similar phenomenon at $1+\sqrt{6}$. At the specific parameter of $r=3$, the orbit is converging *very slowly* towards the $\frac{2}{3}$.

Numerical inspection of fixed points shows a suit of bifurcations at (rounded numbers) $r_1=3, r_2=3.44949$, $r_3=3.54409$ converging towards $r_\infty=3.56994$, with geometric convergence of the increments:

$$\delta=\lim_{n\to\infty}\left(\frac{r_n-r_{n-1}}{r_{n+1}-r_n}\right)=4.66920$$

This is called the Feigenbaum number, who observed it in other iterations (e.g. $f(x)=r\sin(\pi x)$), suggesting it be a universal property.

### 10.3.4 Chaotic behaviour for $r_\infty < r < 4$

In this regime, the orbits have mostly the characteristics of chaos that we further define in section . Numerical analysis shows however some surprising windows of periodic behaviour (look again at the orbit diagram in section 9.2.1, and of *intermittent* behaviour, where the system seems to hesitate between different periods.

### 10.3.5 Fractal set of diverging orbits for $r > 4$

The maximum of $rx(1-x)$ occurs at $x = \frac{1}{2}$ and is $r/4$. Hence, for $r > 4$ there is an interval $A$ comprised between $x\mp = \frac{1}{2}(1 \mp \sqrt{1 - \frac{4}{r}})$ that ejects the points out of the safe interval $[0, 1]$, from where trajectories diverge towards $-\infty$.

However, outside $A$, there are also smaller intervals that will drive $x$ into $A$ at the next iteration(here, denoted $B_1$ and $B_2$), so that their positive orbits also diverge. This reasoning leads us to the construction of an ensemble of diverging orbits. Its complement, the ensemble of non-diverging orbits, is a Cantor set.

This property teaches us a few things.

- ▷ The Cantor set has a Lebesgue measure zero. In other words, if you should "at random" in the $[0, 1]$, you are almost certain to hit an initial condition causing a diverging orbit. In other words, divergence prevails;
- ▷ Yet, there is an infinite, uncountable number of initial conditions with non-diverging orbits. They form a dense, compact set, and every of such initial condition acts as a boundary between two diverging orbits. The Cantor, self-similar nature of this set reflects the geometrical complexity of the structure of trajectories;

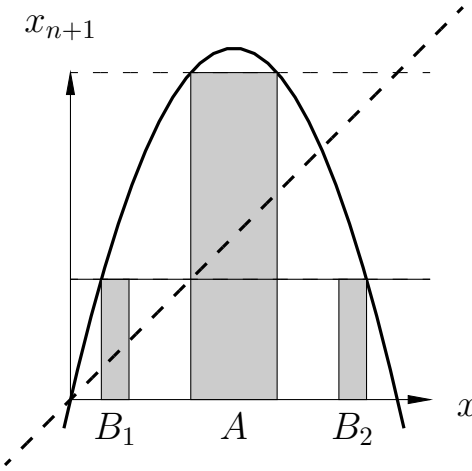


**Fig. 10.5**

# 11 Chaos in 1-d iterations

## 11.1 Chaos of the 2 mod 1 map

We consider an iteration similar to the tent map, but a little bit simpler:

$$x_{i+1} = \begin{cases} 2x_i \text{ for } 0 \leq x_i < \frac{1}{2}, \\ 2x_i - 1 \text{ for } \frac{1}{2} \leq x_i < 1. \end{cases} \tag{28}$$

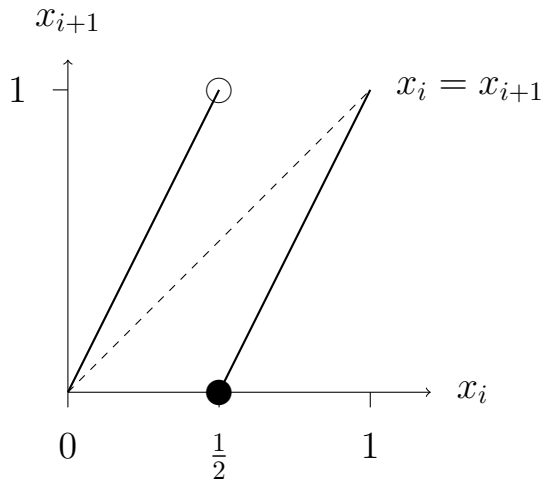


This is also sometimes called the 2 mod 1 map (multiply by 2, and take one off if needed). It is neither continuous, nor reversible. We will now formalise some of the arguments that we have already raised in class when discussing in the class when discussing the tent map. Consider the binary[7] representation of $x = .b_1 b_2 b_3 \ldots$, with $x = \sum \frac{1}{2^i} b_i$.

First, observe that $f(x) = .b_2 b_3 b_4 \ldots$, such that $f^n(x) = b_{n+1} b_{n+2} b_{n+3} \ldots$.

Then, for any $x_0$, and consider $y_0$ such that $|y_0 - x_0| < \epsilon$, with $x_0 = .b_1 b_2 \ldots$ and $y_0 = .c_1 c_2 \ldots$. Then, we generally expect that for $n < -\log_2 \epsilon$, $b_n = c_n$. We can no longer expect this equality to hold after $n = -\log_2 \epsilon$ and the distance $|f^n(y_0) - f^n(x_0)|$ will be of the order of

[7] also called: "dyadic"

$\frac{1}{2}$.

As a general rule, there exists a typical distance $d$ (here, 0.5) such that for any $\epsilon > 0$, $x \subset \Omega$, I can find $y$ such that $|x - y| < \epsilon$ and $|f^n(y) - f^n(x)| \geq d$ for $n$ *not too big*. This is the basis of the definition of *sensitivity to initial conditions*:

**DEFINITION 28 Sensitivity to initial conditions (SIC)**

Let $f : \Omega \to \Omega$. $f$ has SIC iff there is $d > 0$, $0 < C < \infty$ such that $\forall x \in \Omega$ and $\epsilon > 0$, there is a $y \in \Omega$ and $0 < n < C|\ln \epsilon|$ with $|x - y| < \epsilon$ and $|f^n(x) - f^n(y)| \geq d$.

So, our iteration has SIC.



The interval $[0, 1]$ has further properties. All rational numbers in this interval generate finally periodic orbits. Indeed, any rational number comprised in the $[0, 1]$ interval can be expressed an $.b_1 b_2 \ldots$ with the suite $b_n$ finally periodic. Hence, its positive orbit will be finally periodic, too. $\mathbb{Q}$ being dense in $\mathbb{R}$, we find that there is a dense set of points in $[0, 1]$ which generate finally periodic orbits.

More surprising perhaps, observe that the set of points with a finite binary representation (i.e., $x = .b_1 \ldots b_n$ with $n$ finite) is both *enumerable* and *dense*. Call this set $E$.

- ▷ Enumerable: one can enumerate these numbers one by one, by growing $n$ and, for fixed $n$, by enumerating them by lexicographic order;
- ▷ Dense: I can find such a number in any finite, closed interval of the domain.

So, let us consider the set of points with finite binary representation $E = \{f_i, i \in \mathbb{N}\}$.

Now, construct the number made of concatenating all these numbers

in the binary representation (possibly with filling in zeros so that every number appears with any desired floating point accuracy). This one does have an infinity of digits in the binary representation, but its positive orbit passes close to any number in $E$ as close as one wants, and given that $E$ is dense in $\Omega$, we have generated an orbit that passes close to any number in $\Omega$.

At this point, we have gathered all the ingredients of one-dimensional chaos.

**DEFINITION 29 Chaos of a 1-D iteration**

The iteration $f : \Omega \to \Omega$, $\Omega \in \mathbb{R}$ is chaotic iff:

1. it has the SIC property;
2. it has a dense set of periodic orbits;
3. it possesses at least one dense orbit in $\Omega$.

The definition includes the duality of order (dense set of orbits) and unpredictability (SIC); it also combines metric (SIC) and topological (dense character) properties.

In fact, it may be demonstrated that (2.) and (3.) imply (1.).

## 11.2 Chaos in other dynamical systems

The (2 mod 1) map is a starting point to demonstrate chaos in other dynamical systems. To this end, one must find an approach to transfer knowledge from this iteration to other ones. We will briefly review here two approaches.

### 11.2.1 The itinerary approach

**DEFINITION 30 Itinerary**

Consider a set of disjoint intervals forming $\Omega$, that is, $\Omega = \bigcup_i \Omega_i$ with $\Omega_i \cap \Omega_j = \emptyset$ for $i \neq j$. Consider the suite obtained $x_i$ from the iteration $f$. The *itinerary* associated with an initial condition $x_0$ is the suite of indices $s_1, s_2 \ldots$ corresponding to the visited subsets, i.e., $x_{s_i} \in \Omega_{s_i}$.

As a general rule, we expect some information loss when we express the original orbit as its itinerary. But there are special cases, and the $(2 \mod 1)$ map associated with the partition $\Omega_1 = [0, \frac{1}{2}[$ and $\Omega_2 = [\frac{1}{2}, 1[$ is one such special case. There is a bijection between the ensemble $\Omega$ and the ensemble of itineraries, quite obviously so given the fact that the itinerary maps the binary representation of numbers.

Now, consider the tent map. We expect that it behaves somehow similarly to the $(2 \mod 1)$ map but we need the right trick to prove it. This is what itineraries are for. In (very) brief:

- ▷ we can find a mapping between the set of itineraries of the tent map, and the ensemble $\Omega$. Again, we consider the binary representation of numbers, i.e., for $x \in \Omega$, with its binary representation $.b_1 b_2 b_3 \ldots$, one can show (in very brief) that its itinerary will be $s_0 = b_1$ and $s_n = |b_n - b_{n+1}|$. The demonstration (skipped here) consists in demonstrating that any distinct itinerary generates a specific series of $b_1$, thus a unique number in $\Omega$. In other words, any number in $\Omega$ can be denoted by its equivalent itinerary, which we could note $\sim s_1 s_2 s_3 \ldots$.
- ▷ We then observe that the action of the iteration $f$ on $\sim s_1 s_2 s_3 \ldots$ is similar to the action of the $(2 \mod 1)$ map on the binary representation $.b_1 b_2 b_3 \ldots$. All the demonstrations made for the $(2 \mod 1)$

map will work here. The two systems behave similarly.

### 11.2.2 The topological equivalence

We have already defined the notion of topological equivalence for continuous dynamical systems. In brief, there is topological equivalence between two dynamical systems if the domain $\Omega$ can be deformed continuously such as to make the two dynamical systems correspond to each other. Specifically, consider two dynamical systems $f$ and $g$, with $f : \Omega \to \Omega$ and $g : \Omega' \to \Omega'$; there is topological equivalence if there is an homeomorphism $C : \Omega \to \Omega'$ with $C \circ f = g \circ C$. The topological equivalence preserves the $k-$periodic character of orbits, the dense character of orbits, and there repelling-attracting properties. Again, the demonstration rests on the notion of itineraries. One can define to *topologically equivalent* partitions, and given the continuous character of $C$, with such smart partitioning, the dynamical systems $f$ and $g$ iterated from two equivalent points can be associated with the same itineraries.

So, a successful approach to demonstrate the chaotic character of orbits in the logistic equation is to find a topological equivalence with the tent map. Remarkable fact, the topological equivalence can be made explicit. Indeed, the logistic orbit with $r = 4$, that is, the iteration $f : 4x(1-x)$ is topologically equivalent to the tent map $g$ by the homeomorphism $C(x) = \frac{1}{2}1 - \cos(\pi x)$. Indeed, taking the above notation:

- $g(C(x)) = 4\frac{1}{2}(1-\cos(\pi x))\frac{1}{2}(1+\cos(\pi x)) = \sin^2 \pi x$
- $C(f(x)) = \sin^2 \pi x$ (to be verified for the two subcases $x \leq \frac{1}{2}$ and $x > \frac{1}{2}$.

In other words, given a smart choice of partitions, the tent map and the logistic equation with $r = 4$ will generate the same itineraries,

and given that the metrics can be adjusted to work in both sets (two points close to each other in $\Omega$ will remain close to each other in $C(\Omega)$, properties such as density and closeness will be preserved.

# 12 The circle map

## 12.1 Circle map

(These notes are in draft mode. – there are many shortcuts and this is only support to more developed explanation given in class. This is not exam material. )

The circle map provides an model to study and understand flow which display limit cycles. The circle map may be understood as the Poincaré section of a continuous dynamical system: we observe the position the position of the system everytime one of the control angles of the system has been one rotation (it has progressed by an angle $2\pi$). Alternatively, the circle map may be understood as a stroboscopic map: the system position is fixed every time interval.

A circle map maps the interval $[0, 1]$ onto itself. It is a convention to name the variable $\theta$, which symbolises the number of rotations (an angle divided by $2\pi$).

In its simplest version, the circle map reads

$$\theta_{n+1} = f(\theta_n) = \theta_n + \Omega \text{mod} 1 \tag{29}$$

$\omega$ is thus a simple rotation, which, typically, can be understood as an external periodic force perturbing the system.

The operator mod1 effectively keeps $\theta$ in the $[0, 1]$ interval.

Below we represent cobweb diagrams, for $\Omega = 0.2$ and $\Omega = 0.6$, respectively.

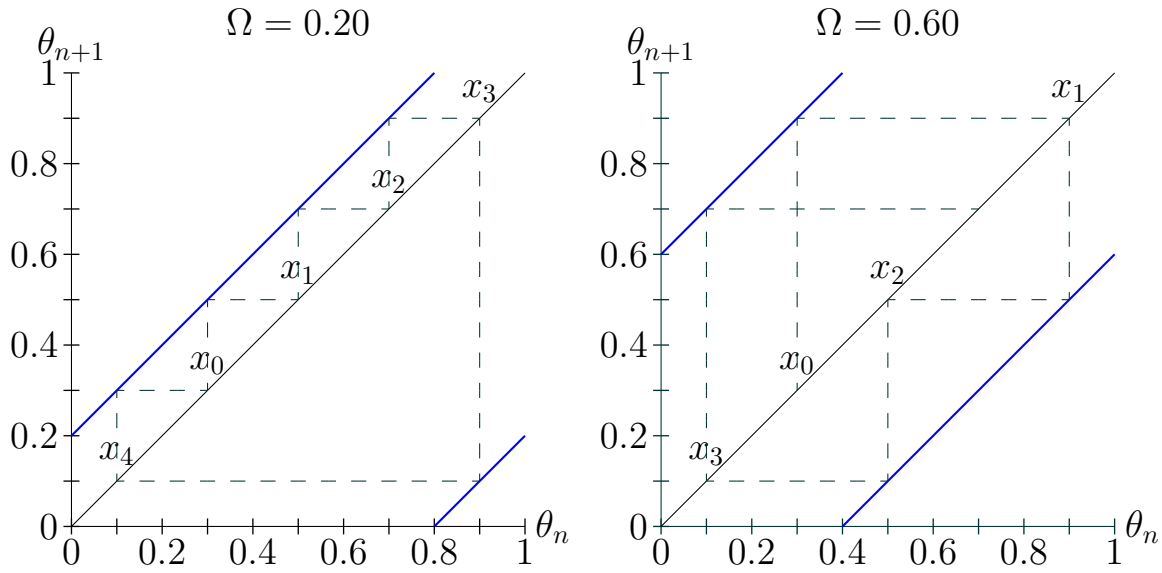




As long as $\Omega$ is a rational number $p/q$, the system will be periodic with period $q$ (here, respectively, q=5 and 3). Later in this chapter, we will sometimes call $\Omega$ the *input* frequency, or, more properly, the input frequency *ratio*, in the sense that everything here is expressed in terms of adimensional units.

The *winding number* is the average number of rotations achieved by the system between two observations.

It is defined as,

$$w = \lim_{n\to\infty} \frac{f^n(\theta_0) - \theta_0}{n} \tag{30}$$

assuming that the limit exist for any initial condition $\theta_0$. For the simple map given in Eq. (29), $w = \Omega$.

Now we consider a more complex example, when the simple map is

further perturbed by a nonlinearity of amplitude $K$:

$$\theta_{n+1} = \theta_n + \Omega - \frac{K}{2\pi}\sin(2\pi\theta) \text{ mod}1. \tag{31}$$

When $\Omega$ is small enough, the system may admit fixed points. This is obtained when the following condition is fulfilled:

$$\theta = \theta + \Omega - \frac{K}{2\pi}\sin(2\pi\theta)$$

As a general rule, we may expect at least one fixed point when $K \geq 2\pi\Omega$, but further inspection of $f'(\theta)$ will show that stability is lost when $K$ gets too large (stability requires $0 < K\cos 2\pi\theta < 2$).



The fixed point obtained when $\Omega$ is small is called a $0:1$ synchronisation. Indeed, we see that the non-linear perturbation is distributed with a period 1 along $\theta$. Hence the number 1. On the other hand, input (driving) force materialised by $\Omega$ is close to zero. This is where the $0:1$ notation comes from. The non-linear perturbation has stopped the natural progression of $\theta$.

However, identical behaviours would be obtained for $\Omega$ slightly smaller than 1: indeed, $\Omega = 0$ and $\Omega = 1$ act in fact very similarly because of the *modulo*1 in the equation. This phenomenon is called *aliasing*.

So far, we identified two synchronisation regimes should appear for $\Omega$ near zero and near 1. Chances of synchronisation increase as $K$ increases, as long as it is not too large.

(diagram to be drawn in class).

Now, as the input frequency $\Omega$ increases, other synchronisation are possible.

Below are two examples. First, take $K = 0.8$, and $\Omega = 0.49$: we represent, on the left-hand-side, the map with a Cobweb diagram, and, on the right-hand-side, the $f^2$ map, which clearly has three stable fixed points, corresponding to the two points being visited by the 2-periodic iteration. This is a case of $\frac{1}{2}$ synchronisation: the action of $\Omega$ is to increase, at every time step, the number of rotation by a little bit less than $\frac{1}{2}$. This is not quite 0.5, but the non-linearity makes it possible to find a sweet spot for $\theta$ such that that the $\Omega$ forcing is enough to enough to meet the next fixed-point of the 2-period iteration.

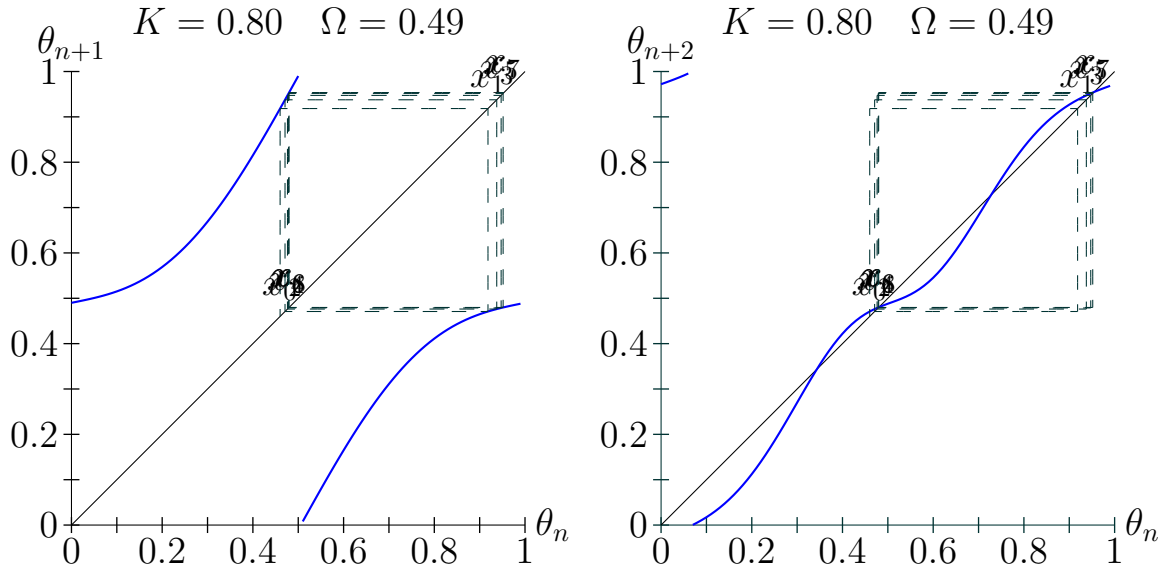


Next, we show a case of $2:3$ iteration, this time obtained for $\Omega = 0.65$. $\Omega$ is not quite $2:3$, but again, non-linearity effectively allows for some tolerance and, in this case, we have synchronisation.

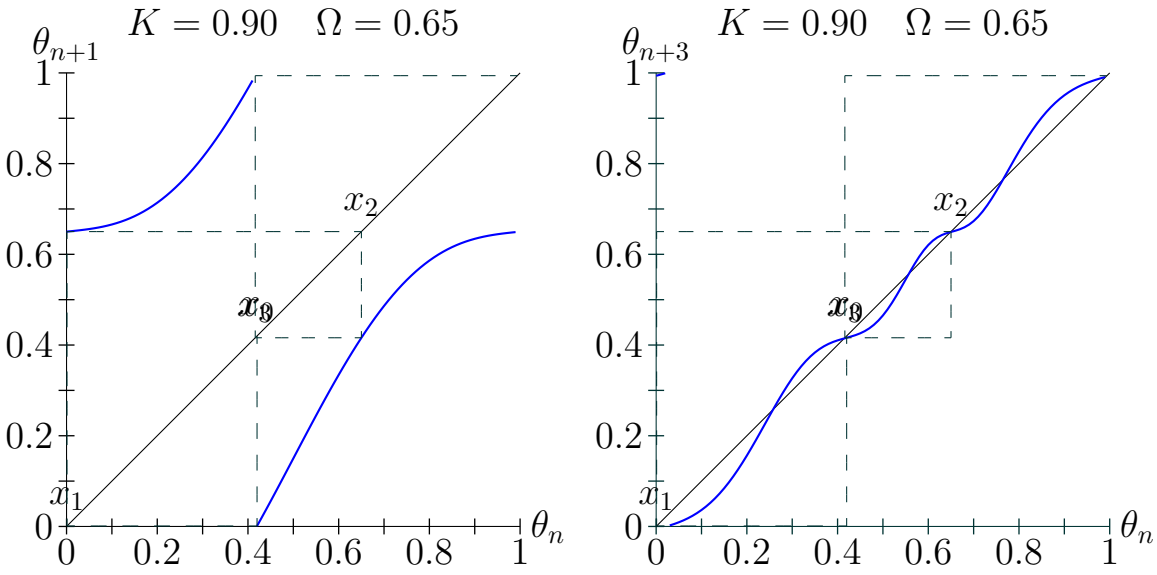


We have just shown synchronisation examples, but in many cases, synchronisation does not occur: there is no fixed point for any iteration, as long as you want it to be.

It is common to represent frequency-locking regimes on a diagram of $\Omega$ vs $K$. Frequency-locking regimes are organised in so-called *Arnold tongues*, named after the Russian mathematician who studied the circle map. The diagram of Arnold tongues is symmetric around $\Omega = 0.5$. Outside the synchronisation regime, $\theta$ is non-periodic, and it will therefore meet all values in the interval $[0, 1]$.

Remember that we defined the circle map as a sketch of what could be the Poincaré section of a continuous dynamical system. If there is synchronisation, the full, continuous system, will appear as periodic, crossing the Poincaré section at a (small) number of points. If there is no synchronisation, then the circle map will appear as the Poincaré section of a torus, and the corresponding trajectories of the continuous dynamical system will be quasi-periodic.

(Arnold tongues at the end of the Jupyter-notebook demo, see below)

With this reasoning, one might think any bare winding number that is rational $p/q$ can be synchronised as long as $K$ is large enough. This actually is what happens for $K = 1$.

There is, for that particular value of $K$, an infinite number of synchronisation regimes, which can be seen as an infinite number of small steps in the diagram of the measured winding number (the *output* frequency) vs the *input* frequency ratio $\Omega$. This is a particular case where the length of the interval of $\Omega$ occupied by synchronisation regime is indeed equal to 1.

[1]:
```
using Plots

omegan = [0:0.002:1.;];
K = 1.0;

function winding(Omega, K)
    x0 = 0.3;
    x = x0;
    n = 1000;
    for i in 1:1:n
      x = x + Omega - K/(2*pi) * sin(2*pi*x)
    end
    x0 = x;
    n = 10000;
    for i in 1:1:n
      x = x + Omega - K/(2*pi) * sin(2*pi*x)
    end
    w = (x-x0)/n
end

staircase = map(x -> winding(x, 0.5), omegan);
plot(omegan, staircase, title="K=0.5")


staircase = map(x -> winding(x, 1.0), omegan);
plot(omegan, staircase, title="K=1")

annotate!(0.2, 0.25,"\$\\frac{1}{4}\$")
annotate!(0.3, 0.33,"\$\\frac{1}{3}\$")
annotate!(0.6, 0.50,"\$\\frac{1}{2}\$")
annotate!(0.45, 2/5,"\$\\frac{2}{5}\$")
annotate!(0.55, 3/5,"\$\\frac{3}{5}\$")
annotate!(0.70, 2/3,"\$\\frac{2}{3}\$")
```

[1]:
```
annotate!(0.80, 3/4,"\$\\frac{3}{4}\$")
```

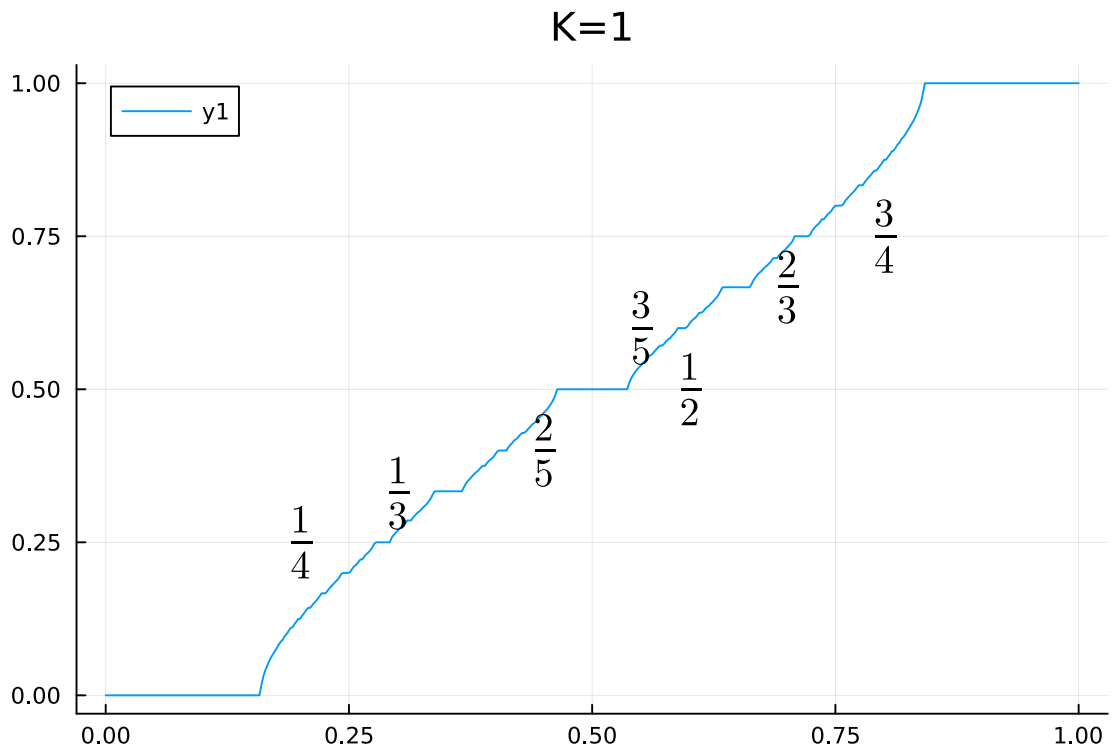


[2]:
```
Ks = [0:0.001:1;]
Omegas = [0:0.001:1;]
tol = 1.e-4

W = map(Iterators.product(Ks, Omegas)) do (K, Omega)
    winding(Omega, K)
end

# filter

WG = map(W) do (x)
   flag = 1
   for test in [0, 1, 1/2, 1/3, 2/3, 1/4, 3/4, 1/5, 2/5, 3/5, 4/5, 3/8, 7/8]

            if (abs(x-test) < 1.e-5) flag = 0   end
    end
    flag
```

```
end;
```

[3]:
```
plot(Ks[end:-1:begin], Omegas, Gray.(WG[end:-1:begin,:]))
xlabel!("\$\\Omega\$")
ylabel!("K")
xlims!(0,1)
xticks!([0,1/4,1/3,1/2,2/3,1], ["0", "\$\\frac{1}{4}\$", "\$\\frac{1}{3}\$",␣
↪"\$\\frac{1}{2}\$", "\$\\frac{2}{3}\$", "1"])
title!("Arnold tongues -- non-linear circle map")
```

[3]:

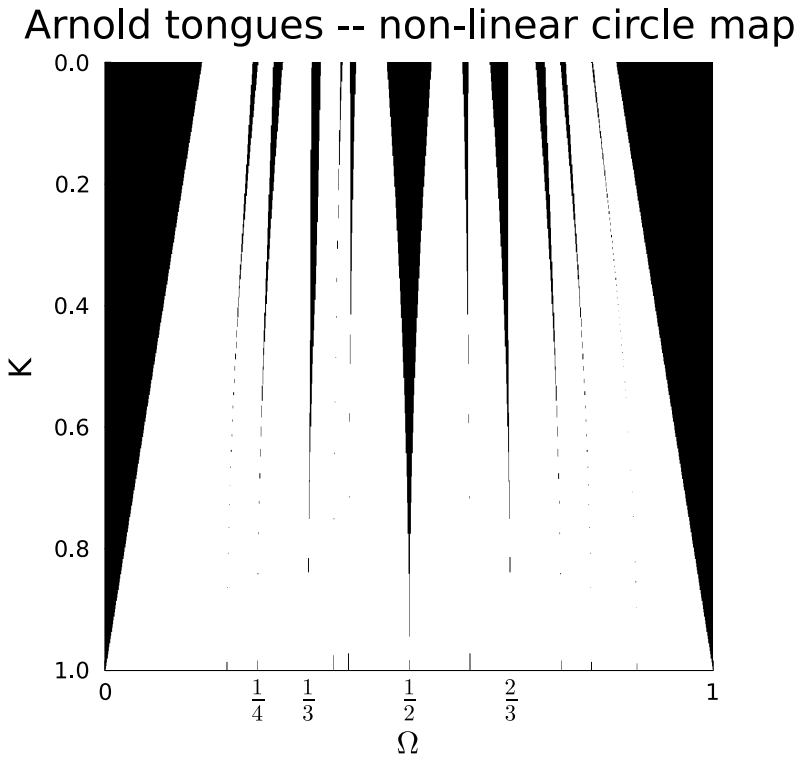


[ ]:
```

```

When $K > 1$, the map ceases to be invertible, in the sense that for a given value of $\theta_{n+1}$, two values of $\theta_n$, in the interval of $[0, 1]$ are possible. Synchronisation regimes remain possible, but it may be shown that they gradually loose stability.

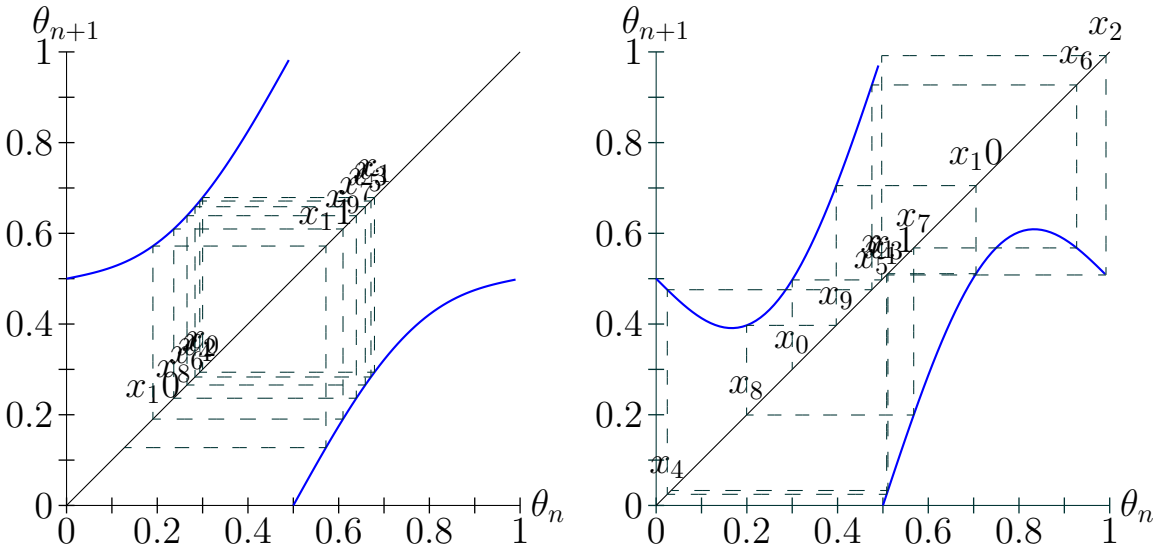


Similar to what has been observed in the logistic map, the stable orbits undergo a succession of bifurcations which are increasingly close to each other, forming the *quasi-period route* to chaos.

# A Appendix: Analysis of the Lorenz 1963 model with Maxima

Here we analyse the fixed points and their stability of the Lorenz - Saltzman model using a symbolic mathematical software Maxima. It is based on the functional programming language lisp. This is not the only software around. Wolfram Mathematica is a well-known, very powerful software under paid licence. Matlab also has a symbolic maths package; SymPy has reached a good level of maturity and presents the huge advantage to be in Python, giving access to the `Jupyter` notebook interface and the `matplotib` interface. This is probably the recommended alternative for someone starting from scratch. Some more discussion of SymPy vs Maxima is available at https://github.com/sympy/sympy/wiki/SymPy-vs.-Maxima.

We first define the system with the three time derivatives:

[20]:
```
dX(X,Y,Z):= σ * (Y-X);
dY(X,Y,Z):=X*(ρ - Z) - Y;
dZ(X,Y,Z):=X*Y - β * Z;
assume(σ>0, ρ>0, β>0);
```
[20]:

$$dX\,(X,Y,Z) := \sigma\,(Y-X) \tag{\%o31}$$

[20]:

$$dY\,(X,Y,Z) := X\,(\rho-Z)-Y \tag{\%o32}$$

[20]:

$$dZ\,(X,Y,Z) := X\,Y-\beta\,Z \tag{\%o33}$$

[20]:

$$[\sigma>0,\rho>0,\beta>0] \tag{\%o34}$$

Solving for all derivatives to be zero generates the fixed points.

[21]:
```
eq1: dX(X,Y,Z)=0;
eq2: dY(X,Y,Z)=0;
eq3: dZ(X,Y,Z)=0;
```
[21]:

$$(Y-X)\,\sigma = 0 \tag{\%o35}$$

[21]:

$$X\,(\rho-Z)-Y = 0 \tag{\%o36}$$

[21]:

$$X\,Y - Z\,\beta = 0 \qquad (\%o_{37})$$

[22]:
```
sols:solve([eq1,eq2,eq3],[X,Y,Z]);
```
[22]:

$$\left[\left[X = \sqrt{\beta}\,\sqrt{\rho-1}, Y = \sqrt{\beta}\,\sqrt{\rho-1}, Z = \rho-1\right], \left[X = -\left(\sqrt{\beta}\,\sqrt{\rho-1}\right), Y = -\left(\sqrt{\beta}\,\sqrt{\rho-1}\right), Z = \rho-1\right], [X=0, Y=0, Z=0]\right] \qquad (\%o_{38})$$

We recognize the trivial fixed point, as well as the two symmetric fixed points on both sides of the $z-$axis, which take real values only for $\rho > 1$.

The Jacobian of the derivatives is computed as follows:

[23]:
```
J:jacobian([dX(X,Y,Z),dY(X,Y,Z),dZ(X,Y,Z)],[X,Y,Z]);
```
[23]:

$$\begin{pmatrix} -\sigma & \sigma & 0 \\ \rho - Z & -1 & -X \\ Y & X & -\beta \end{pmatrix} \qquad (\%o_{39})$$

We first evaluated the Jacobian at the trivial fixed point and consider its eigenvalues. **Maxima** gives us the three eigenvalues and their multiplicity. The **rhs** and **lhs** functions return the right-hand-side and left-hand-side of an expression, respectively

[24]:
```
J0:psubst(sols[3],J);
```
[24]:

$$\begin{pmatrix} -\sigma & \sigma & 0 \\ \rho & -1 & 0 \\ 0 & 0 & -\beta \end{pmatrix} \qquad (\%o_{40})$$

[25]:
```
simp:true$
eJ0:eigenvalues(J0);
```
[25]:

$$\left[\left[-\left(\frac{\sqrt{\sigma^2+(4\,\rho-2)\,\sigma+1}+\sigma+1}{2}\right), \frac{\sqrt{\sigma^2+(4\,\rho-2)\,\sigma+1}-\sigma-1}{2}, -\beta\right], [1,1,1]\right] \qquad (\%o_{42})$$

We recognise the double root (first and second solutions), and the $-\beta$ eigenvalue along the $z$ axis. The trivial fixed point becomes a saddle when the first (and second) eigenvalue reach zero:

```
[26]: solve(eJ0[1][2],ρ);
[26]:
```

$$[\rho = 1] \qquad (\%o_{43})$$

Consider now the non-trivial fixed point, which become real for $r > 1$.

```
[27]: assume(ρ>1);
[27]:
```

$$[\rho > 1] \qquad (\%o_{44})$$

```
[28]: J1:psubst(sols[1],J);
[28]:
```

$$\begin{pmatrix} -\sigma & \sigma & 0 \\ 1 & -1 & -\left(\sqrt{\beta}\,\sqrt{\rho-1}\right) \\ \sqrt{\beta}\,\sqrt{\rho-1} & \sqrt{\beta}\,\sqrt{\rho-1} & -\beta \end{pmatrix} \qquad (\%o_{45})$$

We could repeat the approach for the non-trivial fixed points and also ask `maxima` to compute the eigenvalues but this is unwise. The expressions are very heavy and we can do better. Heaving a computer algebra system should not stop us from thinking. Indeed, consider rather the characteristic polynomial $P(\lambda;\beta,\sigma,\rho)$, defined as the determinant $\det(\lambda 1 - J)$ matrix.

```
[29]: carpol:rat(determinant(diagmatrix(3,λ)-J1), λ);
[29]:
```

$$\lambda\,(\beta\,\sigma+\beta\,\rho)+\lambda^2\,(\sigma+\beta+1)+(2\,\beta\,\rho-2\,\beta)\,\sigma+\lambda^3 \qquad (\%o_{46})$$

```
[30]: dcarpoldl:diff(carpol,λ);
[30]:
```

$$\lambda\,(2\,\sigma+2\,\beta+2)+\beta\,\sigma+\beta\,\rho+3\,\lambda^2 \qquad (\%o_{47})$$

For positive values of the parameters, all coefficients of the polynomial are positive, and the theory of cubic equations tells us that, in this case, all roots *must* be either real negative, or complex. It is easy enough to consider the case $r = 1$, at which the roots are all real, and negative. By continuity, we expect all roots to be real negatives for $r$ slightly above 1. But they could become imaginary.

This transition from negative real to imaginary roots occurs when two roots merge, and occur at an extrema of the $P(\lambda)$. Assuming $\beta$ and $\sigma$ given, the critical value of the parameter $r$ (called $r_1$) at which roots become complex must therefore satisfy $P(\lambda;r) = P'(\lambda;r) = 0$ (where the $'$ symbol denotes a derivative with respect to $\lambda$). So we first solve $P'(\lambda;r)$.

A

[31]:
```
SS:solve(dcarpoldl, λ)$
SS[1];
SS[2];
```
[31]:

$$\lambda = -\left(\frac{\sqrt{\sigma^2+(2-\beta)\,\sigma-3\,\beta\,\rho+\beta^2+2\,\beta+1}+\sigma+\beta+1}{3}\right) \tag{\%o49}$$

[31]:

$$\lambda = \frac{\sqrt{\sigma^2+(2-\beta)\,\sigma-3\,\beta\,\rho+\beta^2+2\,\beta+1}-\sigma-\beta-1}{3} \tag{\%o50}$$

The roots naturally have the form $\lambda_{\pm} = a \pm \sqrt{b}$ and we inspect here the $\lambda_+$ solution (this is the solution for the local minimum, which comes as the second root; see graph below). We substitute this solution in the expression for $P(\lambda; r)$:

[34]:
```
S3:ev(subst(SS[2], carpol), σ=10, β=8/3);
```
[34]:

$$\frac{\left(\sqrt{\frac{961}{9}-8\,\rho}-\frac{41}{3}\right)(8\,\rho+80)}{3}+160\,\rho+\frac{\left(\sqrt{\frac{961}{9}-8\,\rho}-\frac{41}{3}\right)^3}{9}+\frac{41\left(\sqrt{\frac{961}{9}-8\,\rho}-\frac{41}{3}\right)^2}{9}-160}{3} \tag{\%o53}$$

And the critical value for $r$ that we are looking for is the one that will make this expression equal to zero. As the algebraic expression is involved, we provide here a numerical estimate of the root.

[35]:
```
r1 : find_root(S3, ρ, 1, 3);
```
[35]:

1.3456171792329563 (%o54)

We show the behaviour of $P(\lambda)$ for different values of $r$ and this will help us to visualise the specific behaviour at $r$:

[39]:
```
r1;
setoption(legend, "ρ=0.9","ρ=1.3456","ρ=1.7")$
plot2d([ev(carpol, σ=10, β=8/3, ρ=0.9),
        ev(carpol, σ=10, β=8/3, ρ=1),
        ev(carpol, σ=10, β=8/3, ρ=1.7)],
        [λ,-12,0], [legend,"ρ=0.9","ρ=ρ_crit","ρ=1.7"],
        [gnuplot_term, png])$
```
[39]:

1.3456171792329563 (%o64)

```
rat: replaced -5.333333333333332 by -16/3 = -5.333333333333333

rat: replaced 29.066666666666666 by 436/15 = 29.066666666666666

rat: replaced 37.333333333333336 by 112/3 = 37.333333333333336

rat: replaced 31.200000000000003 by 156/5 = 31.2
```

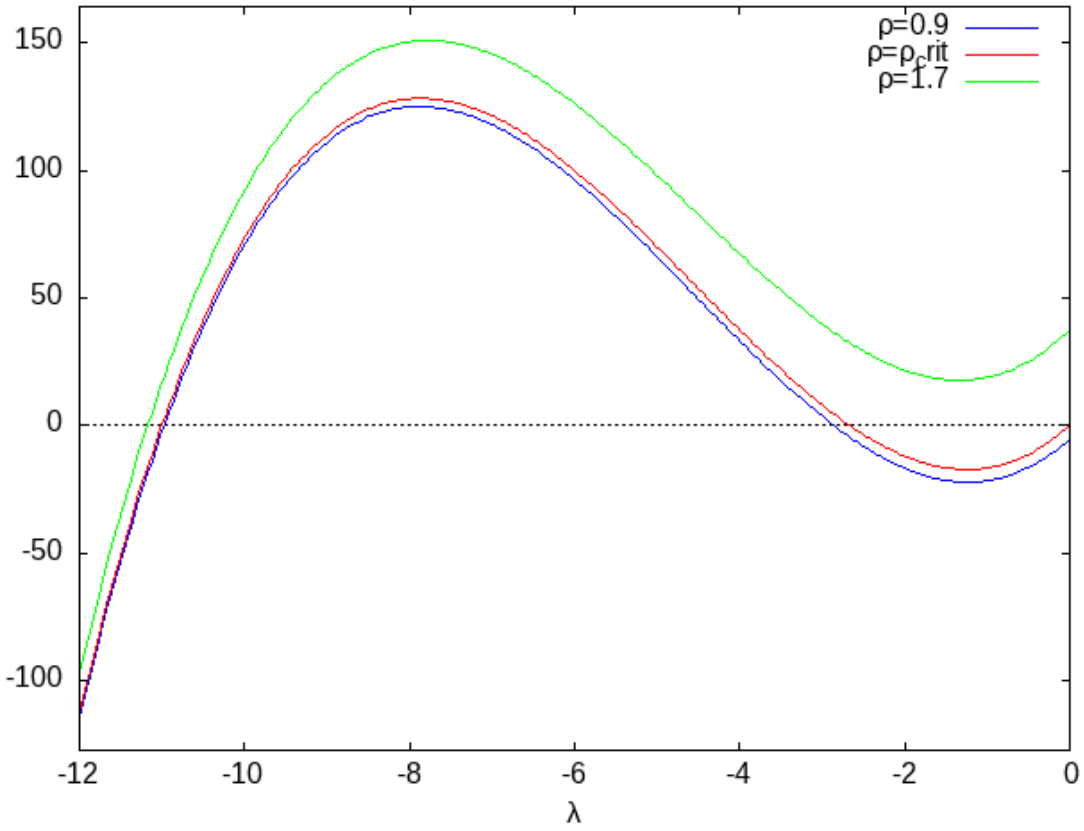

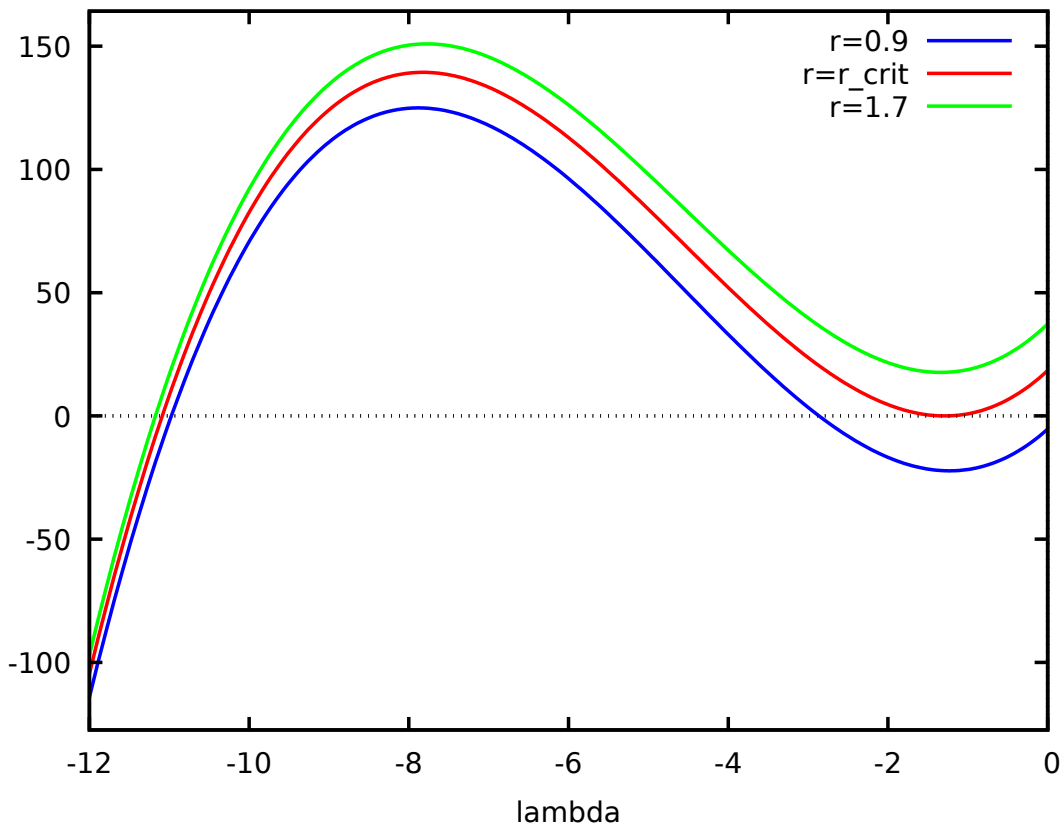


All we can say at this point is that for $r > r_1$ the roots are complex, but numerical inspection shows that the points still act as attracting centers. They become repellers when the real part of the eigenvalue becomes positive. The critical value of the parameter $r$ from where instability emerges, called $r_H$, must then satisfy $P(i\omega; r) = 0$, for real, non-zero $\omega$. This will be the boundary between negative and positive real parts. The correspoding equation reads:

[45]:
```
eqw:subst([λ=sqrt(-1)*ω], carpol);
```
[45]:

$$-\left(i\,\omega^3\right)-\left(\sigma+\beta+1\right)\,\omega^2+i\,\left(\beta\,\sigma+\beta\,\rho\right)\,\omega+\left(2\,\beta\,\rho-2\,\beta\right)\,\sigma \qquad (\%o_{77})$$

And given that all parameters are real, it actually generates two equations by considering together the real and imaginary parts. Solving the combination gives:

[46]:
```
SOL:solve([realpart(eqw), imagpart(eqw)], [ρ,ω])$
SOL[1];
SOL[2];
```
[46]:

$$[\rho = 1, \omega = 0] \tag{\%o79}$$

[46]:

$$\left[\rho = \frac{\sigma^2 + (\beta + 3)\,\sigma}{\sigma - \beta - 1}, \omega = -\left(\frac{\sqrt{2}\,\sqrt{\beta}\,\sqrt{\sigma}\,\sqrt{\sigma + 1}}{\sqrt{\sigma - \beta - 1}}\right)\right] \tag{\%o80}$$

Again we have two roots but the trivial one $\omega = 0$ does not interest us. The second is the relevant one, which we evaluate for the canonical parameers of the Lorenz model:

[47]:
```
rh:ev(rhs(SOL[2][1]), σ=10, β=8/3);
```
[47]:

$$\frac{470}{19} \tag{\%o81}$$

[48]:
```
float(rh);
```
[48]:

$$24.736842105263158 \tag{\%o82}$$

And allows us to conclude about the critical parameter $\rho_H$.

# B Appendix: Analogy of the tent map in the Lorenz - Saltzman model

We pursue our analysis of the Salzman Model Lorenz by reproducing a result actually published by Lorenz 1963, who wanted to have a compelling intuition of the chaotic character of the model, in the chaotic regime. Julia is a strongly-typed language, mainly imperative, that is quite efficient for numerical simulation; as it also integrates Python's matplotlib, it seems to get the best of all worlds for numerical simulation.

[1]:
```
using ODE
using Pkg
```

The Lorenz model can be simply defined and, as we see it, Julia accepts greek symbols.

[2]:
```
function lorenz(t,u)
    σ,ρ,β = p
    dxdt = σ*(u[2]-u[1])
    dydt = u[1]*(ρ-u[3]) - u[2]
    dzdt = u[1]*u[2] - β*u[3]
    [dxdt;dydt;dzdt]
end
```

[2]:
```
lorenz (generic function with 1 method)
```

We know carry out the numerical integration, with the `ode45` Runge-Kutta integration some of you will already be familiar with, on a time grid

[4]:
```
p=(10, 28, 8/3)
dt = 0.001
tf = 100.0
t  = collect(0:dt:tf)
u0=[0.;0.1;0.1]
(t, u) = ode45(lorenz, u0, t);
```

The following commands simply map the three components of the $u$ matrix on vectors $x$, $y$ and $z$.

[5]:
```
x = map(v -> v[1], u)
y = map(v -> v[2], u)
z = map(v -> v[3], u);
```

[6]:
```
using Plots
plot(t,x)
```

[6]:

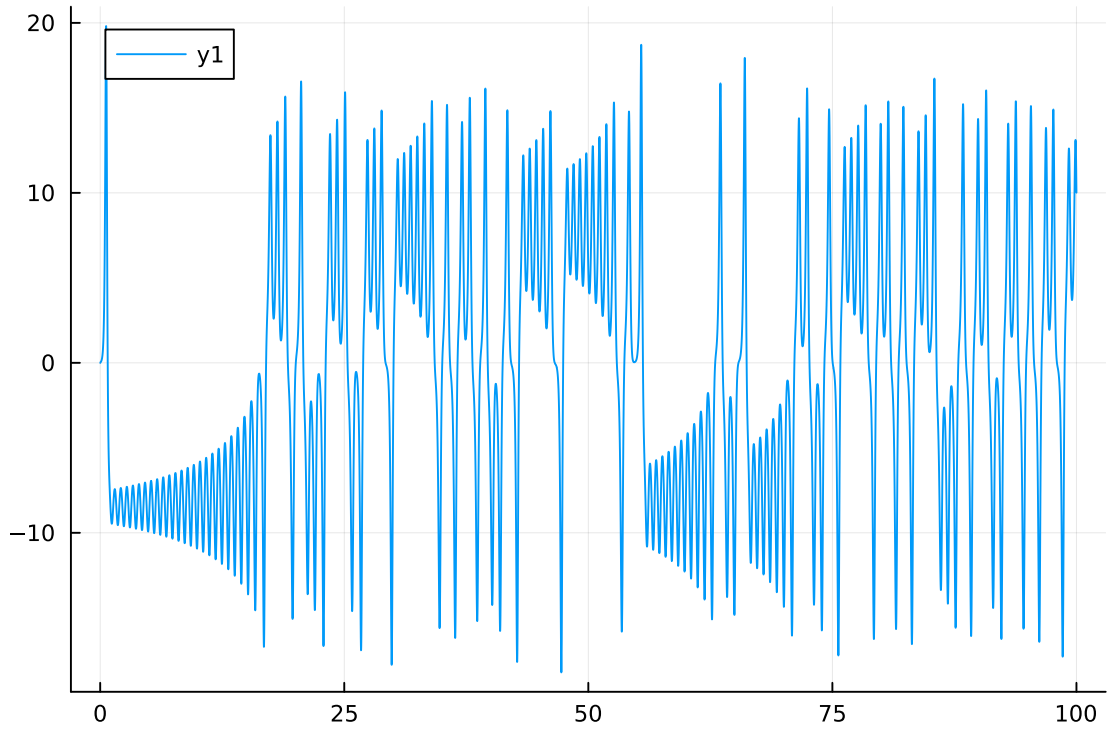




We now use the `Peaks` contributed package to extract the local maxima of the $z-$series

[9]:
```
using Peaks;
```

[10]:
```
Zmax=findmaxima(z);
```

and we plot this series with respect to that same series shifted by one element. Mathematically, we plot $Z_{i+1}$ agains $Z_i$, where $Z$ is the series of maxima

[11]:
```
Zmax1 = Zmax[2][1:(length(Zmax[2]))-1];
Zmax2 = Zmax[2][2:(length(Zmax[2]))];
```

[12]:
```
plot(Zmax1,Zmax2, seriestype = :scatter);
```

[13]:
[13]:
```
plot!([30,45],[30,45])
```

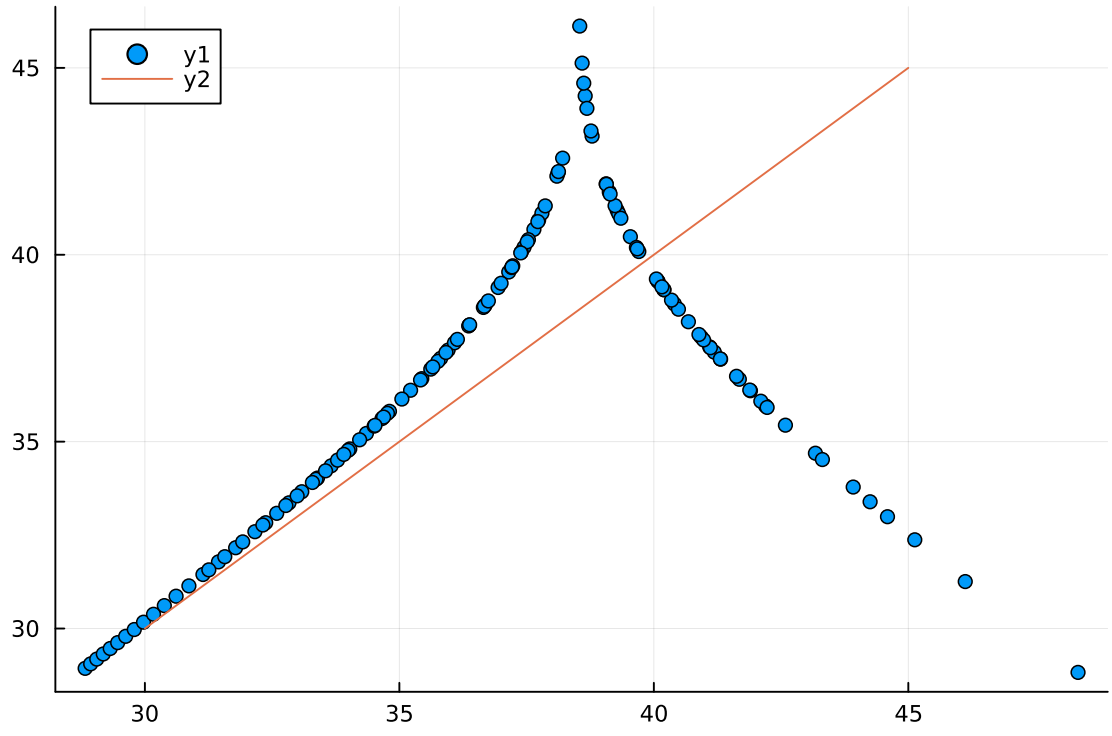


As we see it, the series of $Z$ behaves as a tent-map which, as we will see in the coming section, is indeed chaotic.

[ ]:

# C Appendix: Numerical computation of the largest Lyapunov exponent in the Lorenz-Saltzman model

We now compute the largest Lyapunov exponent according to the algorithm of Benettin 1980. Again, define the Lorenz model

[1]:
```
using ODE
using Pkg
using LinearAlgebra
using Plots
```

The Lorenz model can be simply defined and, as we see it, Julia accepts greek symbols. We provide a function of the parameters, which returns the Lorenz model.

[2]:
```
function lorenz_model(σ,ρ,β)
    function lorenz(t,u)
        dxdt = σ*(u[2]-u[1])
        dydt = u[1]*(ρ-u[3]) - u[2]
        dzdt = u[1]*u[2] - β*u[3]
        [dxdt;dydt;dzdt]
    end
    return(lorenz)
end
```

[2]:
```
lorenz_model (generic function with 1 method)
```

We produce a time series, as in Appendix B.

[3]:
```
dt = 0.01
tf = 2000.0
t  = collect(0:dt:tf)
u0=[0.1;0.1;0.1]
σ=10
β=8/3.
ρ=28.
(t, u) = ode45(lorenz_model(σ,ρ,β), u0, t);
```

We now consider the dynamics of a first-order perturbation $\delta u$ evaluated in $u$:

[4]:
```
function lorenz_linear_tangent(σ,ρ,β)
    function linear_tangent(δu,u)
        dδxdt =  -σ*δu[1] + σ*δu[2]
        dδydt =  (ρ-u[3])*δu[1] - δu[2] - u[1]*δu[3]
        dδzdt =  u[2]*δu[1] + u[1]*δu[2] - β*δu[3]
        return([dδxdt; dδydt ; dδzdt ])
    end
    return(linear_tangent)
end
```

[4]:
```
lorenz_linear_tangent (generic function with 1 method)
```

We consider an arbitrary initial perturbation $\delta u$ of norm $||\delta u|| = 1$, and code it as a column vector

[5]:
```
deltau=[0;1.;0.]
```

[5]:
```
3-element Vector{Float64}:
 0.0
 1.0
 0.0
```

[6]:
```
function iterate_lyapunov(linear_tangent, deltau, u, spinup, iren)

    lambda=1. ; time = 0;
    lambdas=[];
    times=[];
    δu = deltau;
    i=0; j=0;
    for u_ in u;
        # the second order scheme appears here crucial to have good-enough results
        predictor = δu + linear_tangent(δu,u_)*dt
        δu += 0.5*(linear_tangent(δu,u_) +  linear_tangent(predictor,u_)) *dt
        i+=1;
        j+=1;
        if (i==iren);
            ndu = norm(δu)
            δu=δu/ndu
            i=0;
            if(j > spinup);
                time += dt*iren
                lambda+=log(ndu)
                append!(lambdas,lambda)
                append!(times, time)
            end;
        end;
    end
    return(times, lambdas)
end
```

[6]:
```
iterate_lyapunov (generic function with 1 method)
```

[7]:
```
(times,lambdas)=iterate_lyapunov(lorenz_linear_tangent(σ,ρ,β),
    deltau, u,70000,90);
plot( lambdas ./ times)
```

[7]:

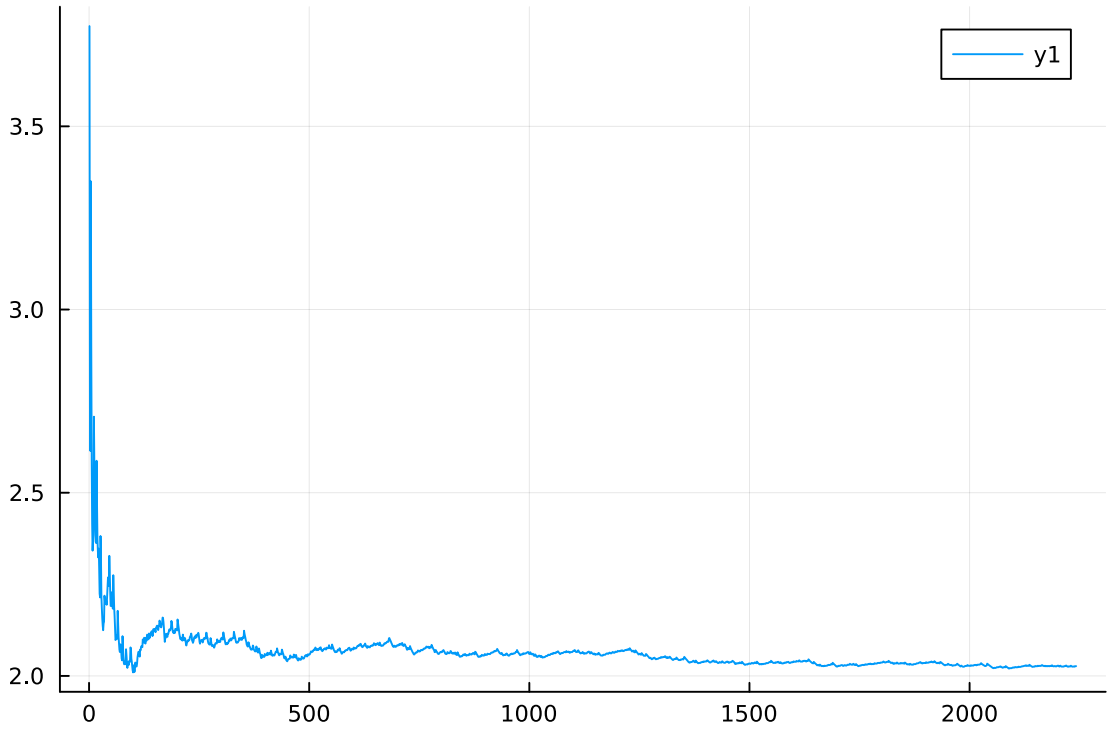


[8]:
```
print(last(lambdas)/last(times))
```

```
2.026722095607501
```

We now wrap up these operations in a function to see the evolution of the largest Lyapunov exponent with $\rho$

[9]:
```
function largestlyap(ρ)
    u0=[0.;0.1;0.1]
    (dummyt,u) = ode45(lorenz_model(σ,ρ,β), u0, t);
    δu=[0;0;1.]
    (times,lambdas)=iterate_lyapunov(lorenz_linear_tangent(σ,ρ,β), δu, u,120000,90)
    last(lambdas)/last(times)
end
```

[9]:
```
largestlyap (generic function with 1 method)
```

[14]:
```
largestlyap(24)
```

[14]:
```
-0.021019446097914816
```

[11]:
```
rhos=collect(1:.4:40)
lambdas = map(largestlyap,rhos);
```

[12]:
```
plot(rhos,lambdas, legend=false)
```
[12]:

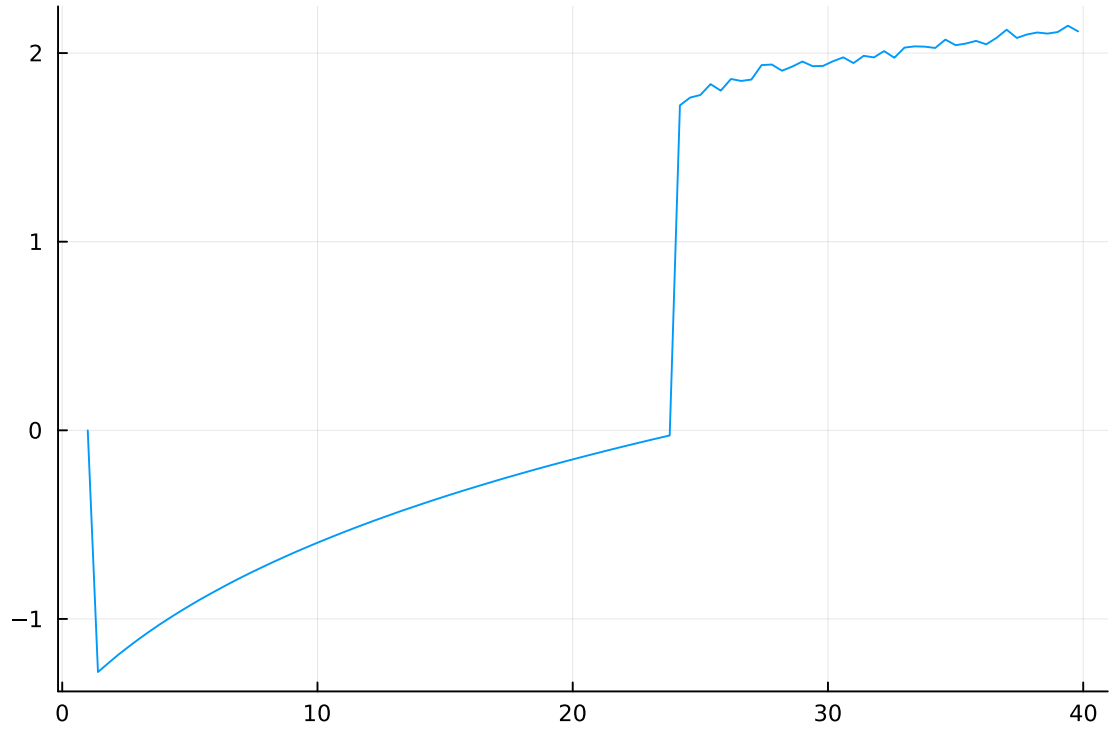


As we see it, the chaotic behaviour emerges for the $r_H$ value that we have predicted analytically.

[13]:
```
rhos[first(findall(lambdas .> 0))]
```

[13]:
```
24.2
```

Note that for further reference, there is actually a Julia library doing this efficiently: https://juliadynamics.github.io/DynamicalSystems.jl/v0.9/chaos/lyapunovs/ I really invite you to exlpore this impressive library.

[ ]:

[ ]:

# D Appendix: Miscellaneous notes

## D.1 Jordan canonical form theorem

The full explanation of the Jordan canonical form theorem is available in [HJ90], Chapter 3, and see its Theorem 3.4.5 for applications in real vector spaces.

The Jordan canonical form theorem states for any linear application, it is possible to find a basis of vectors (called the *genrealised eigenvectors*) such that the application can be expressed as a matrix with Jordan blocs. A Jordan block $J_i$ is a square matrix with a same value $\lambda_i$ on the diagonal, and ones on the upper diagonal:

$$J = \left(\begin{array}{cc|cc|cc} & J_1 & 0 & 0 & 0 & 0 \\ & & 0 & 0 & 0 & 0 \\ \hline 0 & 0 & & \ddots & 0 & 0 \\ 0 & 0 & & & 0 & 0 \\ \hline 0 & 0 & 0 & 0 & & \\ 0 & 0 & 0 & 0 & \multicolumn{2}{c}{J_m} \end{array}\right), \text{with } J_i = \begin{pmatrix} \lambda_i & 1 & 0 & 0 \\ & \lambda_i & 1 & 0 \\ & & \ddots & \\ 0 & & & \lambda_i \end{pmatrix}$$

The $\lambda_i$ are the eigenvalues. This bloc-diagonal matrix is called the canonical form. If the linear application is expressed as a matrix $A$ in an original basis, the canonical form can be obtained by a suitable basis transformation ($J = T^{-1}AT$), where the columns of $T$ are the genralised eigenvectors. The number of Jordan blocs correspond to the number of (true) eigenvectors, which are in general less than the number of generalised eigenvectors. The linear application is said to be *diagonalisable* (all eigenvectors are independent) when all Jordan blocks have dimension one. If at least one Jordan block has 2 or more dimensions, then there will be fewer eigenvectors than the number of dimensions, thus, fewer eigenvectors than *generalised* eigenvectors. In its original formulation, the Jordan canonical form theorem concerns linear applications in algebraic closed spaces, that is, spaces that contain the solutions of all polynomial equations. Vector spaces such as $\mathbb{C}^n$ are algebraically closed, but not $\mathbb{R}^n$. For example, $\mathbb{R}^1$ does not contain the solution of $x^2 + 1 = 0$. As a consequence, what we needed in Section 4.1 is a slightly extended version of the Jordan canonical form theorem. In this case of a *linear* application from $\mathbb{R}^n \to \mathbb{R}^n$, eigenvalues are either real, or appear by pairs of complex conjugates. Real eigenvalues are associated with Jordan blocs. Hence, in this case, we have two options: either accept complex entries in the normal canonical form (associated with complex basis vectors), or opt for a purely real expression, but in this case we need *another* basis of vectors than the actual eigenvectors. In this case, conjugate pairs of eigenvalues $\lambda = \alpha \pm \beta$ are replaced by $2 \times 2$ blocks of the form $\begin{pmatrix} \alpha & \beta \\ -\beta & \alpha \end{pmatrix}$.

Hence, for a linear application $\mathbb{R}^n \to \mathbb{R}^n$, the canonical form is:

$$J = \left(\begin{array}{cc|cc|cc} & C_1 & 0 & 0 & 0 & 0 \\ & & 0 & 0 & 0 & 0 \\ \hline 0 & 0 & & \ddots & 0 & 0 \\ 0 & 0 & & & 0 & 0 \\ \hline 0 & 0 & 0 & 0 & & \\ 0 & 0 & 0 & 0 & & C_m \end{array}\right),$$

where the $C_i$ are either Jordan blocks (associated with a real eigenvalue), or blocks of the form:

$$C_i = \left(\begin{array}{cc|cc|cc} \alpha_i & \beta_i & 1 & 0 & 0 & 0 \\ -\beta_i & \alpha_i & 0 & 1 & 0 & 0 \\ \hline 0 & 0 & \alpha & \beta & 1 & 0 \\ 0 & 0 & -\beta_i & \alpha_i & 0 & 1 \\ \hline 0 & 0 & 0 & 0 & \alpha_i & \beta_i \\ 0 & 0 & 0 & 0 & -\beta_i & \alpha_i \end{array}\right),$$

which are then associated with a pair of eigenvalues $\alpha \pm i\beta$. Hence, in an application of dimension 2, the only remaining possibilities are:

- ▷ $\begin{pmatrix} \lambda 1 & 0 \\ 0 & \lambda_2 \end{pmatrix}$ : two Jordan blocks of dimension 1, associated with real eigenvalues. The matrix is diagonalisable.
- ▷ $\begin{pmatrix} \alpha & -\beta \\ \beta & \alpha \end{pmatrix}$ : two Jordan blocks of dimension 1 but associated with a pair of complex conjugate eigenvalues. We use the adapted version for real applications.
- ▷ $\begin{pmatrix} \lambda & 1 \\ 0 & \lambda \end{pmatrix}$ : one Jordan block of dimension 2. Since there is only one eigenvalue in this case, it must be real (as complex comes as pairs).

## D.2 Biographic notices

- ▷ Henri Poincaré (1854 – 1912): French mathematician and theoretical physicist
- ▷ Vito Velterra (1860 – 1940): Italian mathematician and physicist
- ▷ Alexsandr Lyapunov (1857 – 1918): Russian mathematician and physicist
- ▷ Ivar Otto Bendixson (1861 – 1935): Swedish (check one or two s)
- ▷ Henri Dulac (1870 – 1955): French mathematicia
- ▷ Balthasar van der Pol (1889 – 1959): Dutch physicist
- ▷ Philip Hartman (1915 – 2015) : American mathematician
- ▷ Edwar Norton Lorenz (1917 – 2018): American mathematican and meteorologist
- ▷ David M. Grobman (1922 – 2007): Russian physicist and mathematician
- ▷ Eberhard Hopf (1902 – 1983): Austrian mathematician
- ▷ Alexsandr Andronov (1901 – 1952): Russian (Soviet Union) mathematician

## References


[BGGS80] G. Benettin, L. Galgani, A. Giorgilli, and J. Strelcyn. Lyapunov characteristic exponents for smooth dynamical systems and for hamiltonian systems; a method for computing all of them. part 1: Theory. *Meccanica*, 15(1):9–20, 1980.

[GAD+02] M. Ghil, M. R. Allen, M. D. Dettinger, K. Ide, D. Kondrashov, M. E. Mann, A. W. Robertson, A. Saunders, Y. Tian, F. Varadi, and P. Yiou. Advanced spectral methods for climatic time series. *Reviews of Geophysics*, 40:769–794, 2002.

[HD13] M. W. Hirsh and R. L. Devaney. *Dynamical Systems, and an Introduction to Chaos*. Elsevier, 2013.

[Hil00] R. C. Hilborn. *Chaos and Nonlinear Dynamics: An Introduction for Scientists and Engineers*. Oxford University Press, 2000.

[HJ90] R. A. Horn and C. R. Johnson. *Matrix Analysis*. Cambridge University Press, 1990.

[Kuz23] Y. A. Kuznetsov. *Elements of Applied Bifurcation Theory*. Springer International Publishing, 2023.

[Lor63] E. N. Lorenz. Deterministic non-periodic flow. *Journal of the Atmospheric Sciences*, 20:130–141, 1963.

[MCA15] T. Mitsui, M. Crucifix, and K. Aihara. Bifurcations and strange nonchaotic attractors in a phase oscillator model of glacial–interglacial cycles. *Physica D: Nonlinear Phenomena*, 306:25 – 33, 2015.

[MOF05] K. A. Maasch, R. J. Oglesby, and A. Fournier. Barry saltzman and the theory of climate. *Journal of Climate*, 18(13):2141–2150, 2005.

[Per01] L. Perko. Differential equations and dynamical systems. 2001.

[RS00] K. Ramasubramanian and M. S. Sriram. A comparative study of computation of lyapunov spectra with different algorithms. *Physica D: Nonlinear Phenomena*, 139(1-2):72 – 86, 2000.

[Sal62] B. Saltzman. Finite amplitude free convection as an initial value problem—i. *Journal of the Atmospheric Sciences*, 19(4):329–341, 1962.

[Str14] S. Strogatz. *Nonlinear Dynamics and Chaos: With Applications to Physics, Biology, Chemistry, and Engineering*. Studies in Nonlinearity. Avalon Publishing, 2014.

[Tuc02] W. Tucker. A rigorous ode solver and smale's 14th problem. *Found. Comput. Math.*, 2:53–117, 2002.

[Wig03] S. Wiggins. *Introduction to Applied Nonlinear Dynamical Systems and Chaos*. 2003.


## List of definitions

## List of theorems

# Index

# Index